N6725484

DEVELOPMENT OF AN ADVANCED SOLAR ENERGY THERMIONIC (SET) GENERATOR, FINAL PROGRESS REPORT - 13 AUGUST 1962 TO 12 AUGUST 1963

ELECTRO-OPTICAL SYSTEMS, INC.
PASADENA, CA

MAR 64

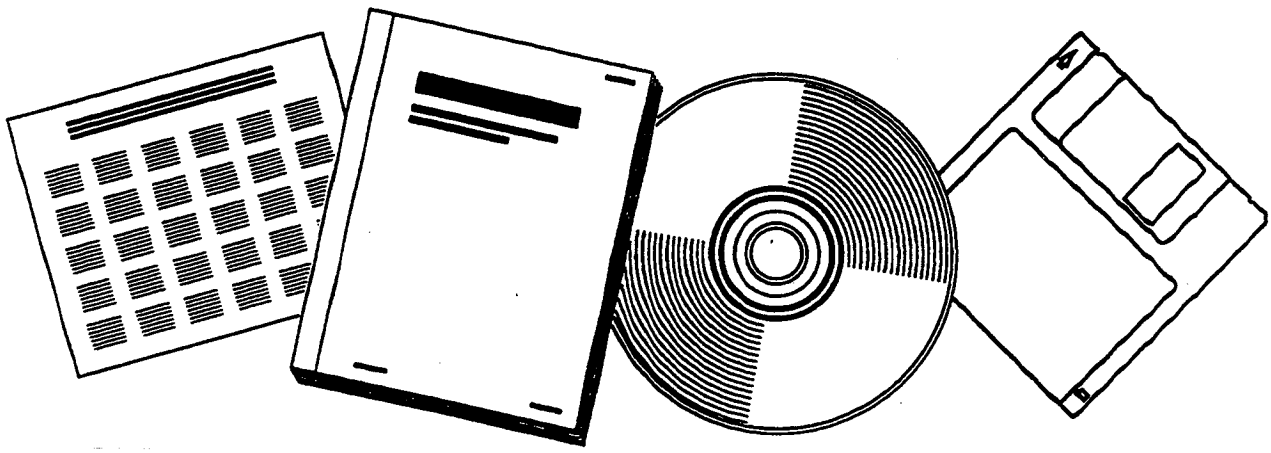

N67-25484

Final Progress Report
13 August 1962 to 12 August 1963

DEVELOPMENT OF AN ADVANCED SOLAR ENERGY THERMIONIC (SET) GENERATOR

Prepared for:

Jet Propulsion Laboratory
4800 Oak Grove Drive
Pasadena, California

Contract No. 950349

EOS-~~Report~~ 3380-Final 13 March 1964

Prepared by

A. E. Campbell
and A. O. Jensen

Approved by

for A. R. Tanguay, Manager
ENERGY CONVERSION DIVISION

REPRODUCED BY
U.S. DEPARTMENT OF COMMERCE
NATIONAL TECHNICAL INFORMATION SERVICE
SPRINGFIELD, VA. 22161

ELECTRO-OPTICAL SYSTEMS, INC., - PASADENA, CALIFORNIA

NOTICE

THIS DOCUMENT HAS BEEN REPRODUCED FROM THE BEST COPY FURNISHED US BY THE SPONSORING AGENCY. ALTHOUGH IT IS RECOGNIZED THAT CERTAIN PORTIONS ARE ILLEGIBLE, IT IS BEING RELEASED IN THE INTEREST OF MAKING AVAILABLE AS MUCH INFORMATION AS POSSIBLE.

CONTENTS

		Page
1.	PROGRAM SUMMARY	1-1
2.	FEASIBILITY INVESTIGATIONS	2-1
	2.1 Positive Spacing Investigation (Materials Compatibility)	2-1
	2.1.1 Direct Contact Spacing Technique (Materials Compatibility)	2-4
	2.1.2 Composite Space Technique	2-16
	2.2 Electrical Insulation of Series Converters	2-19
	2.2.1 Materials Preparation	2-20
	2.2.2 Experimental Measurements and Calculations	2-22
	2.2.3 Experimental Results	2-23
	2.3 Cesium Reservoir Tubulation Design	2-36
	2.3.1 Materials Preparation	2-36
	2.3.2 Experimental Measurements and Calculations	2-37
	2.3.3 Experimental Results	2-41
	2.4 Collector Emissivity Investigations	2-41
3.	CONVERTER DESIGN, FABRICATION, AND TEST	3-1
	3.1 Design and Fabrication (with Manufacturing and Engineering Drawings) of Converter Components	3-3
	3.1.1 Emitter	3-3
	3.1.2 Envelope	3-4
	3.1.3 Envelope Flange	3-5
	3.1.4 Envelope-Flange Assembly	3-8
	3.1.5 Emitter Assembly	3-10

CONTENTS
(contd)

		Page
3.1.6	Collector	3-12
3.1.7	Collector-Flange Assembly	3-14
3.1.8	Radiator and Clamp Assembly	3-14
3.1.9	Collector Flange	3-16
3.1.10	Heat Choke	3-17
3.1.11	Exhaust Assembly	3-17
3.1.12	Flow Chart for Converter No. 1 through No. 6	3-17
3.2	Converter Fabrication and Development History	3-18
3.2.1	The Reservoir Heat Choke	3-18
3.2.2	Collector-Radiator Assembly	3-18
3.2.3	Interelectrode Spacing	3-19
3.3	Converter Test Data Analysis	3-20
3.3.1	Diode No. 2	3-22
3.3.2	Diode No. 3	3-26
3.3.3	Diode No. 4	3-26
3.3.4	Diode No. 5	3-35
3.3.5	Diode No. 6	3-39
3.3.6	Diode No. 7	3-39
3.3.7	Diode No. 8	3-44
3.3.8	Diode No. 9	3-44
3.4	Raw Data from Converter Tests	3-49
3.5	Metallurgical Examination	3-50
3.5.1	Ceramic-Metal Seal	3-50
3.5.2	Envelope-Flange Assembly Braze	3-50
3.5.3	Collector-Reservoir Tubulation Braze	3-50
3.5.4	Collector-Clamp Braze	3-50
3.5.5	Reservoir-Tubulation -- Reservoir Weld	3-50

CONTENTS
(contd)

		Page
4.		
4.1	Generator-Converter Fabrication and Test	4-1
	4.1.1 Generator-Converter Fabrication	4-1
	4.1.2 Generator-Converter Test	4-3
4.2	Generator Design	4-9
4.3	Generator Performance	4-12
APPENDIX		

ILLUSTRATIONS

Figure		Page
2-1	Positive electrode spacing techniques	2-3
2-2	Spacing experiment No. 1 tantalum collector and sapphire rods	2-8
2-3	Spacing experiment No. 3 tantalum-tantalum electrodes spaced with sapphire rods	2-10
2-4	Spacing experiment No. 4 molybdenum-molybdenum electrodes space with sapphire rods	2-11
2-5	Spacing experiment No. 5 molybdenum-molybdenum electrodes spaced with sapphire rods	2-13
2-6	Tungsten emitter showing reaction from thoria rods	2-14
2-7	Molybdenum collector with thoria rod	2-14
2-8	Molybdenum collector with sapphire rods	2-15
2-9	Tungsten emitter after 100.6 hours at 1720°C in contact with sapphire rods	2-15
2-10	Detail of Ta-BeO-Mo spacing experiment after 86 hours at emitter temperature of 1700°C	2-17
2-11	Tantalum-BeO-Molybdenum positive spacing experiment (direct contact)	2-18
2-12	Electrical insulation assembly	2-21
2-13	Electrical insulation data from the first experimental assembly. DC data	2-25
2-14	0.7 hours I-V characteristic rod temperature under coating 1170°C, AC data	2-26
2-15	1 hour I-V characteristic rod temperature under coating 1366°C. AC data	2-27
2-16	2.1 hours I-V characteristic rod temperature under coating 1464°C. AC data	2-28

ILLUSTRATIONS
(contd)

Figure		Page
2-17	3 hours characteristic rod temperature under coating 1462°C. AC data	2-29
2-18	4 hours I-V characteristic rod temperature under coating 1467°C, AC data	2-30
2-19	7 hours I-V characteristic rod temperature under coating 1587°C, AC data	2-31
2-20	Insulation experiment (tungsten rod) Mag. 300X	2-33
2-21	Tungsten Rod-plasma sprayed alumina interface Mag. 300X	2-34
2-22	Sprayed tungsten-sprayed slumina interface Mag. 300X	2-34
2-23	Sprayed tungsten coating Mag. 300X	2-35
2-24	Cesium reservoir tabulation and heater	2-38
2-25	Cesium reservoir tubulation experiment collector at 600°C	2-42
2-26	Cesium reservoir tubulation experiment collector at 700°C	2-43
2-27	Cesium reservoir tubulation experiment collector at 800°C	2-44
2-28	Evaporation rate loss from selected emitter materials	2-46
2-29	Collector emissivity investigation	2-47
3-1	Thermal loss and L/A lead ratio vs current for $\alpha = 0.1$ ($\alpha \equiv$ p elec/p thermal)	3-6
3-2	Envelope/flange assembly brazing jig	3-9
3-3	Inert arc welding apparatus	3-11
3-4	Detail of emitter/collector spacing	3-15
3-5	Maximum power vs interelectrode spacing (at temperature) for EOS diodes	3-21
3-6	Diode No. 2 current-voltage characteristics	3-24
3-7	Diode No. 2 current-voltage characteristics	3-25

ILLUSTRATIONS
(cont'd)

Figure		Page
3-8	Diode No. 2 power output vs cesium reservoir temperature for collector temperature as the parameter	3-27
3-9	Diode No. 2 power output vs cesium reservoir temperature for collector temperature as the parameter	3-28
3-10	Diode No. 2 power output vs cesium reservoir temperature for collector temperature as the parameter	3-29
3-11	Diode No. 3 current-voltage characteristics	3-30
3-12	Diode No. 3 power output vs cesium reservoir temperature for collector temperature as the parameter	3-31
3-13	Diode No. 4 current-voltage characteristics	3-32
3-14	Diode No. 4 power output vs cesium reservoir temperature for collector-temperature as the parameter	3-34
3-15	Diode No. 5 current-voltage characteristics	3-36
3-16	Diode No. 5 current-voltage characteristics	3-37
3-17	Diode No. 5 power output vs cesium temperature for collector temperature as the parameter	3-38
3-18	I-V characteristics for Diode No. 6	3-40
3-19	Power output versus cesium reservoir temperature for diode No. 6	3-41
3-20	I-V characteristics for Diode No. 7	3-43
3-21	Power output vs cesium reservoir temperature for diode No. 7	3-44
3-22	I-V characteristics for Diode No. 8	3-45
3-23	Power output versus reservoir temperature for Diode No. 8	3-46
3-24	I-V characteristics for Diode No. 9	3-47
3-25	Macro-section of Diode No. 1 after 200 hour test	3-50

ILLUSTRATIONS
(contd)

Figure		Page
3-26	11X magnification of ceramic metal seal	3-51
3-27	75X magnification of seal area	3-52
3-28	200X magnification of seal	3-53
3-29	11X magnification of envelope-flange assembly braze	3-54
3-30	11X magnification of collector reservoir tubulation braze	3-55
3-31	11X magnification of clamp-collector braze	3-56
3-32	11X magnification of copper-niobium weld	3-57
4-1	Generator converter emitter structure	4-2
4-2	I-V characteristics for generator-converter No. 2	4-4
4-3	I-V characteristics for generator-converter No. 3	4-5
4-4	I-V characteristics for generator-converter No. 4	4-7
4-5	I-V characteristics for generator-converter No. 5	4-8
4-6	Prototype 3 converter generator	4-10
4-7	Cone mounted in place for completed assembly of generator	4-11

1. PROGRAM SUMMARY

Work on Contract 950349 with the Jet Propulsion Laboratory was initiated August 13, 1962. The effort on this contract was performed in accordance with the contract work statement and EOS technical proposal, BD 62-824A, dated 1 May 1962.

The program for the development of an advanced solar energy thermionic generator was divided into two categories:

1. Feasibility Investigations
2. Thermionic Converter and Generator Development and Design

The feasibility experiments related directly to advancing the state of the art of cesium vapor thermionic converter design and to the integration of reliable, high performance converters into an advanced thermionic generator. The design and development portion of the program was directed to the achievement of long life, high performance reproducible cesium vapor thermionic converters. The design objectives for the converters were: Power density of 10 to 15 w/cm^2, and lifetime capability of 1000 hours at an emitter temperature of 2000°K and a voltage output of 0.8v to 1.0v.

Summarized below are specific accomplishments resulting from this program:

1. A three converter generator was fabricated, assembled and laboratory tested and produced 57 electrical watts with a series-connected output voltage in excess of 2.0 volts.
2. Converter design objectives of 10 $watts/cm^2$ at 2000°K emitter temperature were achieved or exceeded by three converters delivered to JPL.
3. The metallurgical examination of a 200-hour test converter revealed:

a. No evidence of cesium attack on the ceramic-metal seal

b. A completely brazed, high integrity emitter lead

c. A cesium reservoir tubulation that remained attached to the collector during thermal cycle and continuous test

4. A practical materials compatibility study involving the high temperature, long term interaction of ceramics, such as, BeO, Al_2O_3, and ThO_2 with tungsten, molybdenum, and tantalum was completed. The data from this study are an original and useful contribution to the field of thermionic energy conversion.

5. Parametric converter studies have shown the fundamental importance of an optimum collector temperature (and indirectly the collector work function) for achieving maximum output from a cesium vapor thermionic converter. A recommended treatment of the collector to achieve an optimum condition prior to diode fabrication is reported herein. It is believed that this is a significant advance since achievement of a minimum work function on the collector surface adds directly to the converter output voltage and power.

6. High temperature brazing technology was introduced into converter fabrication that supercedes state of the art low temperature copper or nickel brazing. Full details of cleaning procedures, brazing jigs and fixtures, and brazing procedures are reported.

7. Cleaning and processing specifications have been compiled for the proper treatment of metals and ceramics employed in the construction of thermionic converters.

Summarized below are important areas where additional development work is required:

1. Detailed investigations of the high temperature compatibility of ceramic insulating materials and refractory metals. The direct thermal attachment of converters to each other and to an energy absorbing cavity is still considered to be a most efficient and reliable method. The practical utilization of direct thermal interconnection of converters requires more detailed studies of high temperature compatibility of insulation and converter construction materials.
2. Development of positive electrode spacing techniques for high performance, reproducible converters of close spacing is essential. Without continued design and materials assessment, positive (or consistent) interelectrode spacing from converter to converter is not possible.
3. Further development of simple techniques and new design approaches for improving collector heat transfer are required. Proper control of the collector temperature (and consequently the collector work function) at high current density would lead to a converter of more nearly optimum performance and efficiency.
4. Improved thermionic generator designs are necessary in order to reduce cavity losses and improve generator efficiency.

2. FEASIBILITY INVESTIGATIONS

The feasibility investigations encompassed four main areas:

1. Positive electrode spacing techniques
2. Electrical insulation and thermal connection of series converters
3. Cesium reservoir design
4. Collector emissivity

The feasibility investigations were undertaken with the primary objective of advancing the state of the art in thermionic converter design and fabrication techniques. The results of the feasibility investigations were to be integrated into the converter and generator fabrication program in order to achieve long life, high performance, reproducible thermionic converters and generators.

The feasibility experiments were set up and conducted in such a manner that the major proof of feasibility could be obtained in a simple, controlled experiment without resorting to expensive in-converter tests where other variables, such as spacing, cesium purity, and/or improper materials processing, would obscure the fundamental phenomenon under study.

The methods and results of the feasibility investigations are reported in the following sections.

2.1 Positive Spacing Investigation (Materials Compatibility)

The positive spacing investigations were undertaken to develop a method for insuring a fixed spacing between electrodes of a long life converter. In general, the design scheme must be simple, reproducible, and offer minimum thermal losses. Two such schemes were investigated for feasibility. One method, referred to as direct contact spacing, employed precision ground ceramics placed in direct

contact between the emitter and collector. The second method, referred to as composite spacing, incorporated a tungsten ring in direct contact with the emitter, which rested upon a ceramic insert in the collector. Figure 2-1 illustrates the two techniques of spacing.

Results from the first direct contact experiments indicated that the direct contact spacing technique lacked feasibility at high emitter temperature since gross interaction occurred between the electrode materials and ceramic spacing members. However, the experimental data obtained from the direct contact experiments provide an important contribution to the technology of high temperature converter materials compatibility. Carefully controlled experiments have filled some gaps in knowledge pertaining to long time at temperature materials compatibility.

The composite spacing investigations were undertaken to provide an alternate means of achieving a positive spacing between high temperature converter electrodes free from materials interaction. It was felt that the materials reaction experienced in the direct contact technique was primarily due to the reduction of the ceramic by the refractory metals when the two are in contact at temperatures of 1200°C and higher. If the average temperature of the materials at the point of contact is substantially reduced, a reaction would not occur. Therefore, in the composite spacing technique a metallic ring is used which provides only knife edge contact with the emitter and knife edge contact with the ceramic. The reduction in heat flow serves to reduce the average temperature at the point of contact between the ceramic and spacer. A 100 hour test of the composite spacing design demonstrated a positive, unaltering interelectrode space with no evident incompatibility of materials. Details of this investigation are reported in Subsection 2.1.2.3. On this basis, five converters were fabricated that incorporated the composite spacing technique*. Metallurgical

*The environmental influences in a converter such as a high temperature cesium vapor and compressive force on the composite assembly offer the final test for feasibility of any spacing technique.

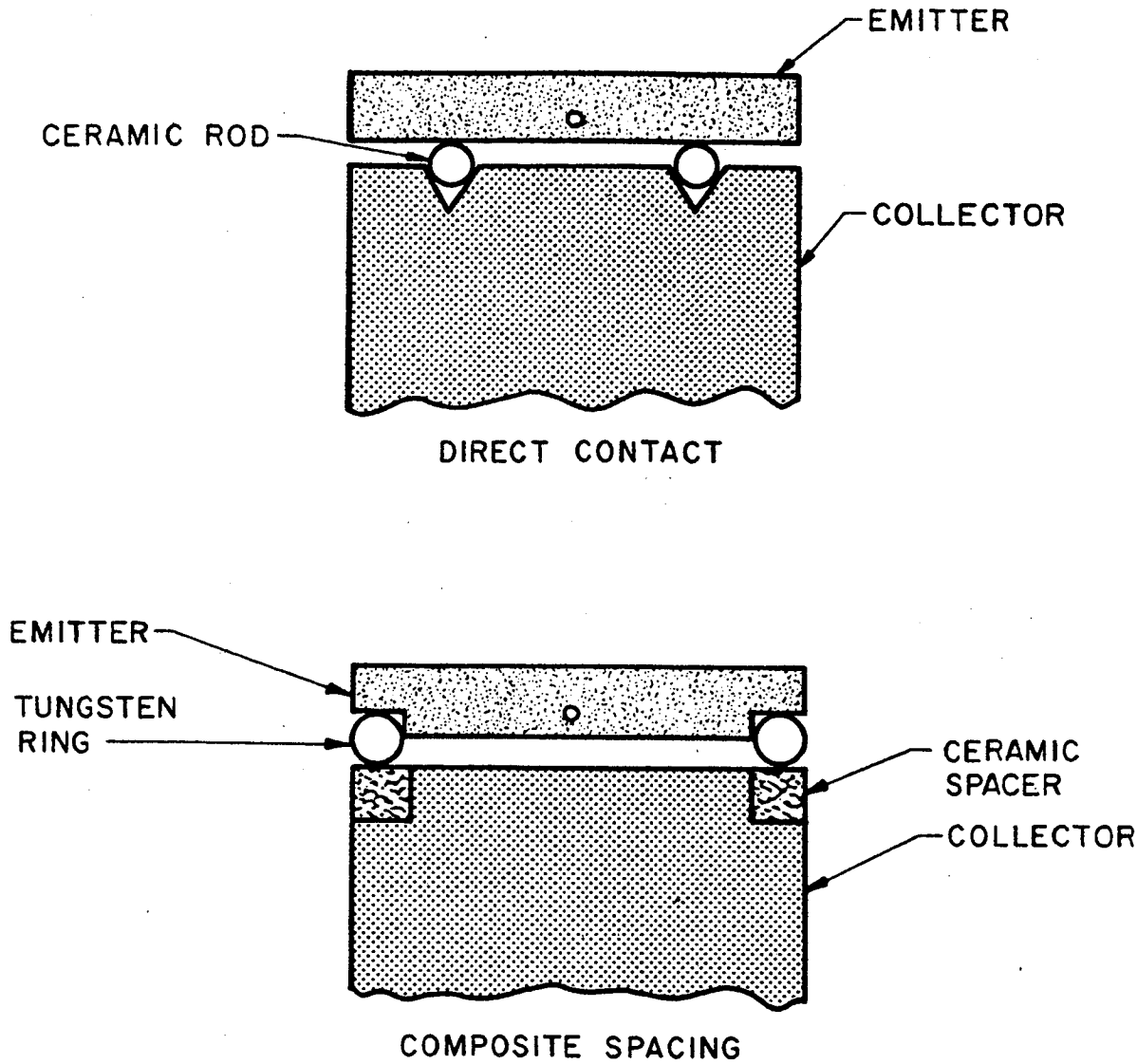

FIG. 2-1 POSITIVE ELECTRODE SPACING TECHNIQUES

examination of one of these converters has shown that during converter operation, reaction occurred between the ceramic insert and the molybdenum collector, contrary to our feasibility investigations. The significance of these observations, and the seemingly contradictory nature of the results, are discussed in Subsection 2.4. For the present, the following text is devoted to the design calculations, materials preparation, and experimental results of these two spacing methods.

2.1.1 Direct Contact Spacing Technique (Materials Compatibility)

2.1.1.1 Materials Preparation

The materials employed in this investigation were chemically cleaned in accordance with the specifications contained in the appendix. After chemical cleaning, the metallic parts were vacuum fired, either in a "gettered" atmosphere or in a vacion pumped environment. Tantalum was outgassed at 2200°C for approximately 30 minutes. Molybdenum was outgassed at 1700°C for the same amount of time. Ceramic parts were air-fired at 1200°C after chemical cleaning.

All materials employed were certified "electron tube grade" with spectrographic analyses indicating 99.9 percent purity or better. The ceramics (sapphire rods) were certified 99.99 percent purity.

With reasonably pure materials as a starting point, followed by dilligent and systematic processing, the direct contact spacing experiments were conducted in a vacion pumped environment at background pressures between 1×10^{-7} mm Hg and 6×10^{-8} mm Hg.

It is felt that the results of the materials compatibility experiments represent what is practically achievable in the way of materials compatibility (between those materials tested) for long term (100 hours and greater) operation. Much of the data reported have not been previously available in the literature.

2.1.1.2 Spacing Measurements and Calculations

The initial interelectrode gap is fixed to within 0.1 mil by precision ground spacer rods. Spacing changes which are likely to occur in reasonably compatible systems over fairly long periods of operation will probably be on the order of 0.1 mil to 0.5 mil. The system used to measure changes in spacing must, therefore, be sensitive to very small spacing changes and should not alter the spacing during measurement. The capacity bridge technique was chosen to measure such small spacing changes. Nominally, the sensitivity of the experimental setup used could easily detect a 2 mmf change in capacity at 80 mmf. This corresponds to the detection of a 0.1 mil change in spacing at 4 mils.

The relation between the capacitance and spacing of two plane parallel surfaces is given in engineering units by $C = 0.224\ A/d$ (micromicrofarads) where A is the area of the surfaces in square inches and d is the distance between parallel surfaces given in inches. In practice, the total capacitance of an assembly is the sum of the electrode capacitance and the lead capacitance. Since changes in spacing are of prime interest, changes in capacitance were observed as a function of sample time at temperature. Parasitic effects were cancelled out in such comparative measurements.

In addition to relative capacitance measurements, an absolute measurement of the capacitance of an assembly of known spacing and area was conducted and the results compared to the calculations. The calculated capacity follows:

$$C_{calc.} = 0.224\ A/d = 0.224 \times 0.44/0.0043 \text{ mmfd}$$

$C_{calc.}$ = 22.9 mmfd (computed for an interelectrode spacing of 0.00433 inches and an electrode surface having a diameter of 0.75 inches)

The results of the capacity measurement on this assembly are as follow:

The total measured capacitance was 65 mmfd, as determined by a capacitance bridge (General Radio Model 1650-A). The total measured capacitance is the sum of the parasitic (lead capacitances) and the electrode capacitance. The parasitic capacitance due to the external test leads, internal potential leads, mounting apparatus, and binding posts was independently measured to be 42 mmfd. Therefore:

$$C_{electrodes_{measured}} = C_{total_{measured}} - C_{parasitic_{measured}}$$

$$C_{electrodes_{measured}} = 65 \text{ mmf} - 42 \text{ mmf} = 23 \text{ mmf}$$

$$C_{electrodes_{measured}} = 23 \text{ mmf}$$

and,

$$C_{electrodes_{calculated}} = 22.9 \text{ mmf}$$

The measured value of 23 mmfd compares favorably with the calculated value of 22.9 mmfd.

2.1.1.3 Experimental Results

The following paragraphs give a detailed account of the experimental results of each direct contact spacing experiment. These results are also summarized in Table 2-1.

Experiment 1

The purpose of this experiment was to establish whether or not there was an interaction between pure alumina (sapphire) and tantalum electrodes at temperatures of operation appropriate to high performance converters. Therefore, a nominal temperature range of 1550 to 1600°C was chosen for 5 hours of operation. Extensive reaction was noted in the region next to the rods as shown in Fig. 2-2. The emitter, and the emitter surface, displayed two noticeable tracks across the surface where the rods had been in contact with the surface.

TABLE 2-1 SUMMARY OF EXPERIMENTAL DATA FOR DIRECT CONTACT TECHNIQUE

EMITTER MATERIAL	CERAMIC	COLLECTOR MATERIAL	COLLECTOR TEMPERATURE	TIME	EMITTER TEMPERATURE	REMARKS
Tantalum	Al_2O_3 (Sapphire Rods)	Tantalum	745°C	6 Hours	1600°C	Gross interaction. Spacing rods flattened. Initial capacitance was 72 mmfd. Final capacitance was 80 mmfd, capacitance change of 8 mmfd.
Tantalum	Al_2O_3 (Sapphire Rods)	Tantalum	508°C	5 Hours	1365°C	No noticeable interaction. Initial capacitance was 68 mmfd, final capacitance was 68 mmfd, no capacitance change
Tantalum	Al_2O_3 (Sapphire Rods)	Tantalum	590°C	6 Hours	1450°C	Slight interaction. Initial capacitance was 65 mmfd, final capacitance was 65 mmfd, no capacitance change
Molybdenum	Al_2O_3 (Sapphire rods)	Molybdenum	496°C	100.2 Hours	1350°C	Moderate interaction. Rods only slightly flattened (<0.0005"). Initial capacitance was 65 mmfd, final capacitance was 65 mmfd, no capacitance changes noted.
Molybdenum	Al_2O_3 (Sapphire Rods)	Molybdenum	590°C	25 Hours	1450°C	Slight interaction. Initial capacitance was 65 mmfd, final capacitance was 65 mmfd, no capacitance change. Rods only slightly flatten (<0.0005")
Tungsten	ThO_2	Molybdenum	770°C	26 Hours	1630°C	Gross interaction. Spacing rod decomposition. Some deposition products on collector. No capacitance measurements made.
Tungsten	Al_2O_3 (Sapphire rods)	Molybdenum	830°C	100.6 Hours	1730°C	Slight interaction. Rods not flattened. No capacitance measurements made
Tantalum	BeO	Molybdenum	817°C	86 Hours	1700°C	Gross interaction. Black collector deposits. Rod decomposition. No capacitance measurements made.

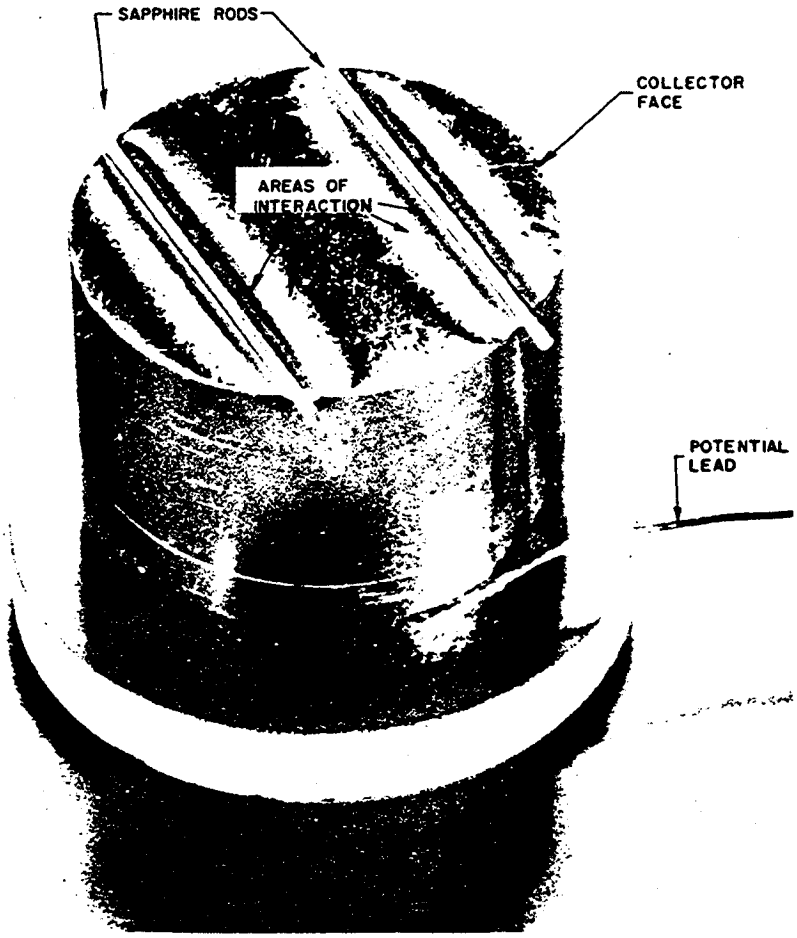

FIG. 2-2 SPACING EXPERIMENT NO. 1
TANTALUM COLLECTOR AND SAPPHIRE RODS
(Tantalum Emitter Operated Over a Temperature Range from 1550°C - 1600°C for 6 hours)

The capacitance was measured initially to be 72 mmfd. The final capacitance measurement was 80 mmfd, therefore, the capacitance of the assembly had changed 9 mmfd during the experiment corresponding to a distance change between electrodes of 0.0005 inches. The capacitance measurements in all cases were conducted with the electrodes at ambient temperature.

Experiment 2

In this experiment the time and temperature conditions were reduced for the purpose of qualifying the observations made in Experiment 1. The same system of tantalum electrodes and sapphire rods was employed. The emitter was operated for 5 hours at 1365°C. No change of capacitance was noted and no interaction products were observed. The capacitance was measured in all cases in the cold condition.

Experiment 3

The results of this experiment, as shown in Fig. 2-3, indicated moderate interaction between the tantalum emitter and sapphire spacer rods. The emitter temperature was maintained at 1450°C for 6 hours. The rods were not observed to be flattened, nor was any change of capacitance detected. The emitter displayed two light, discontinuous tracks across the surface as in Experiment 1, however, they were not as pronounced. The initial and final capacitance measurements are listed in the remarks columns.

Experiment 4

A molybdenum emitter-molybdenum collector assembly spaced with sapphire rods was operated for 100 hours at 1350°C emitter temperature. Figure 2-4 indicates a moderate degree of reaction between sapphire and molybdenum for the given time and temperature. No change of capacitance, however, was noted during the experimental trial, although examination under a bench magnifier showed that the rods were slightly flat along the line of tangency to the emitter. Tracks along the emitter surface were again noted. The initial and final capacitance measurements are listed in the remarks columns.

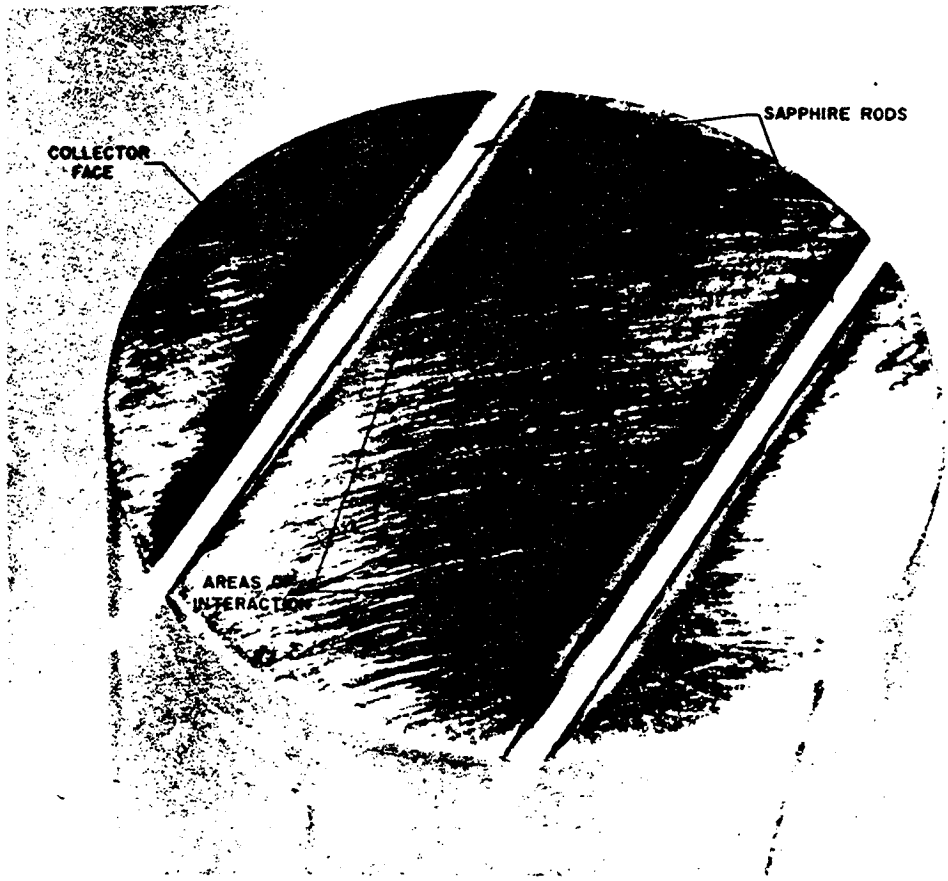

FIG. 2-3 SPACING EXPERIMENT NO. 3 TANTALUM-TANTALUM ELECTRODES SPACED WITH SAPPHIRE RODS (Tantalum Emitter Operated at 1450°C for 6 hours)

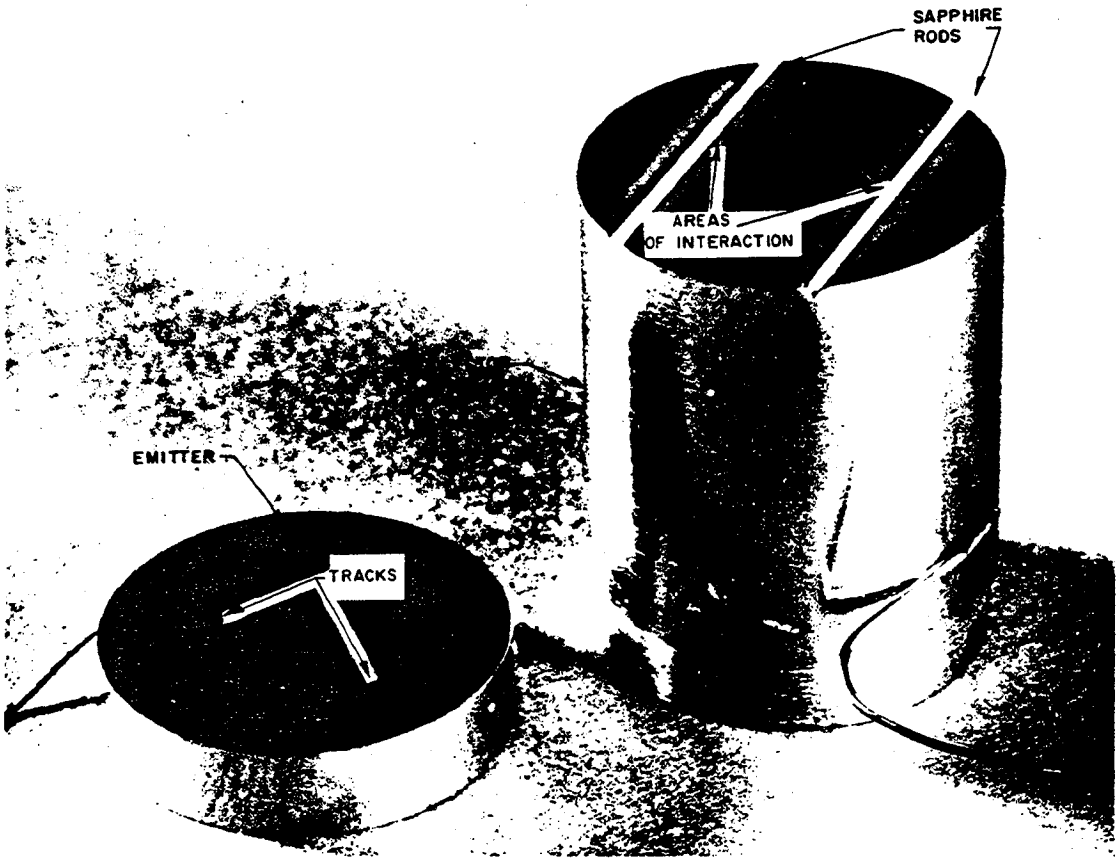

FIG. 2-4 SPACING EXPERIMENT NO. 4 MOLYBDENUM-MOLYBDENUM ELECTRODES SPACED WITH SAPPHIRE RODS (Molybdenum Emitter Operated at 1350°C for 100.2 Hours)

Experiment 5

This experiment was undertaken to add credence to the results of Experiment 4. However, the temperature was increased to 1450°C, and the operational time was decreased to 25 hours. The rods and emitter surface appeared as in Experiment 4. Figure 2-5 identifies the areas of interaction.

It might be well to point out that it was necessary to illuminate the assemblies in Figs. 2-2 through 2-5 in a manner to develop contrast between the clean electrode surfaces and the areas of interaction, which appear as white or gray in all photographs and are labeled as such. The collector faces (other than in a condensation zone), emitter faces, and all refractory surfaces commenced and finished the experiments in a very clean, shiny condition. The initial and final capacitance measurements are listed in the remarks columns.

Experiment 6

A tungsten emitter, thoria spacer rod, molybdenum collector assembly was examined in a direct spacing experiment to evaluate compatibility of these materials. A tungsten emitter was operated for 26 hours at a temperature of 1900°K. Extensive reaction was noted on the emitter surface as shown in Fig. 2-6. One of the spacing rods severed during test. Figure 2-7 illustrates reaction products condensed on the molybdenum collector surface during the operation of the experiment. No capacitance measurements were made.

Experiment 7

Another direct contact spacing experiment was performed to evaluate the interaction of tungsten and alumina. An assembly of tungsten-alumina-molybdenum operated for 100.6 hours at an emitter temperature of 2000°K. Figure 2-8 indicates only slight reaction on the collector surface near the rods. Figure 2-9 illustrates two large continuous tracks on the emitter surface, which appeared to be internal rather than surface contamination products. No capacitance measurements were made.

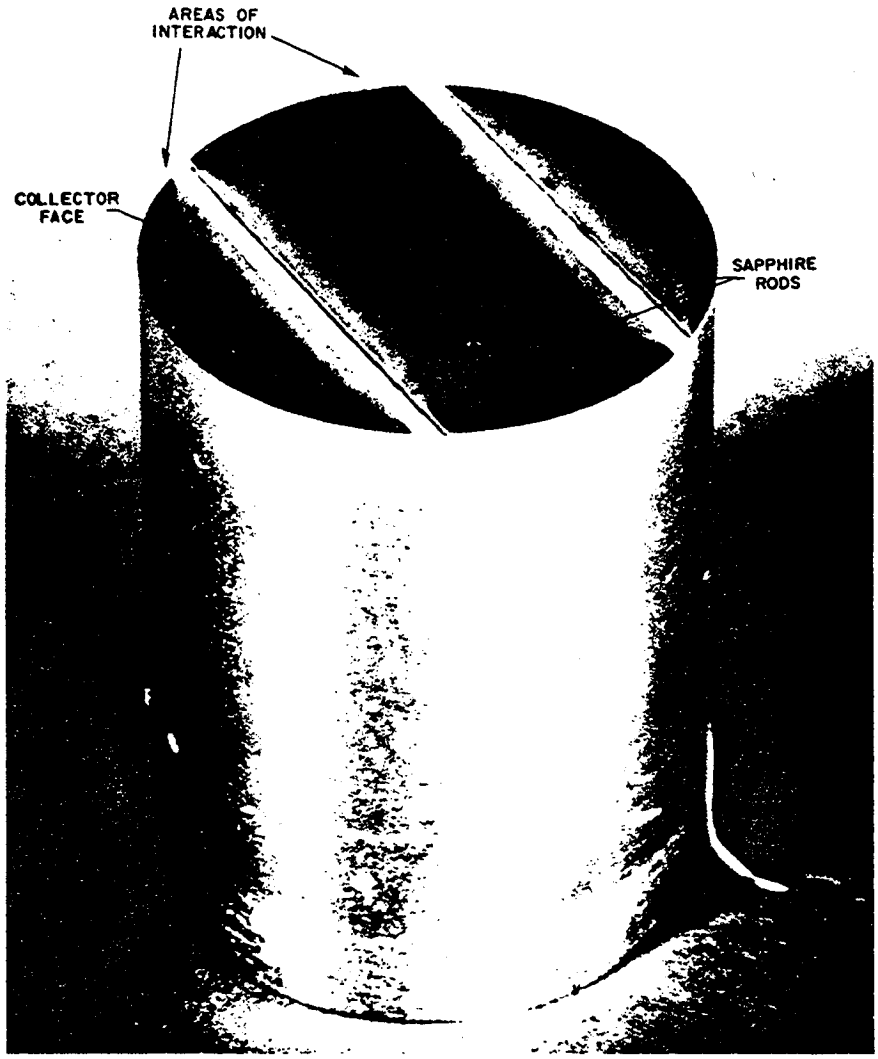

FIG. 2-5 SPACING EXPERIMENT NO. 5 MOLYBDENUM-MOLYBDENUM ELECTRODES SPACED WITH SAPPHIRE RODS (Molybdenum Emitter Operated at 1450°C for 25 Hours)

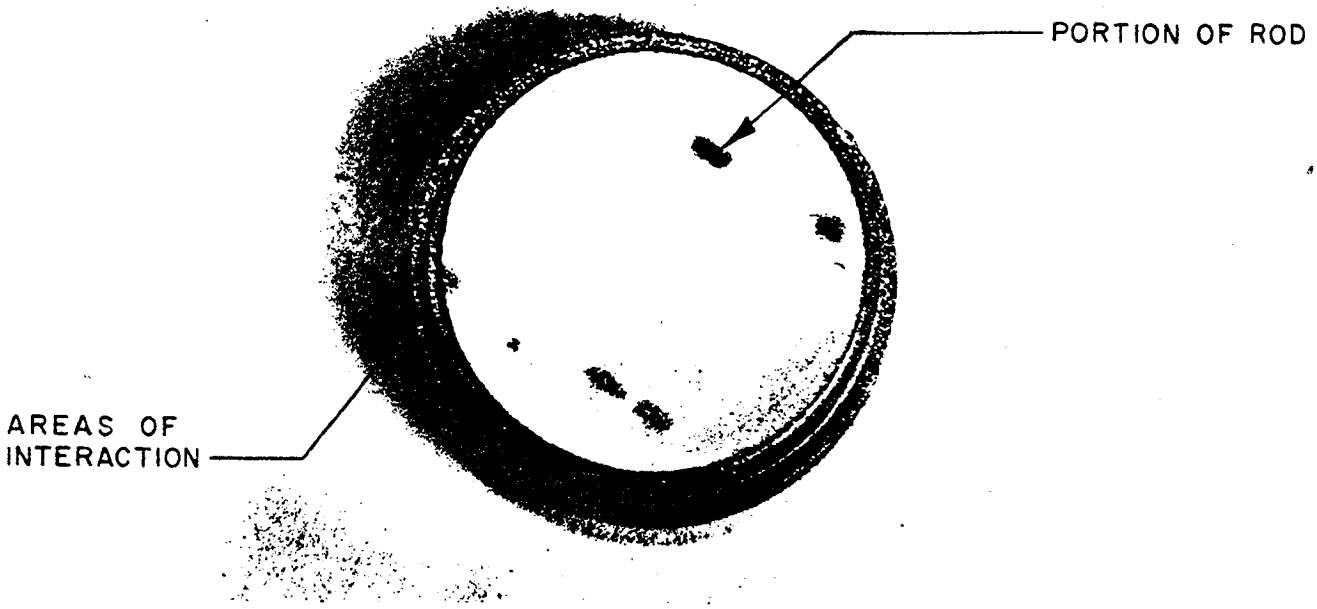

FIG. 2-6 TUNGSTEN EMITTER SHOWING REACTION FROM THORIA RODS

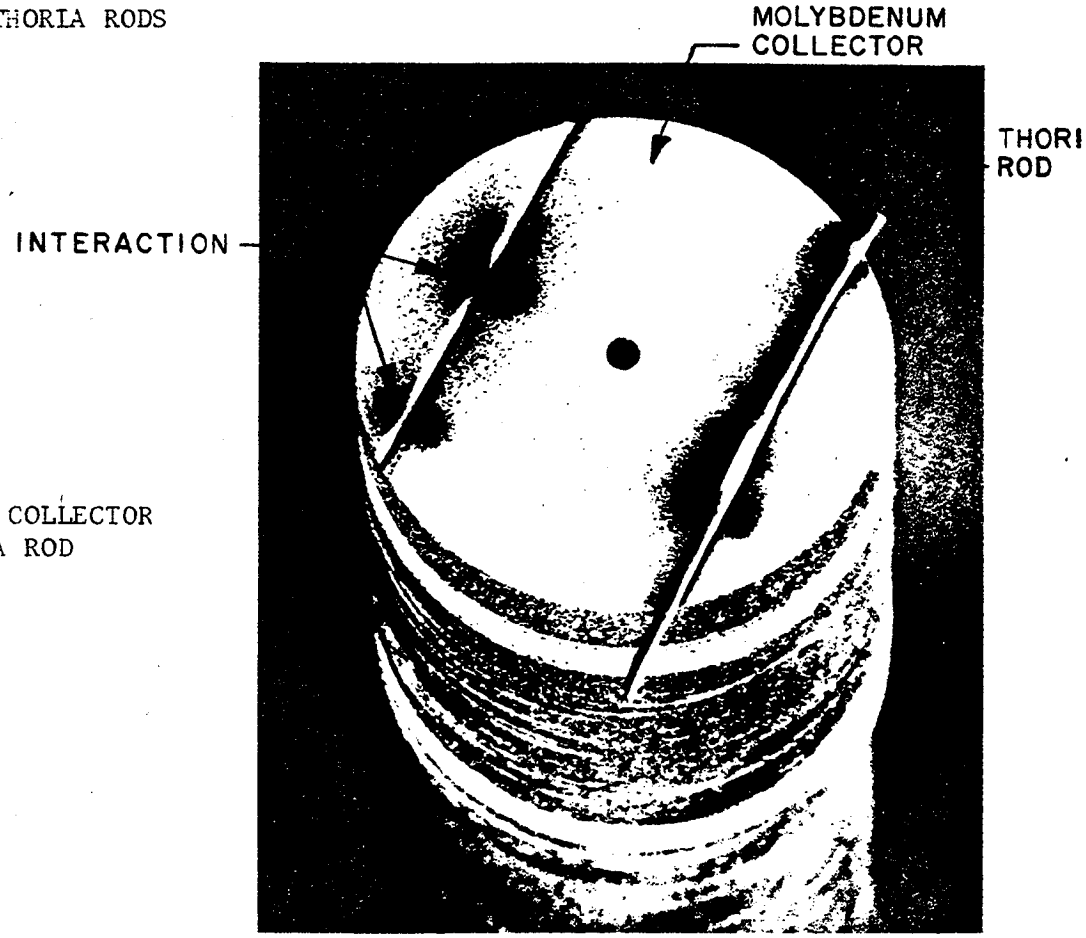

FIG. 2-7
MOLYBDENUM COLLECTOR
WITH THORIA ROD

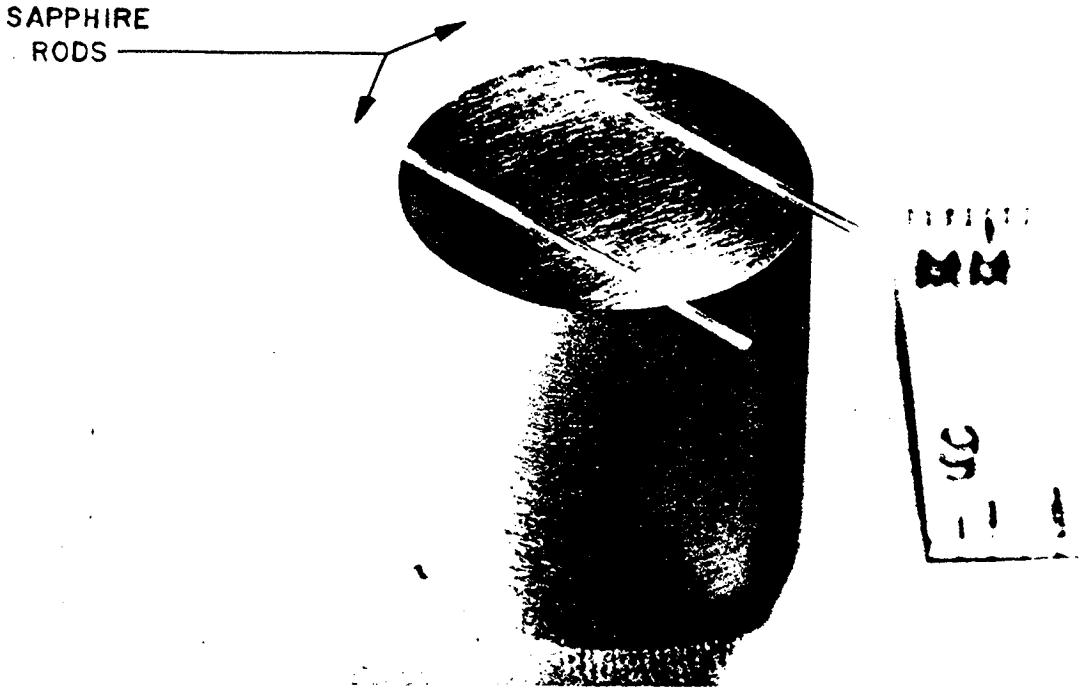

FIG. 2-8 MOLYBDENUM COLLECTOR WITH SAPPHIRE RODS (Tungsten Emitter Operated at 1720°C for 100.6 Hours)

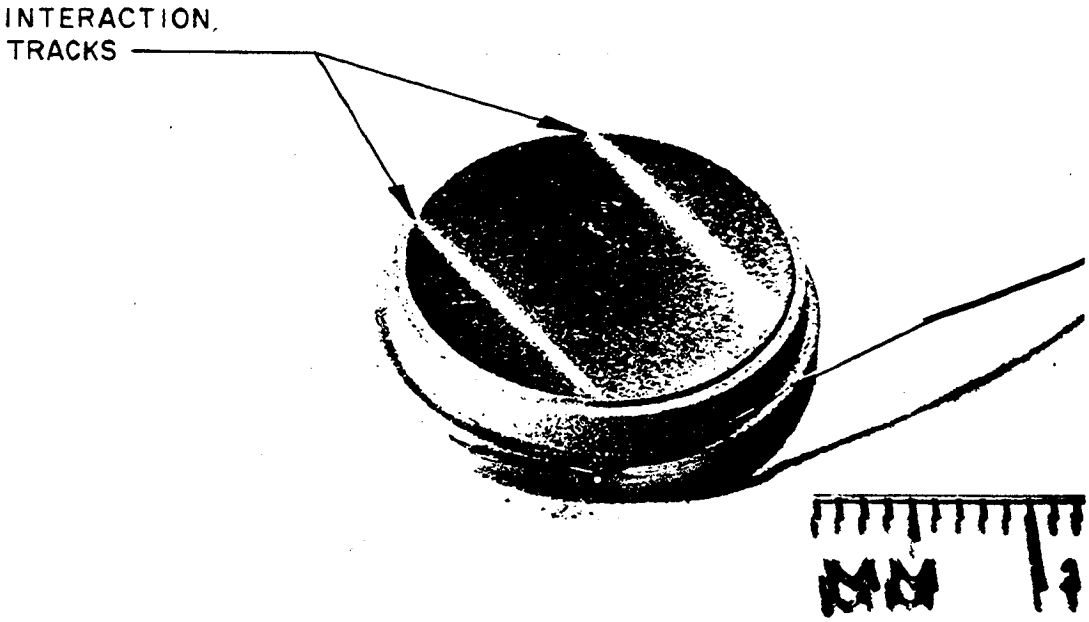

FIG. 2-9 TUNGSTEN EMITTER AFTER 100.6 HOURS AT 1720°C IN CONTACT WITH SAPPHIRE RODS

Experiment 8

The last direct contest spacing experiment was performed to evaluate the compatibility of a tantalum-BeO-molybdenum assembly. The tantalum emitter was operated for 86 hours at an emitter temperature of 2000°K. Figure 2-10 shows the arrangement of the electrodes in the BeO rods. Figure 2-11 indicates the qualitative magnitude of interaction. The molybdenum collector shown on the left has condensed the decomposition products from the BeO rod. The black coating resulted in a requirement for increased electron bombardment power to the emitter in order to maintain constant emitter temperature. The total normal emissivity of this black coating is estimated to be of the order 0.8 to 0.9. The BeO rods suffered severe decomposition during the course of the experiment, and were found to be bonded to the emitter surface. The experiment supporting fixtures contained a metallic coating (probably beryllium) of several hundred angstrons thick at the end of the experiment. No capacitance measurements were made.

The experimental results from the direct contact spacing experiments are summarized in Table 2-1.

2.1.2 Composite Spacing Technique

2.1.2.1 Materials Preparation

The materials employed in the composite spacing experiments received the same chemical cleaning and processing as described in Subsection 2.1.1.1 for the direct contact spacing experiments.

2.1.2.2 Capacitance Measurements and Calculations

Capacitance measuring techniques and the method of performing capacitance calculations supporting the composite spacing technique were identical to those reported in Subsection 2.1.2.

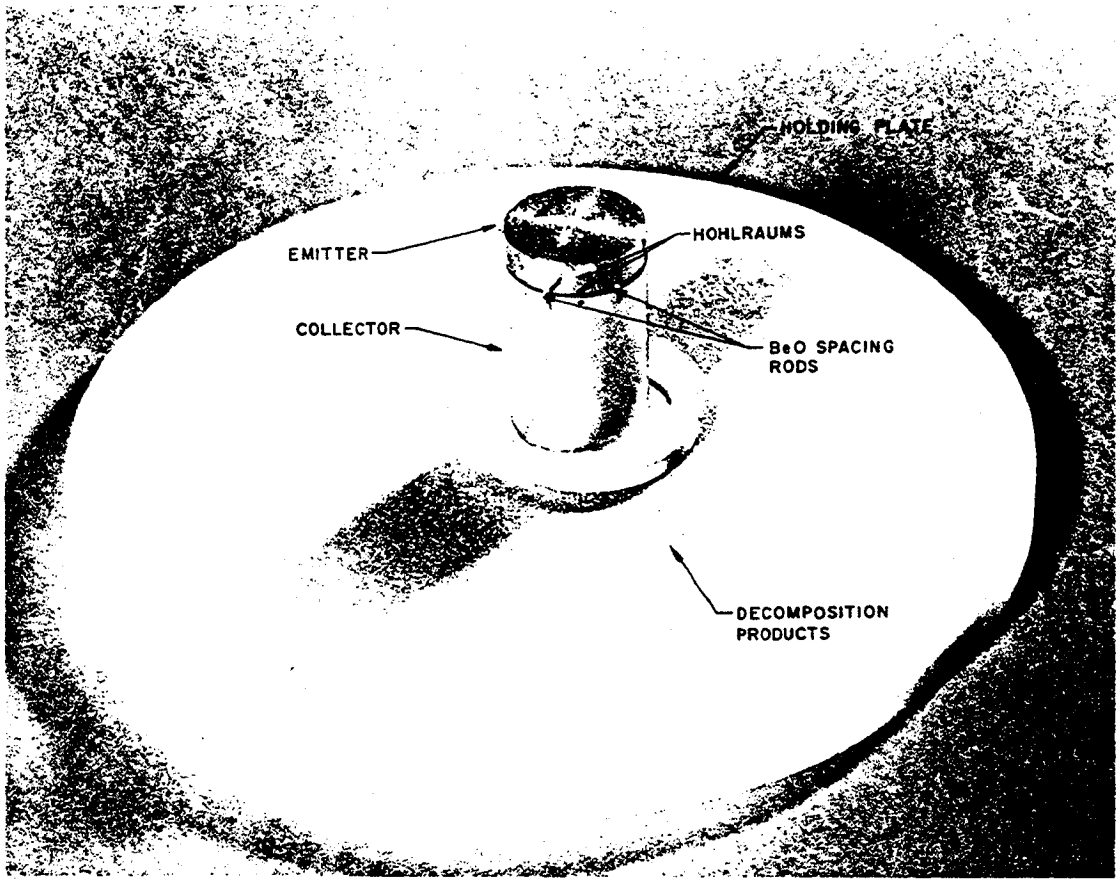

FIG. 2-10 DETAIL OF Ta-BeO-Mo SPACING EXPERIMENT AFTER 56 HOURS AT EMITTER TEMPERATURE OF 1700°C

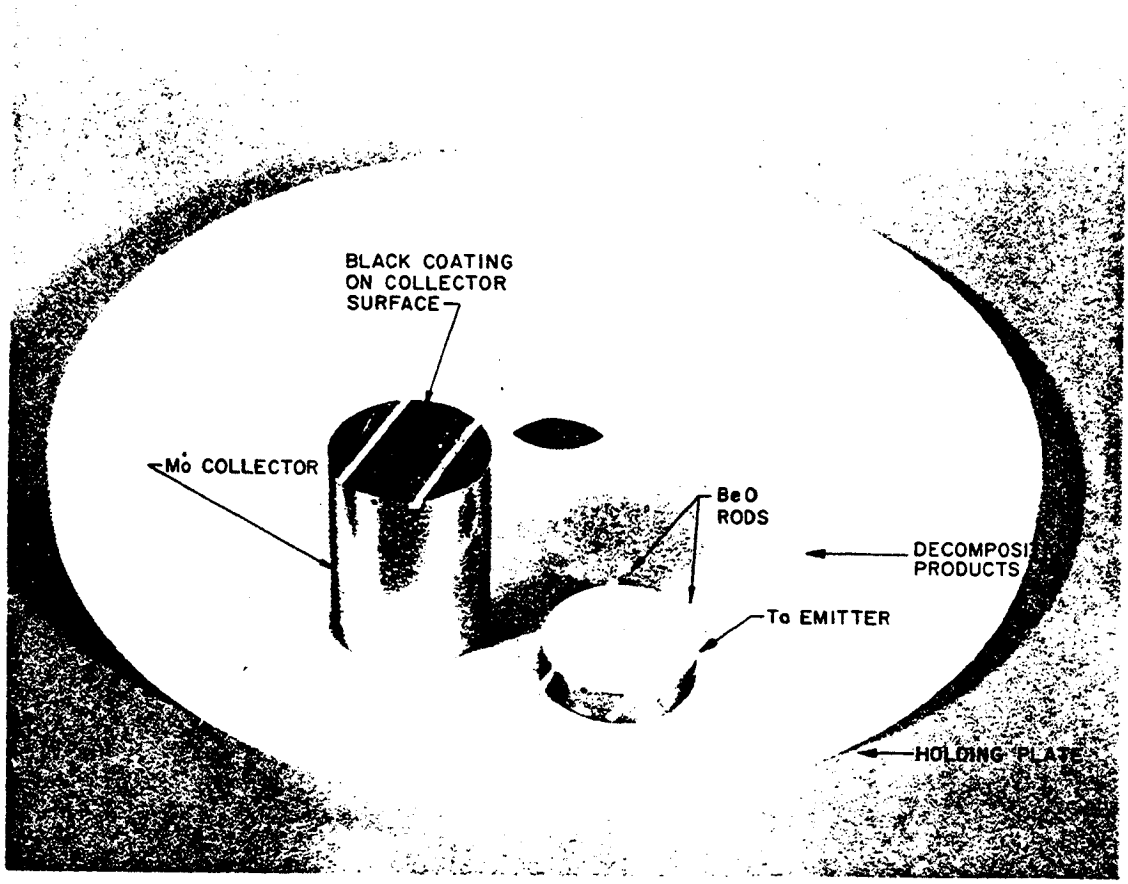

FIG. 2-11 TANTALUM-BeO-MOLYBDENUM POSITIVE SPACING EXPERIMENT (DIRECT CONTACT)

2.1.2.3 Experimental Results

An assembly, consisting of an molybdenum emitter, tungsten spacing ring, ceramic ring, and molybdenum collector operated for 100 hours at an emitter temperature of 1800°K without evidence of interaction or spacing changes. Cold capacitance measurements indicated that the spacing between electrodes remained constant throughout the course of the experiment. The initial capacitance was measured to be 46 mmfd, likewise, the final capacitance was measured to be 46 mmfd. The lack of interaction is explained by the fact that the ceramic had been removed from direct contact with the hot emitter.

A metallurgical examination was performed on Diode No. 1 (which used the composite spacing technique) after 200 hours of operation. The examination of the diode showed decomposition of the ceramic spacer. The detailed results of this examination accompanied by cross-section microphotographs of the ceramic metal seal, emitter lead strap braze and other pertinent areas of concern are reported in Subsection 2.4. The reaction, in the case of the diode, was due to the fact that the collector surface of this particular diode was operating at a temperature of approximately 1200°C, moreover the tungsten spacer ring became bonded to the emitter, increasing the temperature of the ring and ceramic assembly to the reaction range.

2.2 Electrical Insulation of Series Converters

Electrical insulation investigations were conducted to determine the feasibility of direct thermal attachment of converters to each other and to an energy absorbing cavity. The concept of direct attachment involves three problem areas:

1. Voltage hold-off (on the order of 4 or 5 volts) capability of insulation materials at 2000°K.
2. Conduction heat transfer through the insulation and the resulting ΔT.

3. Compatibility of insulation materials with the converter emitter materials.

Our experimental effort was confined to the investigation of these three areas. The initial results indicated:

1. Voltage hold-off Al_2O_3 at temperatures in the range of 1800°K to 2000°K deteriorated during 200 hours of continuous operation.
2. A temperature drop of approximately 80°C was (observed) in the insulating material for a calculated heat flow of 70 watts per square cm.
3. A moderate to considerable interaction was observed between insulation material and converter material.

On the basis of item 3 above, developmental effort on the direct attachment of series converters to an energy absorbing cavity was terminated for the remainder of the program.

The materials preparation, experimental measurements and calculations, and experimental results are given in the following paragraphs.

2.2.1 Materials Preparation

Two assemblies were fabricated for studying the feasibility of electrically insulating a metal structure at temperatures of 1800°K to 2000°K. Tungsten was chosen to be the metal structure, and pure alumina was the insulating material. The choice was dictated in part by the minimum interaction of tungsten-alumina as observed in the direct-contact spacing investigations.

Two samples of heavily swaged tungsten bar at 99.9 percent theoretical density were plasma sprayed over an inch length with 0.020 inches of 100 percent pure alumina. This area was in turn plasma sprayed with 0.050 inches tungsten (resulting in a structure as shown in Fig. 2-12) where the center slug functions as the emitter, and the tungsten coating as the cavity wall. Plasma Kote Inc. of Los Angeles performed all plasma spraying operations required for the fabrication of these two assemblies.

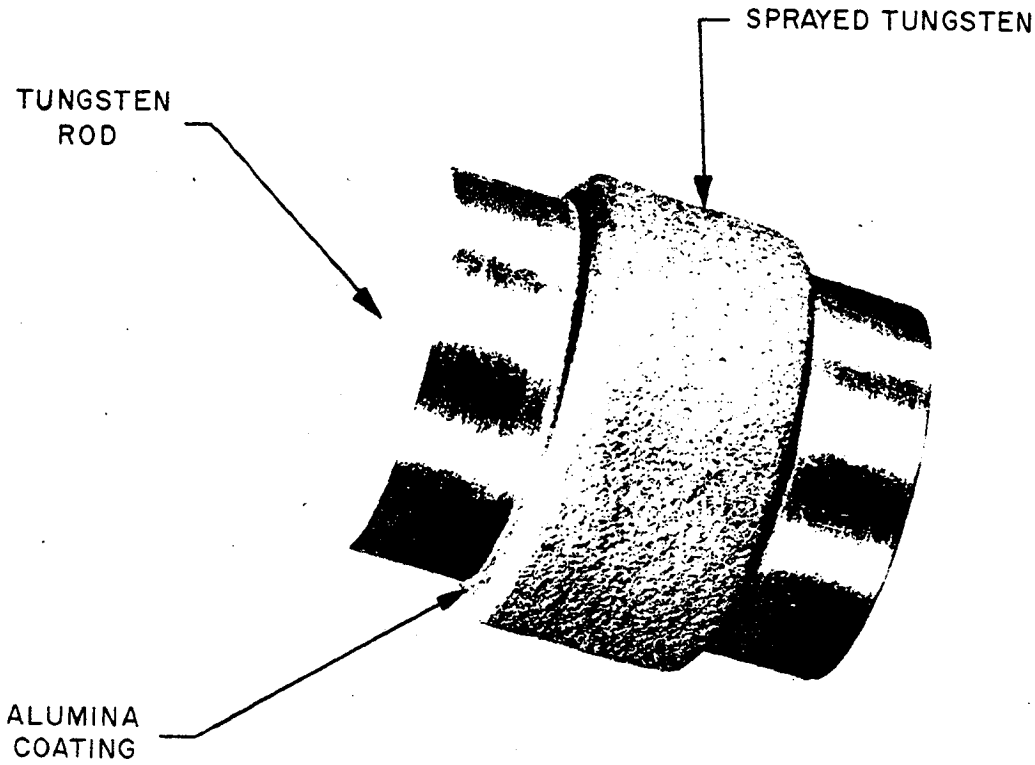

FIG. 2-2 ELECTRICAL INSULATION ASSEMBLY

The initial impedance of this structure measured a few megohms. Upon electron bombardment in vacuo the tungsten began to discolor and the system pressure steadily increased. It was concluded that the alumina would require sintering in an atmosphere of dry hydrogen to reduce any moisture or contaminants introduced in the spraying process. Both structures were hydrogen fired at 1800°C for 10 hours at a dew point of -70°F. Impedance measurements were made on both assemblies after treatment the coating resistance was essentially infinite.

2.2.2 Experimental Measurements and Calculations

The center slug of tungsten was electron bombarded with a counter wound pancake heater to insure uniform heating. The temperature of this slug was measured by viewing a hohlraum of 10:1 depth to diameter ratio. Temperature of the outer tungsten sleeve, which simulated the wall cavity, was measured with a platinum/platinum-10 percent rhodium thermocouple, and monitored with a pyrometer.

At temperature, the electrical characteristics of the assemblies were obtained by: (1) application of dc voltages from a battery or power supply, and (2) application of ac voltages from a stepdown transformer. The data taken from either method were consistent with each other, and at a fixed temperature an entire set of volt-ampere data were obtained.

The resistance of the insulating layer of alumina, at approximately 1500°C, was estimated from the values currently available in the literature (Ref. 1).

From expression of resistance in terms of the geometry,

$$R = \frac{\rho L}{A}$$

where ρ = the resistivity of the material at temperature (in the case of Al_2O_3 it was taken to be 10^5 ohm-cm at 1500°C)

L = the path length of current flow = 0.05 cm

A = the cross section of area supporting current flow = $2.4\pi cm^2$

For the dimensions of the investigated assemblies,

$$R = \frac{10^5 \times 5 \times 10^{-2}}{\pi \times 2 \times 1.2} \simeq \frac{5 \times 10^3}{2.4\pi}$$

$$R \approx 660\Omega$$

This calculated resistance agreed fairly well with the measured resistance of 1×10^3 ohms at a temperature near 1500°C, taken at the start of the initial 100 hours test of the second structure.

2.2.3 Experimental Results

The first assembly test ended in catastrophic failure, when a voltage breakdown occurred and allowed an estimated two amperes of current to be drawn through the insulator. The structure suffered permanent damage from this breakdown as indicated by a direct short across the alumina at room temperature. Prior to failure, a satisfactory amount of heat transfer data were obtained from the assembly that is summarized in Table 2-2. The volt-ampere data acquired from the first structure are subject to some question since the current drawn through the insulator, assumed ohmic in nature, displayed a preferential direction of flow as shown in Fig. 2-13.

The second assembly was tested over a period of 200 hours. During the first 100 hours of test, volt-ampere data were obtained by ac and dc methods. Figures 2-14 through 2-19 are a record of raw data obtained. The resistance of the structure, at a rod temperature under the coating of 1587°C was on the order of 1×10^3 ohms when the 100 hour test commenced. A constant dc voltage of 2 volts was applied across the insulation material at the start of the test.

TABLE 2-2

ELECTRICAL INSULATION THERMAL CHARACTERISTICS

Hohlraum	Surface Next to Hohlraum	Δt Surface Vs. True	Surface Middle	Middle Surface + Correction	T/C	Δt Through Coating	Heat Conducted Through Coating
1345°C	1235°C	110°C	1198°C	1284°C	1216°C	68°C	57 watts/cm^2
1443	1333	110	1276	1371	1295	76	66
1525	1390	135	1336	1439	1370	69	57
1620	1465	155	1405	1515	1437	78	66
1742	1569	173	1483	1606	1516	90	75

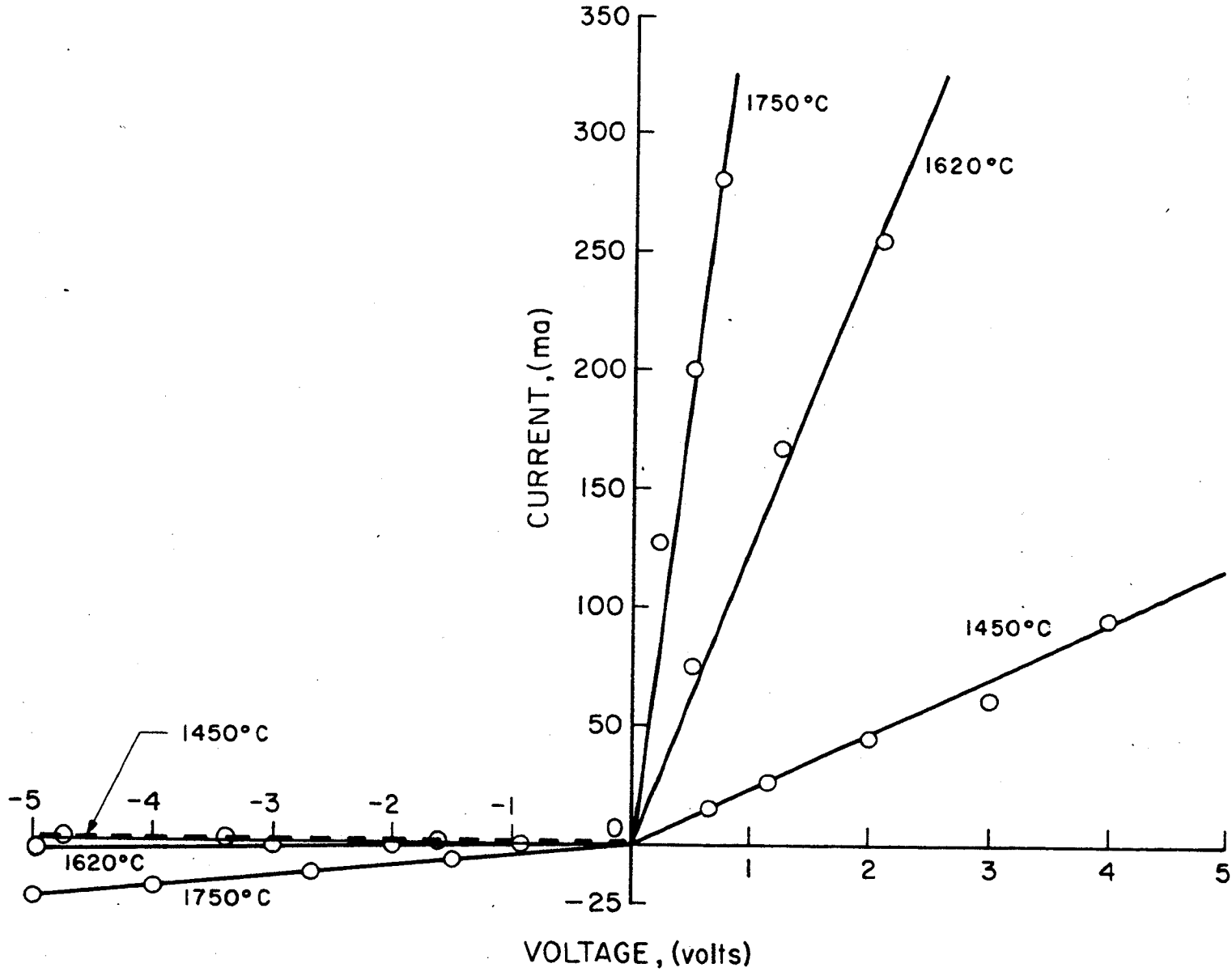

FIG. 2-1[illegible] ELECTRICAL INSULATION DATA FROM THE FIRST EXPERIMENTAL ASSEMBLY. DC DATA

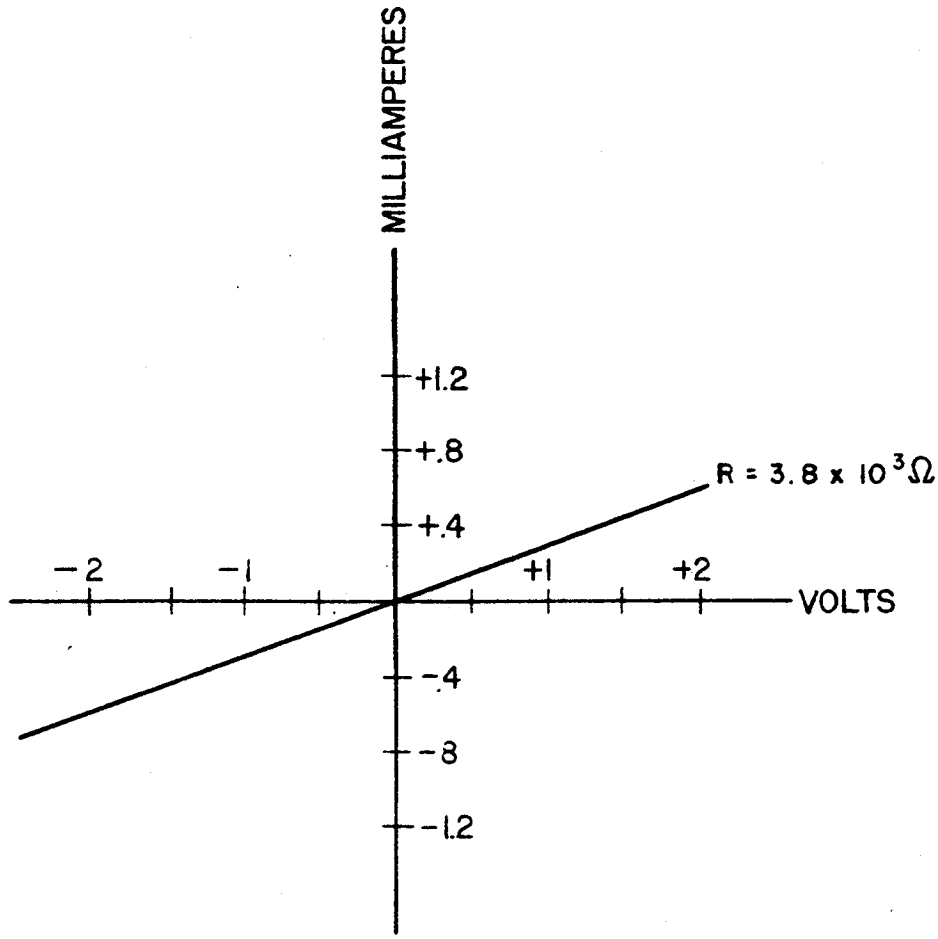

FIG. 2-14 0.7 HOURS I-V CHARACTERISTIC ROD TEMPERATURE UNDER COATING 1170°C, AC DATA

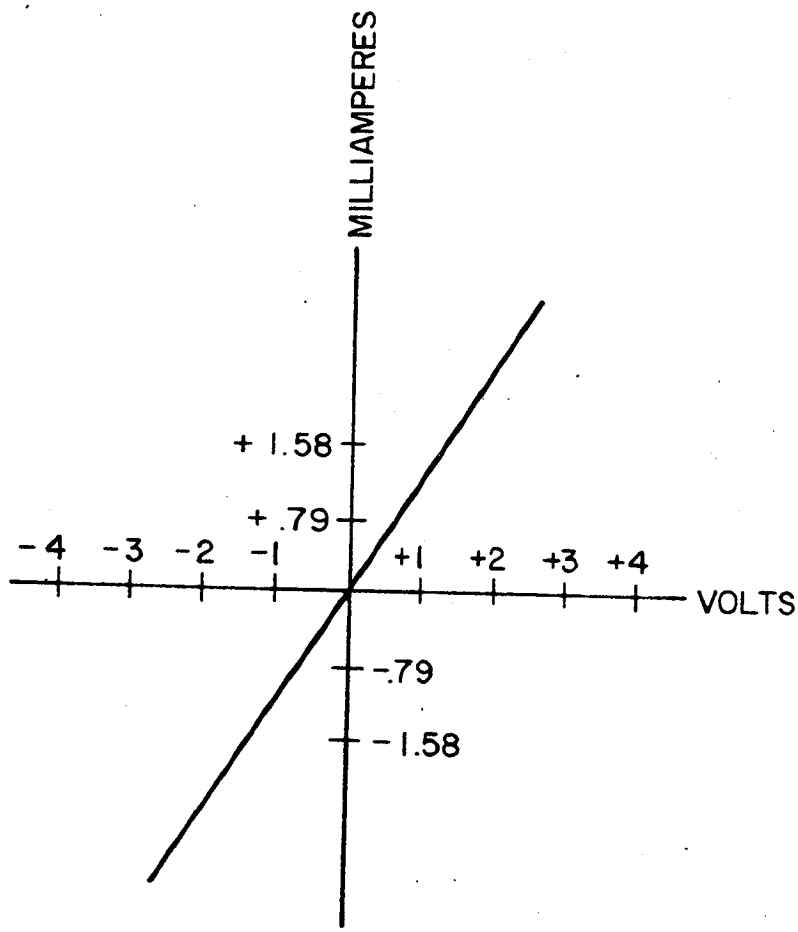

FIG. 2-15 1 HOUR I-V CHARACTERISTIC ROD TEMPERATURE UNDER COATING 1366°C. AC DATA

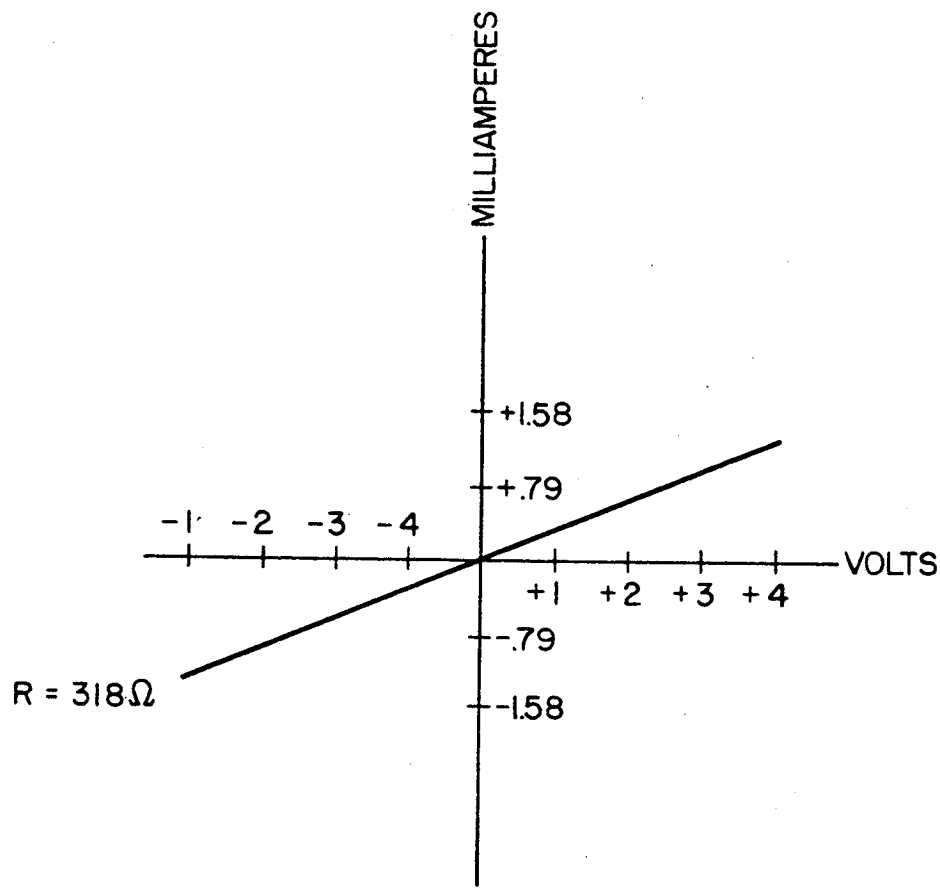

FIG. 2-16 2.1 HOURS I-V CHARACTERISTIC ROD TEMPERATURE UNDER COATING 1464°C. AC DATA

7369438

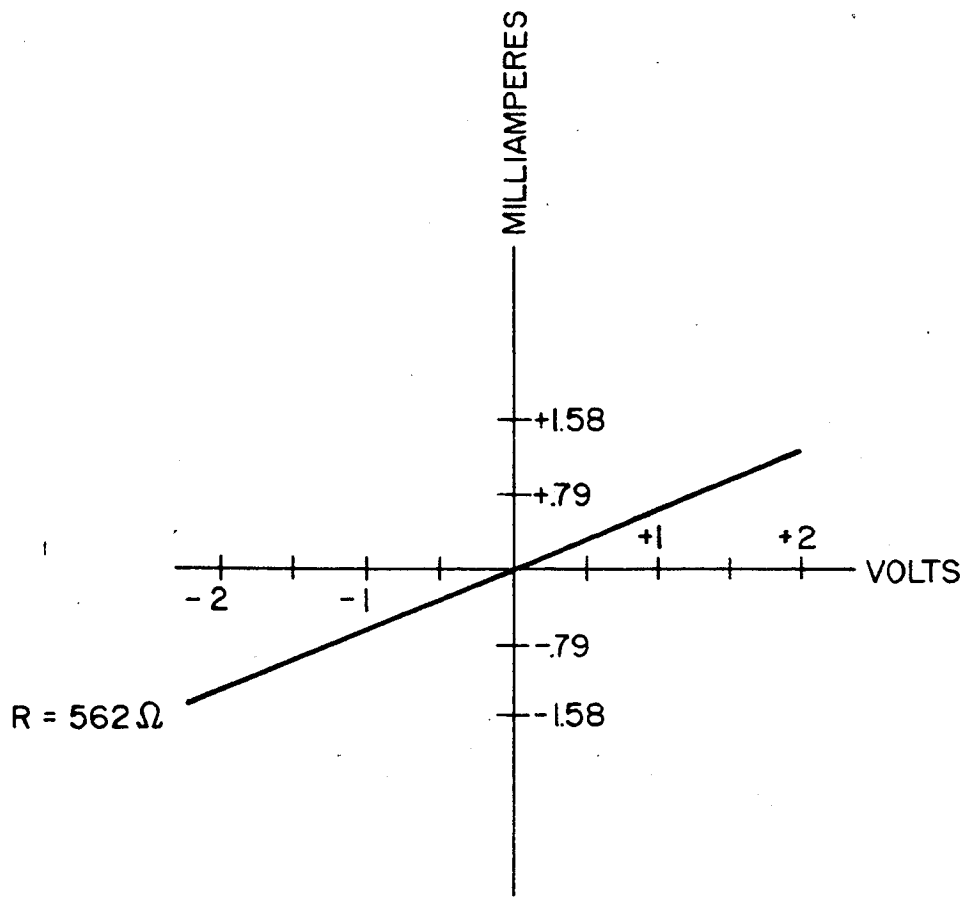

FIG. 2-17 3 HOURS CHARACTERISTIC ROD TEMPERATURE UNDER COOLING 1462°C. AC DATA

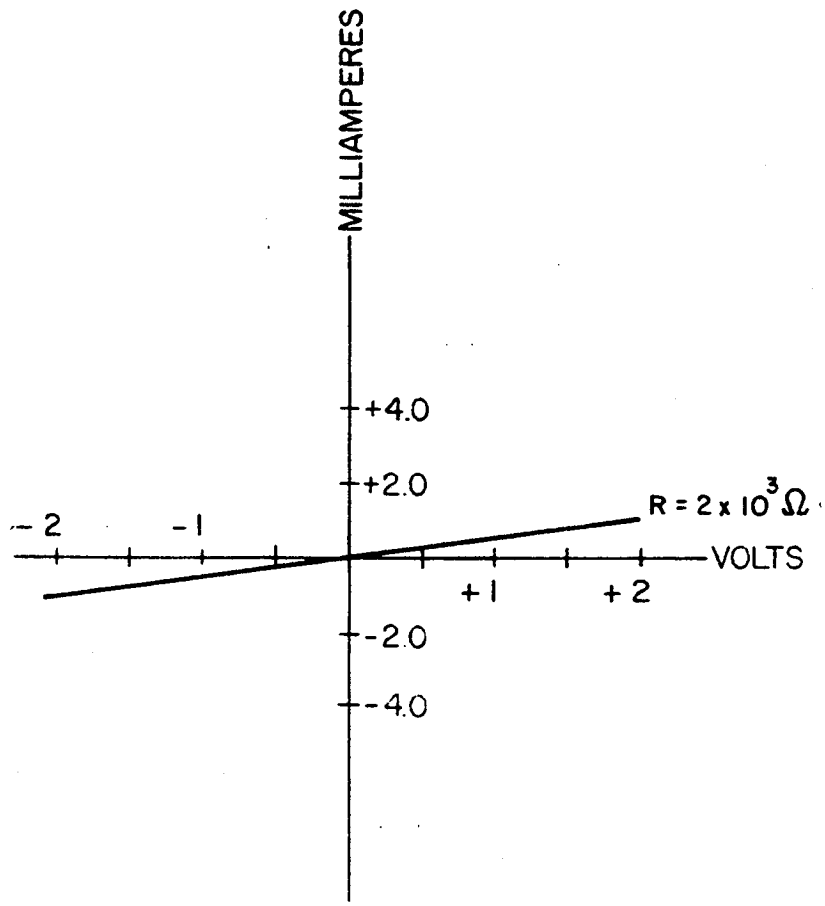

FIG. 2-18 4 HOURS I-V CHARACTERISTIC ROD TEMPERATURE UNDER COATING 1467°C, AC DATA

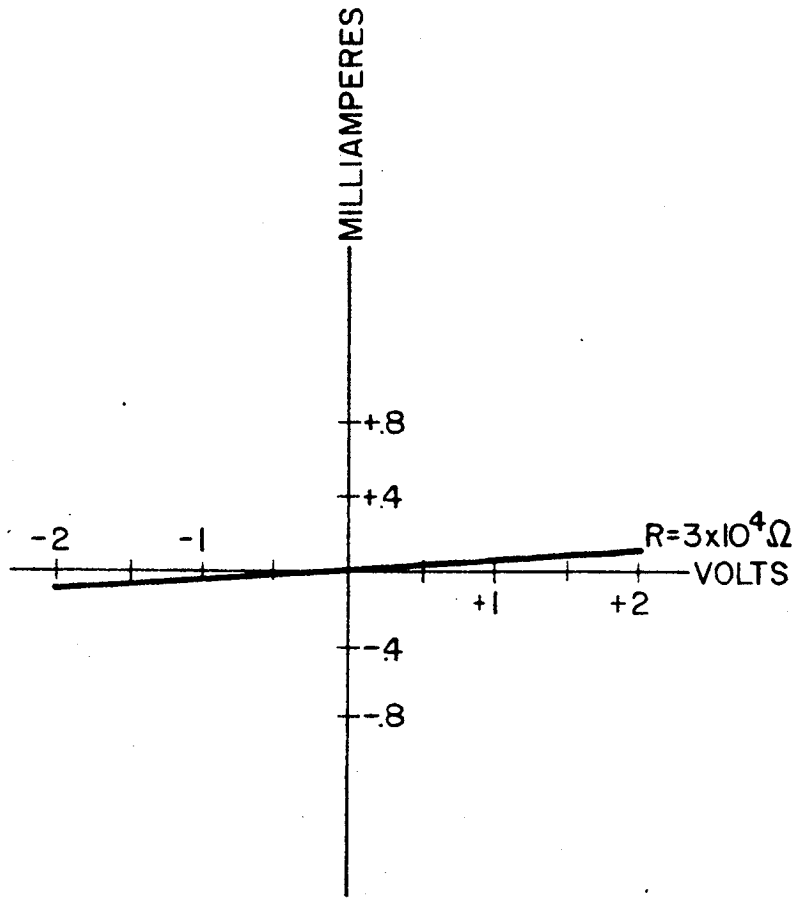

FIG. 2-19 7 HOURS I-V CHARACTERISTIC ROD TEMPERATURE UNDER COATING 1587°C, AC DATA

After 50 hours the voltage was increased to 4 volts. At this voltage, the current drawn through the insulation was on the order of 2 milliamperes after 100 hours of test. The resistance was computed to be 1×10^3 ohms. The rod temperature was 1730°C at the hohlraum, and 1590°C under the coating during the test duration.

TABLE 2-3

DEGRADATION OF INSULATOR RESISTANCE DURING SECOND 100 HOUR TEST

Hohlraum rod temperature (°C)	Elapsed time	Applied voltage	Current leakage	Approximate resistance
1560	0 hours	2	2 ma	1000Ω
1580	20 hours	2	22 ma	90Ω
1531	44 hours	2	80 ma	25Ω
1510	91 hours	2	84 ma	24Ω
1485	95 hours	2	86 ma	23Ω

During the next 100 hours of test, this assembly was maintained at an approximate temperature (hohlraum) of 1800°K. A potential of 2 volts was continuously applied across the alumina insulation. A steady decrease of the insulation resistance as a function of time was observed. Table 2-3 illustrates this deterioration. The final value of 23 ohms resistance at temperature is still useful, for some applications, considering that at 5 volts potential difference a current leakage of 250 milliamperes is small compared to converter currents of 25 to 80 amperes.

A metallurgical examination of the 200 hour test specimen was undertaken to determine the integrity of the various structure interfaces. Figures 2-20 through 2-23 are photomicrographs of the interfaces and areas of interest.

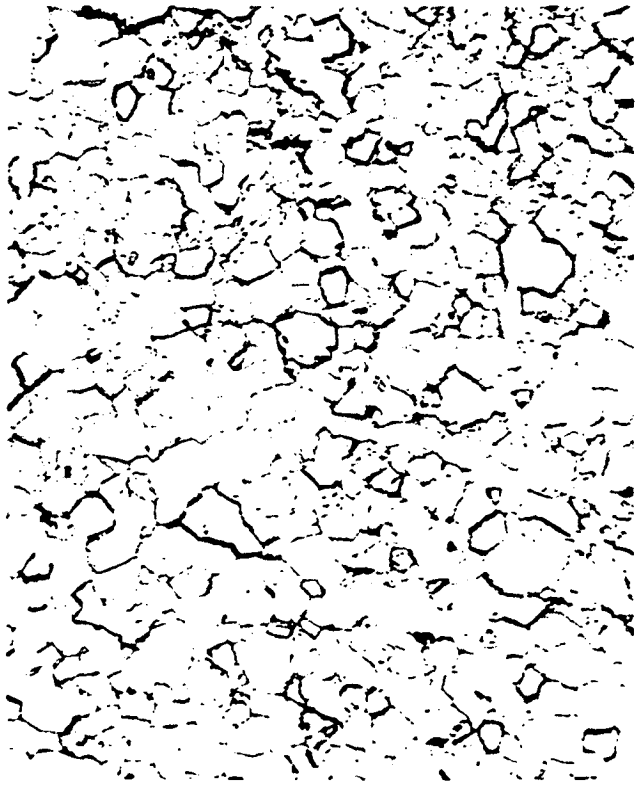

. 2 2

FIG. 2-21

TUNGSTEN ROD-PLASMA SPRAYED ALUMINA INTERFACE MAG. 300X

FIG. 2-22

SPRAYED TUNGSTEN-SPRAYED ALUMINA INTERFACE MAG. 300X

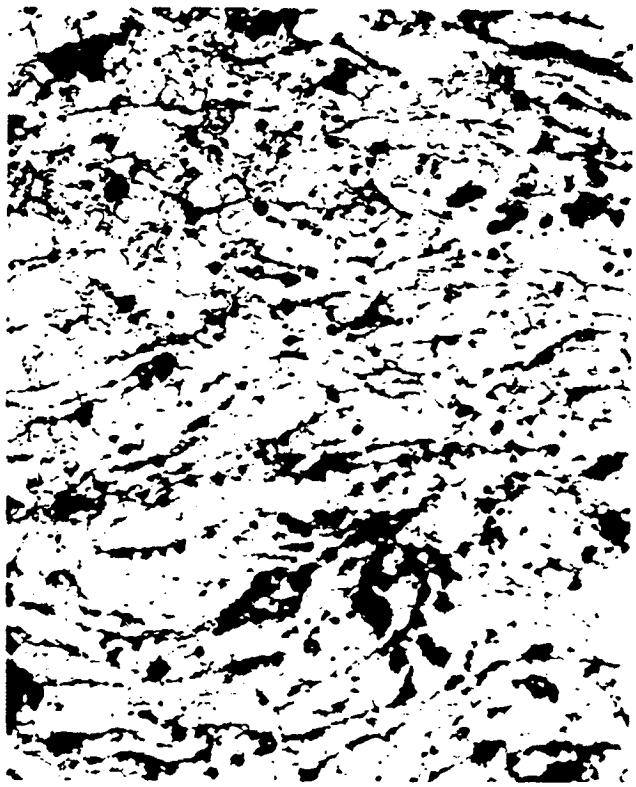

FIG. 2-23 SPRAYED TUNGSTEN COATING
MAG. 300X

2.3 Cesium Reservoir Tubulation Design

An investigation was conducted to select the materials, establish the best geometry and develop a suitable joining technique for the cesium reservoir tubulation. Generally, the reservoir tubulation must support a sharp temperature gradient between the collector and reservoir to establish a unique cesium vapor pressure in the converter. The tubulation material must be capable of high-temperature operation without mechanical failure. In addition, the tubulation must be joined to both the reservoir and collector without embrittling either structure or reducing their high-temperature stability through the use of improper or low-temperature braze materials.

Heat transfer calculations supporting the tubulation design are presented in detail in the following text. There is excellent agreement between these calculations and the experimental data. The materials preparation, experimental measurements, and experimental results are reported in the following paragraphs.

2.3.1 Materials Preparation

Niobium was selected for the reservoir tubulation material because:

1. It has excellent high-temperature strength.
2. It has no material phase changes through which thermal cycling could induce mechanical failure.
3. It has a low value of thermal conductivity that reduces the conduction heat transfer from the collector to reservoir.
4. Niobium has "gattering" properties for active gases that might conceivably still be in the device during operation.

Tantalum could also be used as a reservoir tubulation material for the above reasons. Nickel was considered but is not recommended since it experiences a phase change near 400°C. This phase change can produce mechanical failure during continuous thermal cycling. Copper is not recommended because it has a high value of thermal conductivity and also has poor high temperature strength.

A molybdenum slug, simulating a collector, was machined to receive the niobium tube. All materials were chemically cleaned in accordance with the cleaning specification in the appendix. The parts were close-fitted and the molybdenum-cobalt braze powder (100 mesh) was packed around the inner face. The braze was attempted in a high vacuum bell jar atmosphere using rf induction heating. The assembly was held at 1600°C for 3 minutes. The resulting braze indicated that the molybdenum-cobalt did not adequately wet the niobium tubulation. It was assumed that the surface oxides/nitrides of niobium were not reduced during the braze operation. For this reason, titanium was chosen for a test braze. The braze conditions were 1650°C for 3 minutes. The resultant braze was highly successful as evidenced by the complete wetting of the niobium, and a leak tight joint between the molybdenum and niobium. The copper reservoir was heli-arced to the niobium tubulation. Copper-tantalum heli-arc joining is also a common technique requiring no special setup other than a purged dry box. The atmosphere purity, rotation speeds and current setting are discussed elsewhere in this report. A nichrome sheathed heater wire, obtained from Aeropak Co., was B.T. brazed onto the copper reservoir, and coated with 0.010 inches of Rokide "C" by the L.A. Metalizing Company of Los Angeles. The copper reservoir was chemically cleaned and vacuum fired prior to applying Rokide.

After the fabrication techniques were established, the niobium tubulation was machined to a length of 0.8 inches and a wall thickness of 0.008-inches. These dimensions were calculated to be approximately correct for limiting the heat transfer to the cesium reservoir. The calculations are explained in detail in the following paragraphs.

2.3.2 Experimental Measurements and Calculations

Chromel-alumel thermocouples which were used to measure the heat choke temperature profile were spot-welded to the niobium tubulation at accurately measured intervals. Figure 2-24 illustrates

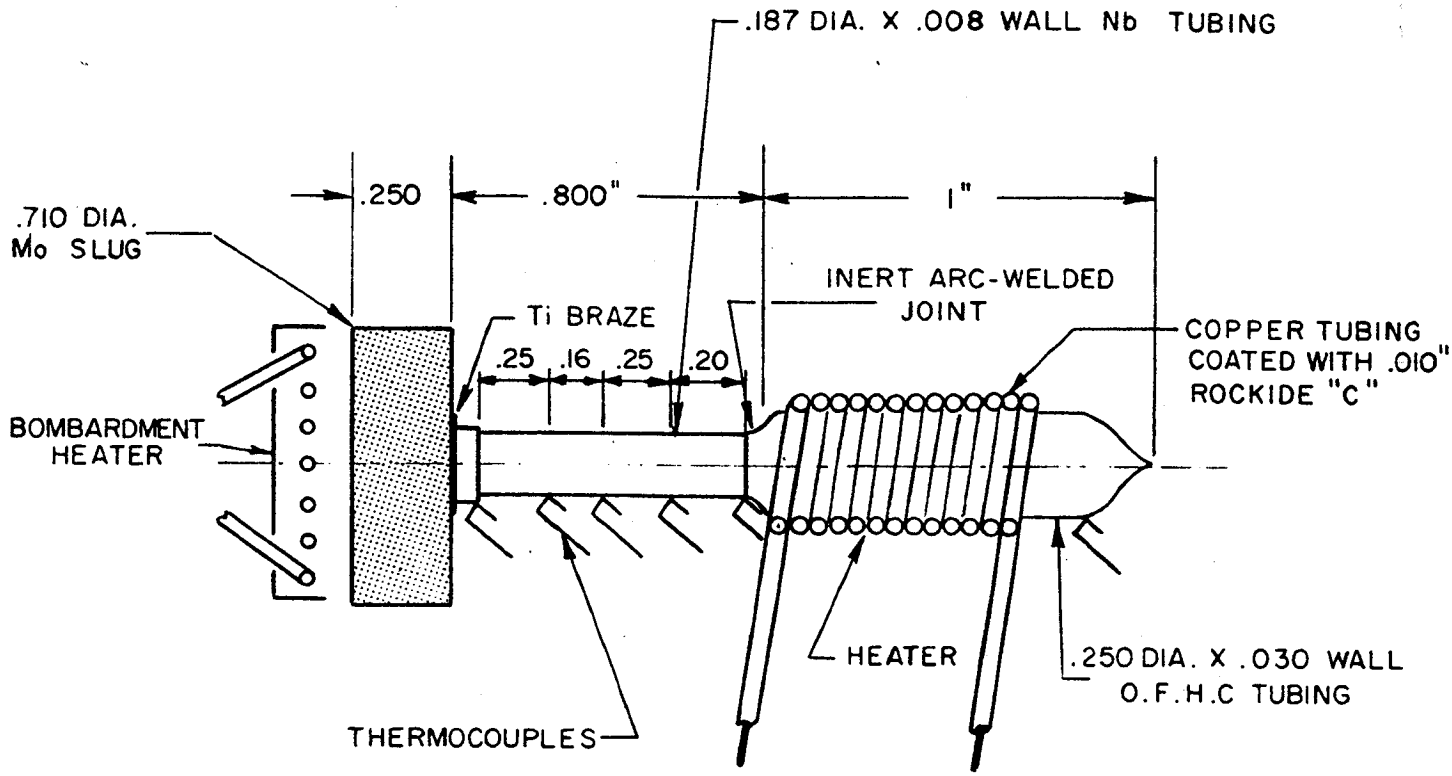

FIG. 2-24 CESIUM RESERVOIR TABULATION AND HEATER

7367618

the experimental assembly. Chromel-alumel base plate lead throughs were utilized to eliminate erroneous thermal voltages generated at "hot" junctions inside the bell jar. The effect of having "hot" junctions (that is, thermocouple connections to heated posts, or leads in a Bell jar of material different than the couple) was demonstrated by the comparison of the output from two thermocouples placed on the same heated junction. The output of one of the couples which employed a chromel-copper "hot" junction heated to 41°C had an error of 1 millivolt. On a cesium reservoir measurement this would be equivalent to an error difference of 2 mm Hg at 2 mm Hg pressure.

Supplementing the experimental work detailed calculations were performed to determine the heat balance of the reservoir. The results of these calculations are given in Table 2-4. The analysis proceeds as follows: Radiation losses from the tubulation are neglected due to the low values of the emissivity and temperature envolved for the clean portion of the heat choke. Heat transfer by conduction from the collector to the reservoir is given by the equation,

$$Q = KA\ \Delta T/\Delta X$$

where Q = the heat flow conducted in watts

K = the thermal conductivity of the material

A = the cross sectional area supporting heat flow

$\Delta T/\Delta X$ = the thermal gradient that drives the heat flow

A specific calculation for 0.008 inch wall now in tubulation 1-inch in length attached to a collector at a temperature of 700°C and a reservoir at a temperature of 350°C, proceeds as follows:

$$Q = KA\Delta T/\Delta X$$

$$Q = 1.5 \times 10^{-1} \times 4.186 \times 0.028 \text{ sq. cm} \times 350^{\circ}C/2.54$$

$$Q = 2.44 \text{ watts}$$

This amount of heat is in turn rejected by the Rokide coating (ε = 0.8) on the reservoir, as follows:

TABLE 2-4

HEAT TRANSFER SUMMARY OF RESERVOIR TUBULATION CALCULATIONS
(1 inch length heat choke)

Wall thickness (inches)	Cross sectional area (cm^2)	Temperature coll. (^oC)	Temperature res. (^oC)	Q (watt) 0.004	0.008	0.015	Δt (^oC)
0.004	0.014						
0.008	0.028						
0.015	0.053						
		800	300	1.81	3.49	6.65	500
		700	300	1.45	2.79	5.35	400
		600	300	1.13	2.18	4.19	300
		800	350	1.62	3.15	6.04	450
		700	350	1.26	2.44	4.70	350
		600	350	0.91	1.78	3.36	250
		800	400	1.45	2.79	5.35	400
		700	400	1.13	2.18	4.19	300
		600	400	0.72	1.39	2.68	200

$$Q = \epsilon \sigma A T^4$$

$$Q = 0.8 \times 3.75 \text{ sq. cm} \times 0.8 \text{ watts/sq. cm}$$

$$Q = 2.35 \text{ watts}$$

A balance is therefore achieved with the reservoir radiating the conducted heat from the collector.

The calculations in Table 2-4 were all made for a length of 1 inch (2.54 cm). The heat conduction for any particular tubulation length may be computed by directly dividing Q for 1 inch by the desired length. Likewise, a wall thickness of dimensions different from 0.008, 0.004, or 0.015 inches would require a similar "scaling" process whereby the Q rom the calculations in Table 2-4 would be modified by a direct multiplication. Likewise, a material different from niobium would require scaling the calculations in Table 2-4 for the appropriate K value.

2.3.3 Experimental Results

The data from the reservoir tubulation experiments are plotted in Figs. 2-25, 2-26, and 2-27 for simulated collector temperatures of 600, 700, and 800°C. The power input necessary to achieve a particular reservoir temperature is included in each figure. The reservoir temperature and power input data from operating converters have essentially verified these data except where there was poor thermal contact between reservoir heater wire and the reservoir.

2.4 Collector Emissivity Investigations

The formation of black deposits on the surface of converter collectors has been observed and reported by several investigators. These coatings were analyzed and found to be predominately composed of (1) impurities, emitter material, and cesium; (2) emitter material and cesium. In the first case, we have shown these impurities most probably originate from improperly processed emitter structures. If the converter emitter is outgased in the final converter assembly contaminants evaporated from the emitter are condensed on the collector

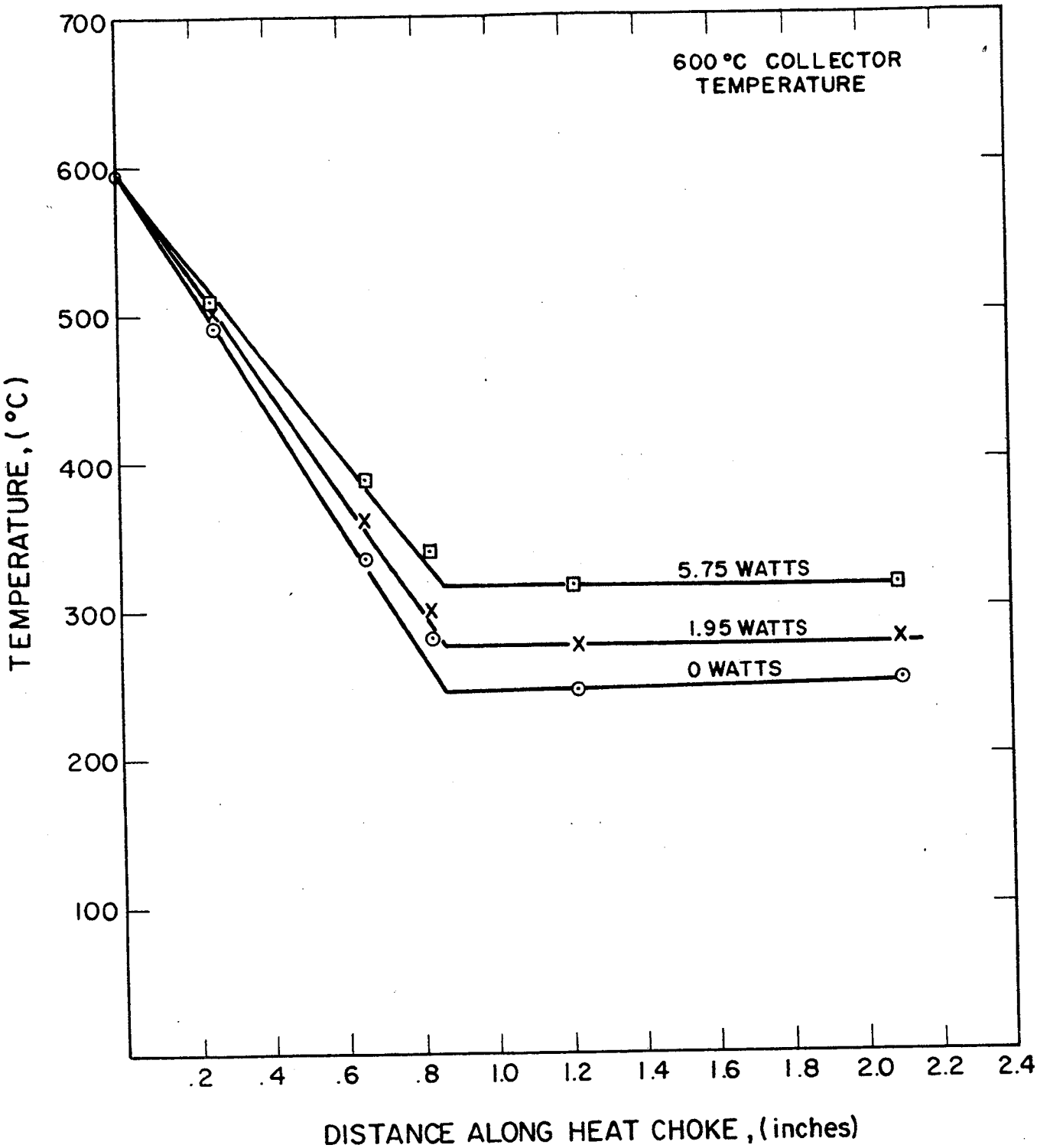

FIG. 2-25 CESIUM RESERVOIR TUBULATION EXPERIMENT COLLECTOR AT 600°C

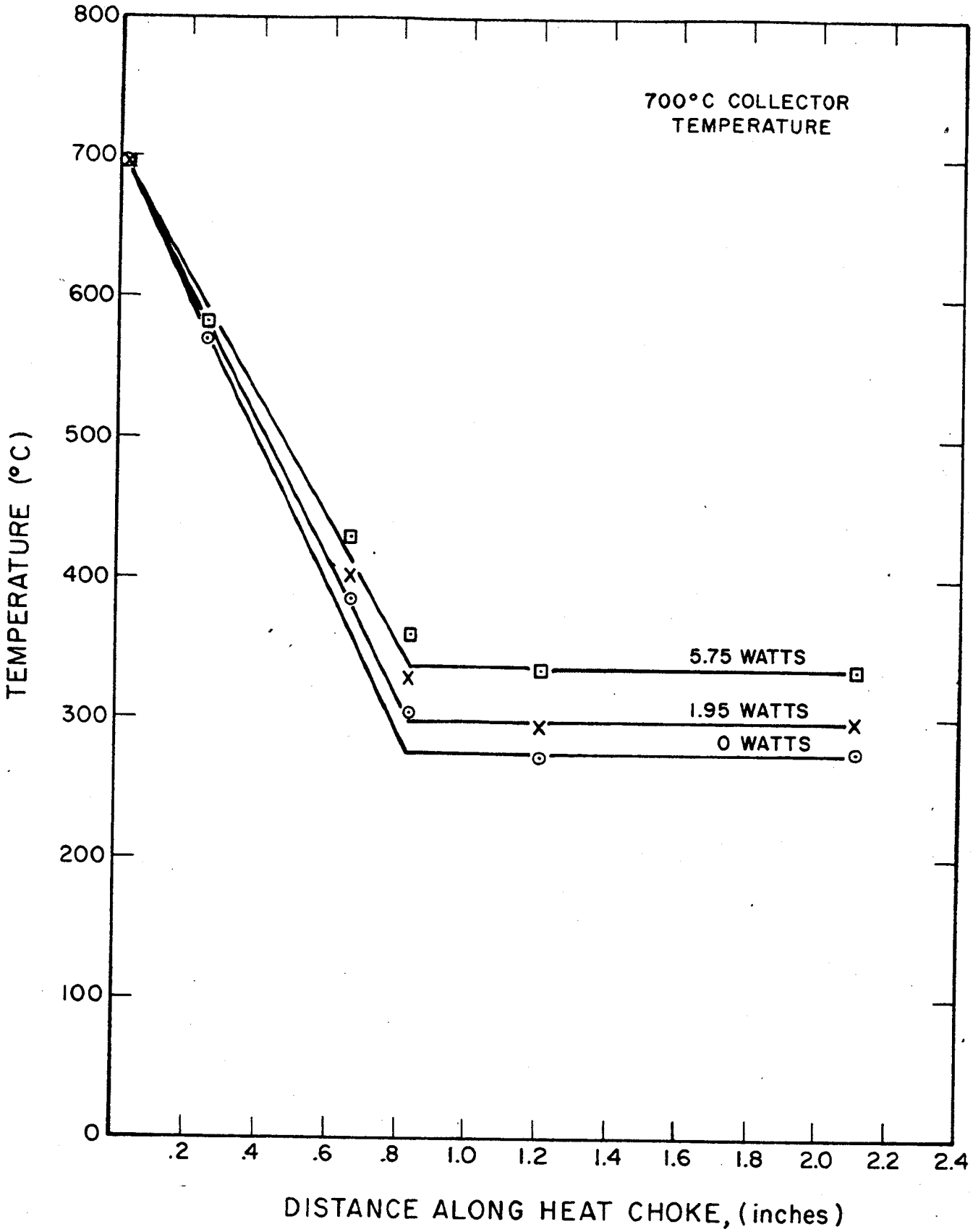

FIG. 2-26 CESIUM RESERVOIR TUBULATION EXPERIMENT COLLECTOR AT 700°C

368729

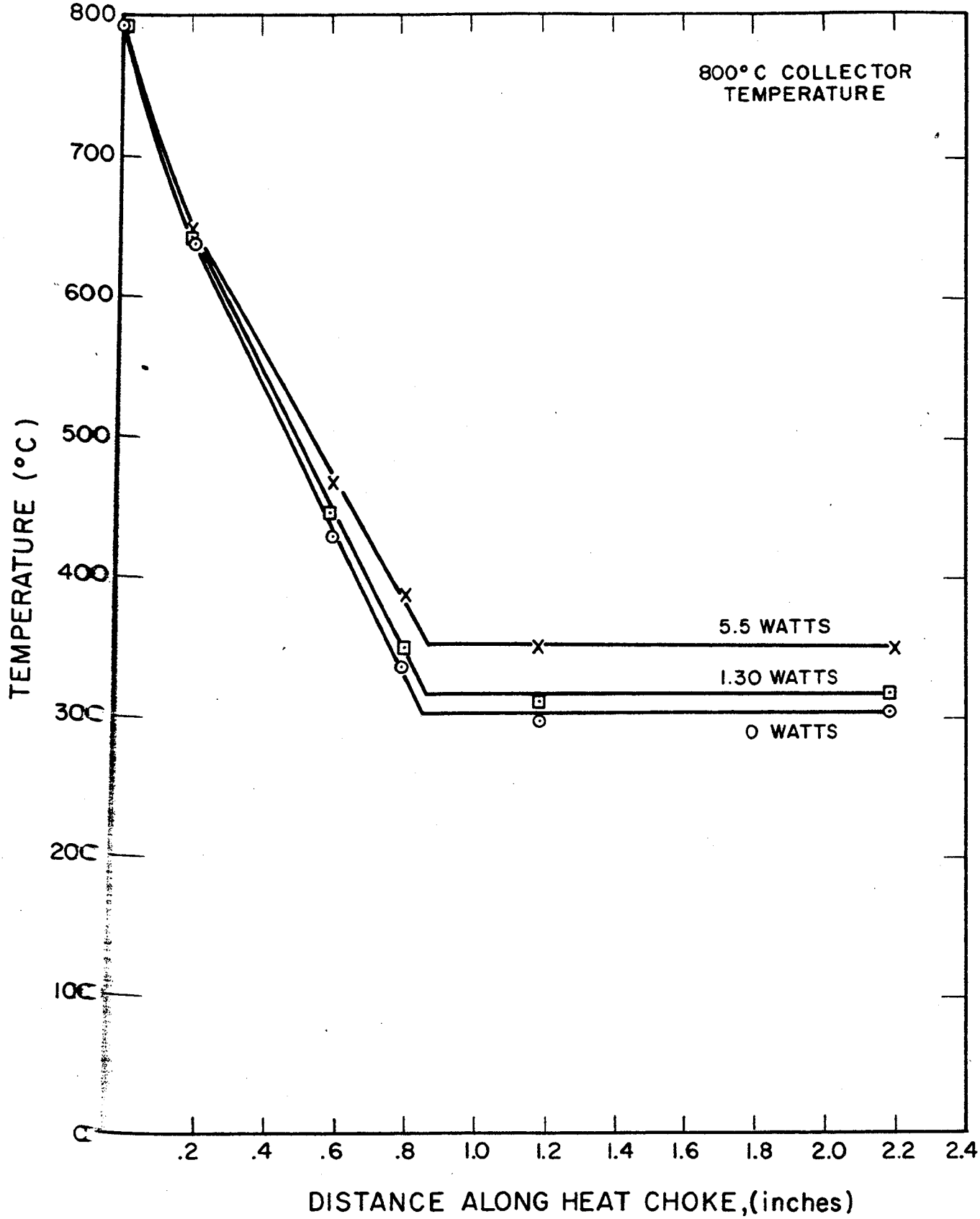

FIG. 2-27 CESIUM RESERVOIR TUBULATION EXPERIMENT COLLECTOR AT 800°C

surface giving rise to coatings that contain silicon, nickel, copper, iron, chromium, etc. It is also possible that the use of impure cesium is a source of contamination which would promote collector deposits.

In the second case (emitter material and cesium in the deposit) we feel that the emitter temperature may be too high for long term (thousands of hours) operation. From evaporation rate calculations which acknowledge a factor of 8 or less suppression by a high pressure cesium vapor, we contend that tantalum should be operated at a temperature of 2000°K or less for high converter efficiency and long life (see Fig. 2-28).

EOS No. 1 converter was operated for 200 hours at 2000°K to observe any possible evidence of collector coatings. This diode was positively spaced with a tungsten ring-alumina ceramic insert which suffered gross interaction masking any lesser effect of emitter material evaporation. Figure 2-29 illustrates the areas of interaction on the collector. The inset in the collector which retained the alumina ring was decorated with a white, powdery substance presumed to be decomposed alumina. The collector face was covered with a dark, tightly adhering layer which may have contained condensed droplets of aluminum as a result of the ceramic reduction. Aluminum has been identified on the surface of converter No. 5 which also was positively spaced (Ref. 2).

A smooth, tightly adhering collector deposit may not have the same emissive properties as an amorphous or flaky deposit. This is hypothesis, but the grounds for accepting it have come from the optical industry where black coatings have been fabricated which have both high and low emissivity values. The emissivity of a material appears to be a function of the surface smoothness rather than its color in the visible spectrum.

An additional and perhaps more serious consequence of collector coatings is the change in collector work function which may result from such coatings. EOS data indicates that a work function of approximately 1.5 ev may be achieved for cesium on clean polycrystalline

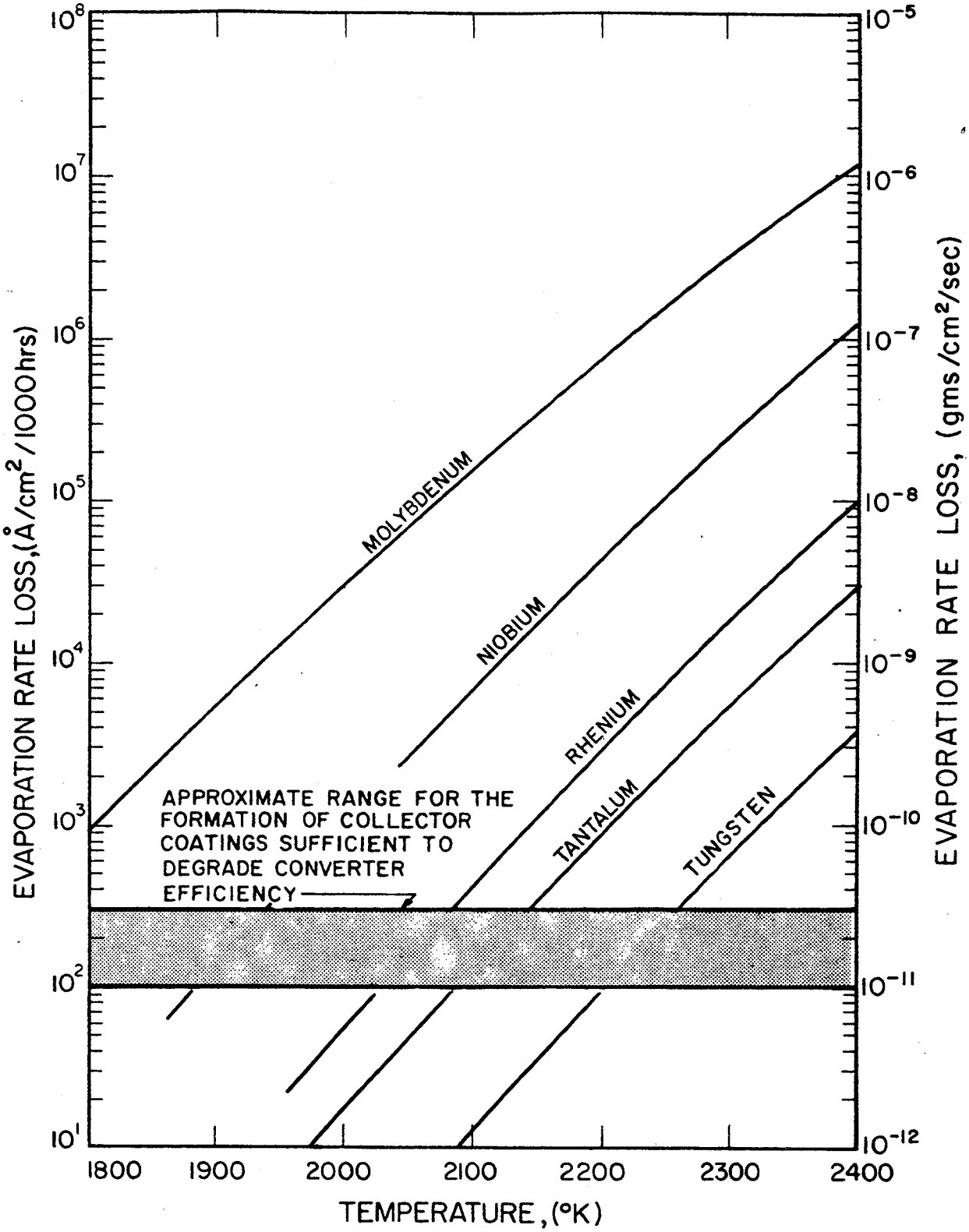

FIG. 2-28 EVAPORATION RATE LOSS FROM SELECTED EMITTER MATERIALS

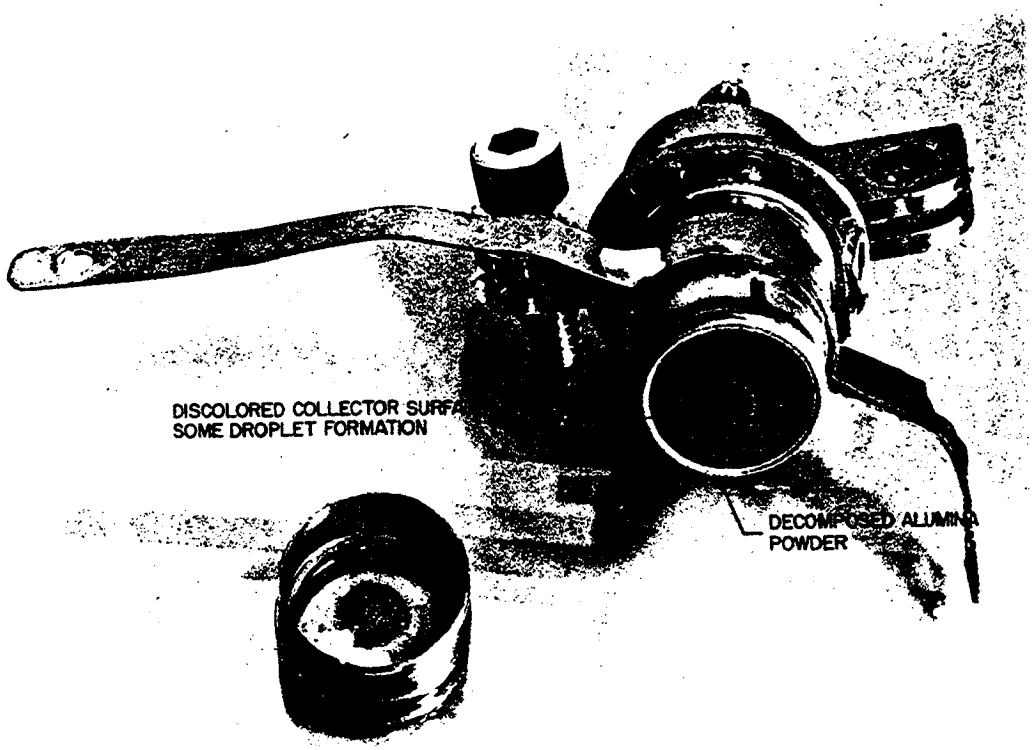

FIG. 2-21 COLLECTOR EMISSIVITY INVESTIGATION

molybdenum. The minimum work function achievable on the same molybdenum with coatings appears to be closer to 1.7 to 1.8 ev. This difference shows up as a direct 0.2 to 0.3 volt reduction in converter output voltage at a fixed current.

3. CONVERTER DESIGN, FABRICATION, AND TEST

The design approach and materials combinations selected for the initial converter fabrication effort on this contract were arrived at through careful consideration of the contract design objectives and by attempts to eliminate the weak points in other designs that are state of the art. The converter design objectives of this contract are nominally to design, fabricate, test and deliver (to JPL) cesium-vapor thermionic converters that have the following characteristics:

1. power density 10 to 15 watts/cm^2
2. efficiency 15 to 20 percent
3. output voltage 0.8 to 1.0 volts
4. life (minimum) capable of 1000 hours
5. $T_{emitter} = 2000^{\circ}K$
6. $T_{collector} = 1100^{\circ}K$

Converters No. 1 through No. 6 employed a composite spacing technique of a tungsten ring-ceramic washer assembly between emitter and collector. These converters have suffered shorting problems and/or materials interaction, thus limiting their useful life and efficiency. Five of these converters achieved a power output ranging from 12 watts to 24 watts, with a well-defined emission area of 2 square centimeters. The converter data on the first five were obtained primarily by ac sweep methods since a poor radiator to collector thermal bond made it impossible to transfer the heat away from the collector surface under dc conditions. This latter situation resulted in collector temperature approaching $1200^{\circ}C$ under high current dc conditions. If it had been possible to keep the collector surface temperature in the $800^{\circ}C$ range, the dc data would have been identical with the ac data.

Converter No. 7, No. 8, and No. 9 were fabricated without positive spacing between electrodes. The output power from these diodes was

approximately 25 watts as measured by ac sweep methods and 20 watts by dc methods. The lifetime and performance of these last two diodes should exceed any of the first six.

A supplement to this report will be issued 15 September that will complete the converter design calculations and fabrication technique as required.

The following section discusses the design and fabrication of component parts and subassemblies; detailed information is reported on cleaning, machining, welding, brazing, and jigging of various converter parts, and a section of test data and analysis of performance is included.

3.1 Design and Fabrication (with Manufacturing and Engineering Drawings) of Converter Components

3.1.1 Emitter

Converters No. 1 through No. 6 employed a tantalum emitter to the exact specification in Drawing 12102 (see Appendix). Converters Nos. 7 and 8 deleted the .015-inch deep retaining groove which accommodated the tungsten spacing ring. Regardless of configuration, the treatment of these tantalum emitters has been identical.

Tantalum was chosen as an emitter material for two reasons:

1. Cesiated emission data for tantalum have appeared to be as good as the other body-centered cubic materials.
2. Evaporation rate calculations indicate that at 2000°K tantalum will evaporate less than 100 Å layers in 1000 hours. We feel that the evaporation of more than 100 Å layers of emitter material subsequently deposited on the collector deteriorates converter efficiency.

After the tantalum emitter has been machined to size and chemically cleaned in accordance with the cleaning specifications, it is machined-lapped to achieve the proper surface finish. A Strausbaugh Lap Master, model 6-J, automatic lapping machine is employed to achieve an optical finish on the active surface of the tantalum emitter. The polishing and lapping schedule for a particular emitter specimen is a function of its machined finish. However, an average lapping procedure is as follows: A lapping speed of 30 to 50 rpm is maintained during the entire operation. Pure alumina grit, mesh No. 240, No. 125, and No. 50 is employed at the operator's discretion. Linde A (particle size 0.3 microns) and Linde B (particle size 0.05 microns) are used in a final lapping operation. The overram weight varies in this schedule from 1/2 to 25 pounds. No wetting agents are employed. A slurry of

alumina and distilled water is the sole lapping compound. The surface of an emitter lapped in this manner is flat to within approximately 1/10 wavelength of the mercury greenline as determined by an optical flat. Such a finish is considerably better than would ordinarily be required for achieving a low emissivity surface. The emitter is put through a chemical cleaning procedure before use in a device.

3.1.2 Envelope

All converters fabricated on this program contained an envelope structure machined in accordance with Drawing No. 12103 (see Appendix) and processed in accordance with our cleaning specifications. The material choice for the envelope evolved from a detailed theoretical analysis of the electrical leads for a thermionic converter. This analysis and the accompanying assumptions are as follows: Let α be defined as the ratio of electrical loss to thermal loss, Δt is the temperature difference across the lead, I is the current through the lead in amperes, ρ is the electrical resisitivity in ohm-centimeters, and K is the thermal conductivity in watt/cm^{-1} $^{o}C^{-1}$. The electrical loss may be written immediately as $I^2(\rho L/A)$. The thermal loss may be written as $K\Delta t(A/L)$ when no current is flowing in the lead. When current flows, it is assumed that half the joule loss will flow in either direction. Hence, $1/2\ [I^2\rho(L/A)]$ is conducted in the wrong direction. (i.e., to the hottest end), and must be subtracted from the thermal loss without current. Therefore,

$$\alpha = \frac{I^2\rho(L/A)}{K\Delta t(A/L) - 1/2\ (I^2\rho(L/A)}$$

It is assumed in this analysis that the radiation loss is insignificant, which is a reasonable assumption for $\alpha < 0.2$. Additionally, a more exact treatment of the problem would account for the resistance varying along the lead due to a non-uniform temperature distribution.

Figure 3-1 is a plot of the thermal loss and optimum L/A lead ratio versus current drawn from the emitter for $\alpha = 0.1$. Two commonly used materials in converter fabrication, tantalum and tungsten, were reviewed for application as converter envelope materials.

Tantalum with an L/A ratio of 21 was chosen for the envelope material due to the fact that this is about optimum for an $\alpha = 0.1$ and a current of 70 amperes. The envelope was fabricated from raw stock tantalum tubing, rather than machining solid tantalum round stock. This method of fabrication produced a part of uniform wall thickness with very high yield. The machining schedule for 0.020 inch wall tantalum tubing is as follows: Cemented carbide or high-speed steel (Vascoloy Ramet grade 2A-5) was found to be the most satisfactory tool material. A cutting speed of 57 feet per minute, a tool approach angle of 30 degrees, and a tool trail angle of 45 degrees, in conjunction with a feed-finishing of 0.0008 inch maximum per revolution resulted in a controlled, and accurate machined section of tantalum tubing. Two different lathes were used with equal success. The first lathe was a South Bend 10-inch lathe, catalog No. CL8187A, with a bed length of 4 feet. The second lathe was an 11-inch Delta, model PM1778, with a bed length of 5 feet. Essential to satisfactory machined parts was the use of Squibb mineral oil as a cutting lubricant or, on operator's discretion, Basic-H cleaning solution, a special type of liquid detergent having a PH of 7. Collapsing of the tantalum tube during machining operations was prevented by the insertion of a stainless steel rod of tight-sliding fit within the tube. The entire assembly is chucked into a collet before machining and indicated to within 0.0005 inch true on the diameter.

3.1.3 Envelope Flange

Niobium was chosen as the envelope flange material (see Drawing No. 12104 in the Appendix), primarily because it has a coefficient of thermal expansion that is very close to that of high density alumina. The material is formed by metal spinning. At present

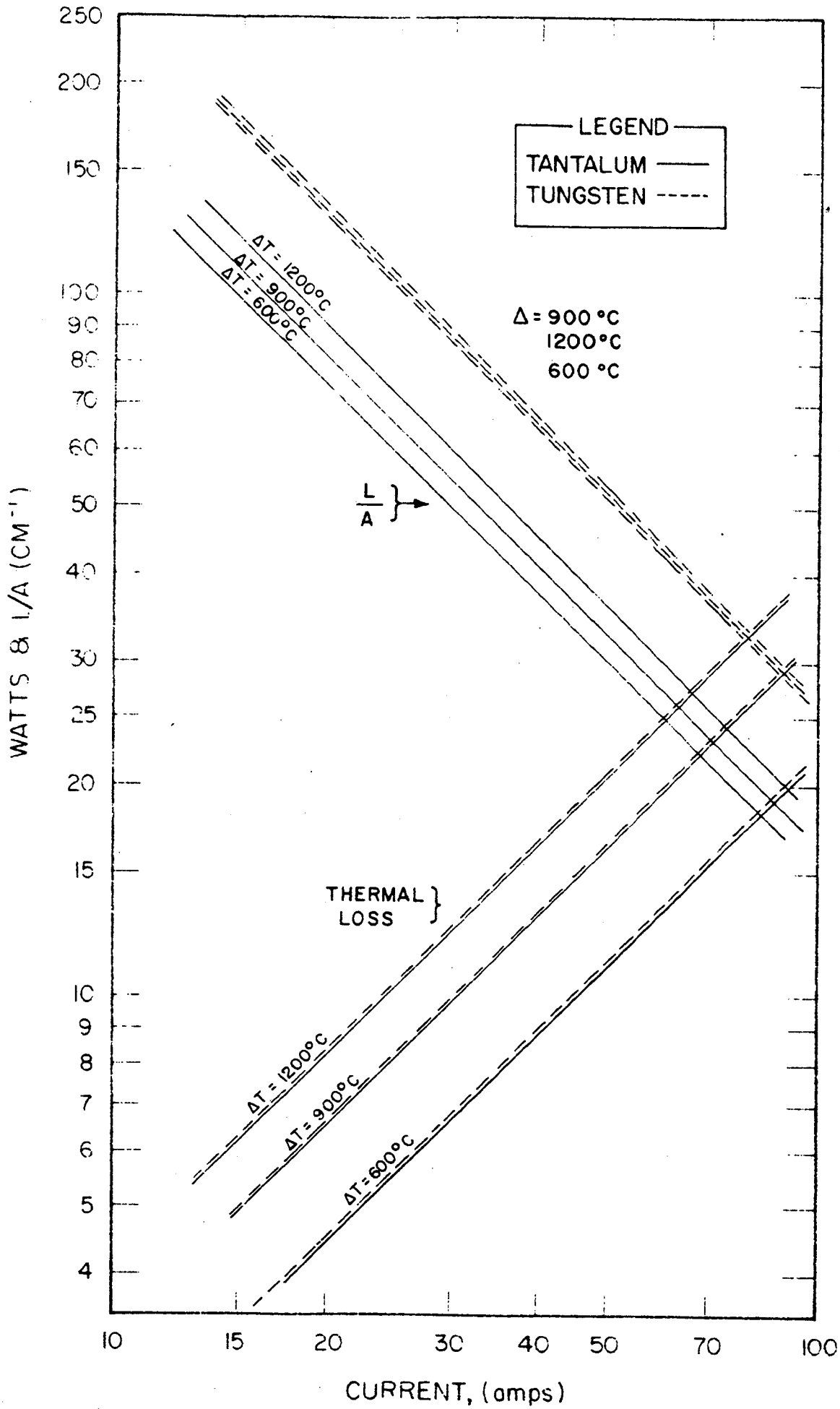

FIG. 3-1 THERMAL LOSS AND L/A LEAD RATIO VS. CURRENT FOR σ = 0.1 ($\sigma \equiv$ p elec/p thermal)

7365489

this spinning operation is accomplished by a local company, Hermann's Metal Spinning of Glendale. The flange fabrication consists of three distinct steps. The first step is accomplished at the spinning source, which amounts to the first rough spin of the flange. This part is highly work-hardened, and requires stress relieving. The stress relieving is performed at Electro-Optical Systems by way of vacuum annealing the part at 1250°C for thirty minutes. The part is subsequently returned for the final spinning operation, wherein flange flatness and critical dimensions are achieved. We have attempted some grinding of the flange surface in order to achieve tolerable flatnesses on otherwise reject parts. This grinding operation is not performed too frequently, since the spinning source has become more competent in maintaining flange dimensions.

We have included a calculation of the induced stresses at the flange-ceramic interface as a result of the sealing operation. The ceramic wall thickness of approximately 0.11 inch and the ceramic outside diameter of approximately 1.1 inches results in

$$S_{max}/hT_{yp} \approx 6.5 \text{ or } 7,$$

where S_{max} is the maximum axial stress in the ceramic-metal seal, h is the surface thickness of the metal member, and T_{yp} is the yield strength of the metal member. This relationship is derived from the chart on page 3-54 of a thermionic literature survey conducted by Electro-Optical Systems for JPL under Contract JPL-950188. At room temperature for a niobium flange of 0.010 inch thick, and a value of 40,000 psi to 45,000 psi of tensile strength,

$$S_{max} = 7 \times 4.2 \times 10^4 \times 1 \times 10^{-2}$$

$$S_{max} = 3{,}000 \text{ psi}$$

3.1.4 Envelope-Flange Assembly

The envelope-flange assembly (Drawing No. 12108 in the Appendix) joint should satisfy the following criteria:

1. The braze material must have a low vapor pressure at temperatures as high as 1000°C.
2. The braze material must be capable of wetting satisfactorily the tantalum and niobium surfaces. This is usually accomplished by the active reduction of surface oxides in the vacuum environment in which the joint is made.
3. The braze material must be resistant to the corrosive effects of cesium.

Commonly known braze materials, such as copper and nickel, were rejected because of their high vapor pressure at temperatures near 1000°C. On the basis of our fabrication experience of joining the niobium reservoir tubulation to the molybdenum collector, titanium was chosen for making feasibility tests for joining this assembly.

Since the main problem of joining the envelope flange at the emitter lead appeared to be one of proper jigging, we prepared a brazing fixture or jig as shown in Fig. 3-2. Initial feasibility joints were highly successful, demonstrating leak-tight integrity. There was some difficulty, however, in the assembly becoming brazed to the jig. This was corrected by machining a relief as indicated in Fig. 3-2 and upon the insertion of a molybdenum shim, which prevented excess braze material from bonding the assembly to the jig.

The detailed brazing schedule is as follows: The parts are placed in a susceptor can inside a high-vacuum bell jar. An rf induction coil is mounted on the exterior of the bell jar and energy is coupled from the coil into the susceptor can, thus creating a vacuum furnace. After a suitable brazing vacuum is achieved, usually in the range of 1×10^{-6} mm.Hg, the furnace and its parts are raised to a temperature of 1400°C and allowed to "soak" at this temperature for

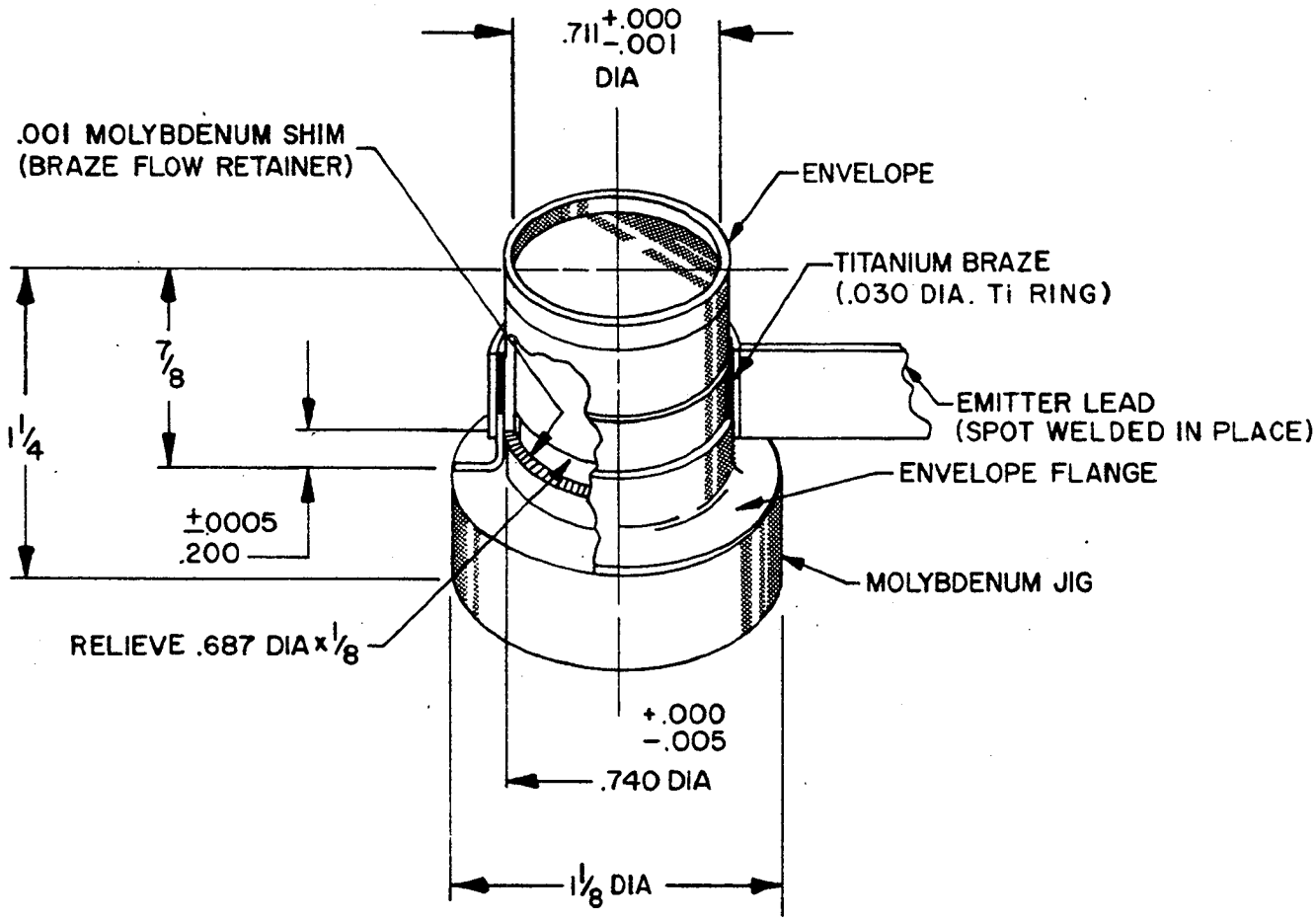

FIG. 3-2 ENVELOPE/FLANGE ASSEMBLY BRAZING JIG

approximately 10 minutes. The temperature is then quickly raised to 1700°C for a period of three minutes, at that time the brazed material achieves a melt. The rf unit is secured and the assembly cooling rate is governed by radiation.

3.1.5 Emitter Assembly

After the envelope flange and emitter lead assembly have been titanium-brazed together, the polished emitter is joined to this subassembly to complete the emitter assembly (see Drawing No. 12115 in the Appendix). The tantalum is joined to the envelope-flange assembly by inert heliarc welding. The welding schedule for this assembly is as follows: The purging gas employed is reactor grade helium (99.99 percent pure) supplied by Gordon Duff of Glendale. Helium is admitted into the weld area from two points, as shown in Fig. 3-3. A Miller Model No. SR-200-LA welding machine, with a SR-32A panel and rf start, has been utilized for all heliarc operations. The current setting on this machine is 40 to 50 amperes, with foot control at the operator's discretion. The rotation speed of the turn table shown in Fig. 3-3 is approximately 5 rpm. The welding electrode is tungsten rod of 0.040 inch diameter. No particular jig has been found necessary to effect this joining process. The parts are placed on a work holder, which is held in the cluck of the rotation table. This welding schedule for tantalum-tantalum parts, has proven quite successful as evidenced by the high yield of leak-tight assemblies.

Of particular importance to the technique of welding the emitter-to-envelope assembly is the weld area joint design. Note that the emitter and envelope press-fit together and that there is an area of contact between parts that forces a smooth temperature distribution from emitter to envelope during converter operation. A sharp temperature difference between these parts could induce hoop stresses in the joint that would lead to failure. The exact dimensions of the joint area are a result of practical considerations rather than detailed calculation.

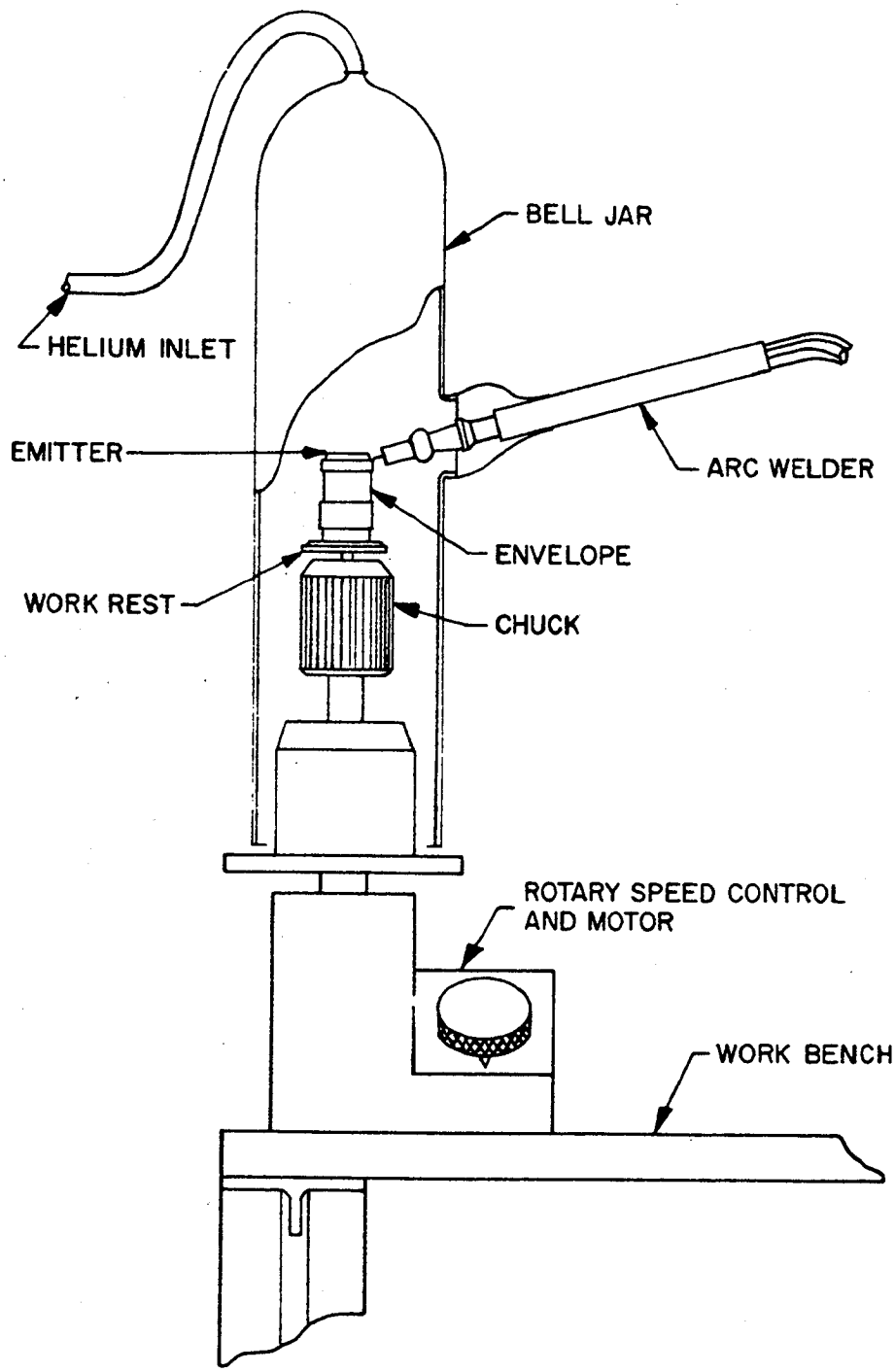

FIG. 3-3 INERT ARC WELDING APPARATUS

7369453

3.1.6 Collector

A heat transfer analysis of the collector (see Drawing No. 12109 in the Appendix) in an operating converter has indicated the approximate temperature and work function of the collector surface.

For 30 amperes of current being drawn through an assumed collector work function of 1.8 volts plus the plasma electron temperature of 0.35 volts, 65 watts electrical heating of the collector results. Assuming low emissivity emitter and collector surfaces of tantalum and molybdenum, respectively, 18 watts of radiated power are transferred (9 w/cm^2 times 2 cm^2). (See reference EOS final 2210, p. 4-6, JPL Contract 950188).

An estimated 5 watts are conducted by the cesium vapor from emitter to collector. (Ref. S. Kitrilakis and M. Meeker, Advanced Energy Conversion Journal, Vol. 3, March 1963, p. 59)
The summation of these individual contributions is 88 watts, which must be dissipated by the collector-radiator system. From the heat conduction equation

$$Q = \frac{KA\Delta T}{\Delta X}$$

$$\frac{Q}{A} = 44 \text{ watts/cm}^2 = \frac{K\Delta T}{\Delta X} \text{ (for 2 cm}^2 \text{ of collector surface)}$$

For molybdenum at approximately 1000°K,

$$K \simeq 1.1 \text{ watt cm}^{-1}\ {}^\circ\text{C}^{-1}$$

(Ref. EOS final 2210, p. 2-85, JPL Contract 950188)

Therefore,

$$\Delta T \simeq 44\ \Delta X$$

where: ΔX is the collector length of 1.5 inches equivalent to the distance in a practical converter.

$\Delta T \approx 150^{\circ}C$, the calculated difference in temperature between the collector at the radiator clamp and collector face in the device.

The 1.5 distance was used to allow ample room for the metal-ceramic seal, the lead straps, and the 0.4 inch length heat choke section in the envelope. This length can easily be reduced in a redesign.

The temperature measurements on the collector at the radiator clamp have been in doubt, since the thermocouple is not immersed in the collector nor spot welded to the clamp. Thermocouple measurements have indicated $650^{\circ}C$ temperature at the clamp during dc operation when the current is 30 amperes. The true temperature of the collector at the clamp could be 700 to 800 degrees C, resulting from a poor thermocouple connection at the clamp interface. It is therefore probable that the collector face temperature was $1000^{\circ}C$ to $1050^{\circ}C$. The work function of cesiated molybdenum at this temperature is 1.8 to 1.9 volts; however, a work function of 1.55 volts or lower is available at collector temperatures near $750^{\circ}C$ (EOS report 3410 Q3, Contract NAS3-2529).

It might be well to point out that a work function of 1.55 volts from molybdenum bar stock is attained only if the molybdenum is vacuum-fired at $1700^{\circ}C$ or higher for 20 minutes in order to recrystallize the surface properly. We observed the improvement of converter No. 5 as the collector "aged-in" for eight hours at a lower temperature.

In a final attempt to modify the clamping procedure, which has prevented a lower collector face temperature and consequently an improper work function adjustment of the collector surface, we have attempted to braze the clamps onto converters No. 1, No. 7, and No. 8. This technique is discussed in the next section.

As Drawing No. 12109 (see Appendix) indicates, slots are machined into the side of the collector to receive sapphire alignment rods. The alignment rods accomplish two purposes:

1. They insulate the collector positively from the envelope-emitter structure.
2. They provide a 0.010 inch space between the envelope sidewall and collector. This spacing is large enough to insure that no current is drawn from the envelope or emitter surface, which is not spaced 0.002 inch or less from the collector. Evidence in support of this hypothesis is the minimal power output of a 0.010 inch space converter at a cesium reservoir temperature of 380°C (see Fig. 3-4).

We therefore define the area of the emitter in diodes 1 through 6 to be 2 cm^2. Diodes 7 and 8 possess 2.35 cm^2 of active emitting area.

3.1.7 Collector-Flange Assembly

This assembly, is shown in Drawing No. 12110 of the Appendix. A titanium braze ring 0.030 inches in diameter is placed in the solder groove. The entire assembly is then placed in an rf induction furnace and brought to a temperature of 1700°C for 3 minutes to accomplish the braze. The braze process is essentially identical to that used on the envelope - flange assembly (See paragraph 3.1.4).

3.1.8 Radiator and Clamp Assembly

At present the radiator assembly is clamped onto the collector with a 0.001 inch B.T. braze shim in place for brazing the two structures together (see Drawing No. 12239 in the Appendix). The radiator fins are pre-brazed onto one clamp before joining the clamp to the collector.

Prior to brazing, the external surfaces of the clamp and the side fins are sprayed with 0.002 inch of Rockide "C". The parts are chemically cleaned and vacuum-fired prior to emissive coating to insure good adhesion of the Rockide.

The problem of radiator attachment has become more complex than originally envisioned. The first converter operated with a mechanically attached radiator that first operated too low in

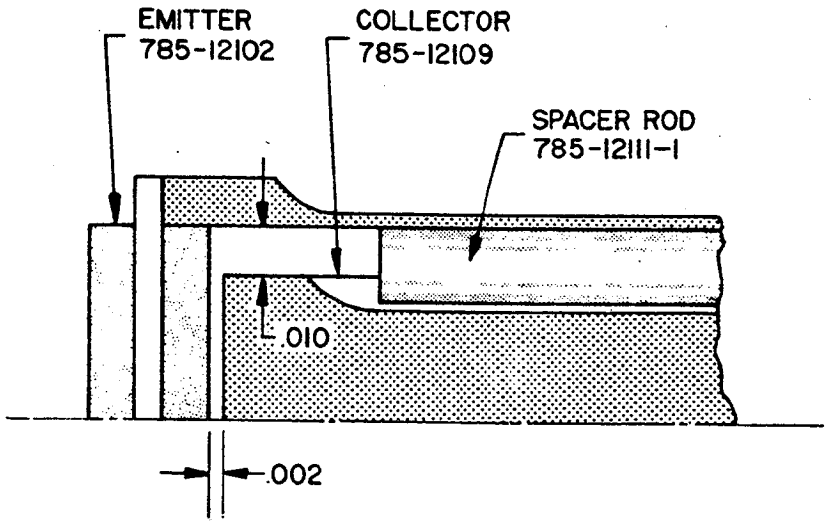

FIG. 3-4 DETAIL OF EMITTER/COLLECTOR SPACING

temperature due to low current. The radiation area was reduced and the radiator external heater input was increased. The radiator then operated too high in temperature. The original radiator area was computed on the basis that 88 thermal watts must be radiated (see Section 3.1.6).

Assuming a total normal emissivity of 0.85 for a Rokide "C" covered radiator operating at 600°C, a radiator area of approximately 32 cm^2 would be required to radiate the 88 watts to space.

Converters Nos. 2 through 6 maintained the original radiation area, but still operated too high in temperature, because the current drawn through these devices was three to four times higher than in the first one. In fact, the radiator heaters were used only to demonstrate that too high a collector temperature reduced the converter performance. The collector temperature could be lowered by applying ac sweep methods to obtain a lower average device current and consequently less collector heating.

The clamp is fabricated from molybdenum to minimize expansion problems with the collector. The clamp is machined to close tolerances in order to improve the fitting and brazing operation. The clamps on Converters Nos. 7 and 8 were B.T. brazed at 750°C when the diode was first taken to 1700°C at a voltage value near short circuit. This operation insured that a high current passed through the collector, heating it sufficiently to affect the braze. A feasibility braze was first attempted on converter No. 1. The results of this braze are discussed more fully in the metallurgical examination section.

3.1.9 Collector Flange

The fabrication techniques for the collector flange (see Drawing No. 12109 in the Appendix) are the same as for those of the emitter flange, namely, the spinning operation, the interstage annealing, and the overall precaution used in maintaining flange flatness and flange dimensions.

3.1.10 Heat Choke

The parametric calculations, the heat choke (see Drawing No. 12216 in the Appendix) dimensions and choice of materials for the reservoir tubulation have been discussed in the feasibility investigation section. All converters fabricated, with the exception of No. 1, have employed the dimensions and materials selection as indicated in Drawing No. 12216. Converter No. 1 was inadvertently fabricated with a 0.015 inch wall heat choke, which resulted in an inability to maintain the proper reservoir temperature. At the conclusion of the initial testing of diode No. 1, the diode was carefully chucked into a lathe and rotated at low speed while a jeweler's hand file was employed to reduce the thickness of the reservoir tubulation. The reservoir control on converters Nos. 2 through 8 has been maintained properly with the correct heat choke dimensions.

3.1.11 Exhaust Assembly

The exhaust and heat choke tubulations are joined by heliarc welding in a helium-purged atmosphere (see Drawing No. 12120 in the Appendix). The conditions for heliarc welding including current setting, purity of gas used, and electrode diameter have been discussed previously in the emitter-envelope assembly. The current setting for welding copper to niobium is somewhat higher than that used for tantalum-tantalum. The high value for the thermal conductivity of copper results in a considerable amount of heat being withdrawn from the weld area; therefore, a current setting of 100 amperes is recommended.

3.1.12 Flow Chart for Converter No. 1 Through No. 6

Converters No. 1 through No. 6 received the treatments and the sequence of treatments as indicated in Drawing No. 12124 of the Appendix. Converters 7 and 8 received idential treatment with the exception that positive spacing was not incorporated in those converters that would exclude the retaining ring and insulator ring from the flow chart. The material sources, chemical cleaning, and other procedures are listed in the Appendix and should be used in connection with the flow chart.

3.2 Converter Fabrication and Development History

A number of converter design and fabrication changes were made as the program progressed. These changes were generally based on performance data or fabrication experience obtained from previous converters.

Three problem areas of special concern evolved during the succession of converters 1 through 8. They were identified as:

1. The reservoir heat choke
2. The collector-radiator assembly
3. The interelectrode spacing

The following paragraphs are devoted to a discussion of these areas.

3.2.1 The Reservoir Heat Choke

Converter No. 1 suffered low performance initially from a high cesium reservoir temperature. Design calculations and feasibility test data concerning the reservoir tubulation wall thickness and length were inadvertently not incorporated into converter No. 1. Moreover, the interelectrode spacing of converter No. 1 was larger than first the design value, which contributed heavily to a further loss in performance.

Subsequent converts (No. 2 - No. 8) employed reservoir heat chokes of the design 0.800 inch length and 0.008 inch wall thickness. These values were derived from the design calculations presented in Section 2.

3.2.2 Collector-Radiator Assembly

The radiator assembly in converters No. 1 through No. 6 was mechanically attached to the collector by means of a clamp. Generally, the result was a poor heat transfer path. In addition, the collector-radiator thermocouple at this interface responded erratically, owing to the lack of conduction transfer to the couple. Some of the radiator fin edges were "scalloped" in order to position the radiator heater wire during rockide application. In general, the method of

rockiding heater wire, either to a reservoir or radiator, was found unsatisfactory, since the heat from the wire is not efficiently transferred.

3.2.3 Interelectrode Spacing

The proper choice of a spacing for a high performance converter follows a general rule: within practical limits the closer, the more output. Converts No. 1, than No. 3 were fabricated with positively spaced electrodes decreasing from 8 to 3 mils with the optimum power doubling over the range of spacings. The problem of materials interaction however, prohibited a definitive analysis of the data due to collector coating formation and intermittent shorts caused by decomposition products. After converter No. 6, the positive spacing schemes was abandoned. These preliminary results do not mean however, that positive spacing is not possible for practical converters. The results imply that better techniques are required.

3.3 Converter Test Data Analysis

The electrical characteristics of the first eight diodes which have been fabricated and tested to date will be discussed in numerical order. Of the five diodes, diodes 2, 3, 4, 5, 6, 7, and 8 have been tested at EOS and delivered to JPL under contractual commitment. Diode No. 1 was retained at EOS for metallurgical examination and collector emissivity studies. A general summary of the maximum power output of each diode at 1700°C emitter temperature is shown in Figure 3-5. Figure 3-5 is a plot of the maximum power output of the diodes versus interelectrode spacing. Shown on the curves is the cesium reservoir temperature at which each of these diodes was optimized. The curve is drawn for one emitter temperature, namely, 1700°C. Diode No. 1 which had a interelectrode spacing of approximately 8 mils was found to have a maximum power output of approximately 6 watts or 3 watts/cm^2. This diode optimized at a emitter temperature of approximately 1500°C and only a slight gain in power output was achieved by increasing the emitter temperature approximately 200°C to 1700°C.

Of further interest is the fact that with plate stock tantalum emitters and bar stock molybdenum collectors it is necessary to achieve spacings at temperature of less than approximately 1 mil in order to obtain power densities on the order of 10 to 15 watts/cm^2 at 1700°C emitter temperatures. Such spacings are considerably smaller than those predicted at the start of the present program. Spacings of approximately 4 mils were predicted to be adequate for achieving power densities of the order 12 to 14 watts/cm^2. This prediction was based upon the assumption that tantalum emitter surfaces could be achieved which would exhibit predominately a 110 crystal surface after high temperature recrystallization. The particular material from which these emitters were fabricated appears

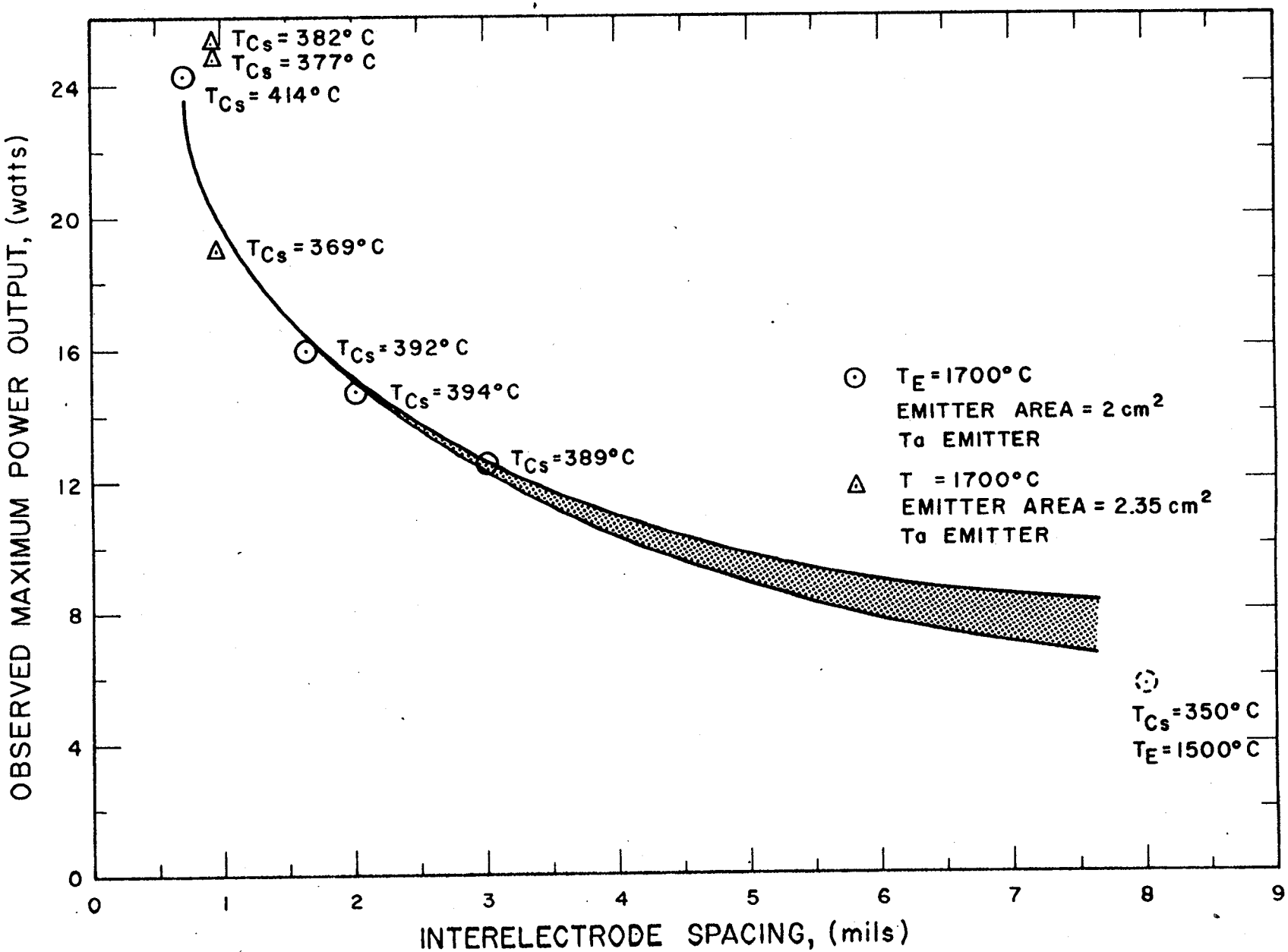

FIG. 3-5 MAXIMUM POWER VS. INTERELECTRODE SPACING (AT TEMPERATURE) FOR EOS DIODES

to have predominately a {111} crystal surface structure after recrystallization. In the case of tungsten the {111} crystal surface has a work function intermediate to that of the {100} and the {110} surfaces. In essence, the same emission density can be achieved from any one of these crystal surfaces in the cesiated condition, but at the expense of a higher cesium arrival rate (and hence cesium vapor pressure) for those crystal faces having the lowest bare work function. The higher the cesium arrival rate necessary to achieve a given emission density from the emitter, the closer must be the interelectrode spacing in order to minimize the electron-atom collision losseslosses in the plasma. It is still our feeling that the predicted emission densities can be achieved at spacings on the order of 4 mils, but more work will be required in order to achieve a predominately 110 crystal surface on the tantalum or tungsten substrate.

The collector thermocouple temperatures on several diodes appear to be in doubt as a result of lacking good thermal contact with the collector. In addition the collector heat transfer equations indicate that the collector surface temperature may be 150°C higher than the collector base. At any rate, an <u>increase</u> or <u>decrease</u> in temperature is positive, and gives a definite indication of collector temperature influence upon the converter power output.

3.3.1 <u>Diode No. 2</u>

Diode No. 2 had a spacing of approximately 3 mils. The minimum spacing was fixed by the positive spacing technique described in the section on feasibility experiments. The 3 mil spacing is achieved at the braze temperature wherein all components of the converter have come to a uniform temperature of approximately 1000°C. The actual spacing at operating temperatures is then calculated through a knowledge of the converter temperature distribution under operating conditions. Such a calculation indicates that the converter spacing will open up by approximately 0.5 to 0.7 mils for an emitter temperature at 1700°C and with collector and side wall temperatures on

the order of 850 to 900°C. The calculation proceeds as follows: The emitter structure expands characteristic of tantalum in the stress free condition at 850°C since this was the estimated temperature at which the seal braze stress-relieved.

$$\alpha_{\substack{\text{total}\\ \text{envelope}}} \cong \alpha_{\substack{\text{emitter}\\ \text{at } 2000^\circ K}} + \alpha_{\substack{\text{heat}\\ \text{choke at } 1000^\circ C}}$$

$$\alpha_{\substack{\text{total}\\ \text{envelope}}} \simeq (0.8 + 0.2)\ 0.8 \times 10^{-3} \cong 0.8 \text{ mil}$$

the collector expansion of molybdenum at 800°C

$$\alpha_{\text{collector}} \simeq (0.4)\ 0.75 \times 10^{-3} \simeq 0.3 \text{ mils}$$

The total expansion, $\alpha_{\text{envelope}} - \alpha_{\text{collector}}$, approximate 0.5 mil. Thus, although converter No. 2 has a fixed minimum spacing of 3 mils at the braze temperature, the actual spacing under operating conditions may be as large as 3-1/2 mils. The volt ampere characteristic for diode No. 2 is shown in Figure 3-5. In evidence in this figure is the general characteristic of the arc mode converter wherein there is: (1) a range of the voltampere characteristic (near open circuit voltage) where the current is essentially limited by space charge, (2) a portion of the characteristic near maximum power where the current is almost independent of voltage except for a small internal loss in the plasma, and (3) a portion of the characteristic where the current becomes saturated except for the Schottky effect. The maximum power point in these converters is approximately at the break in the characteristic corresponding to the current saturation. The curves in Figure 3-6 were taken at a constant collector temperature of 690°C. For comparison purposes, an equivalent set of characteristics taken for a collector temperature of 618°C is shown in Figure 3-7. The main difference between these two sets of characteristics is the shift of the whole pattern of curves to

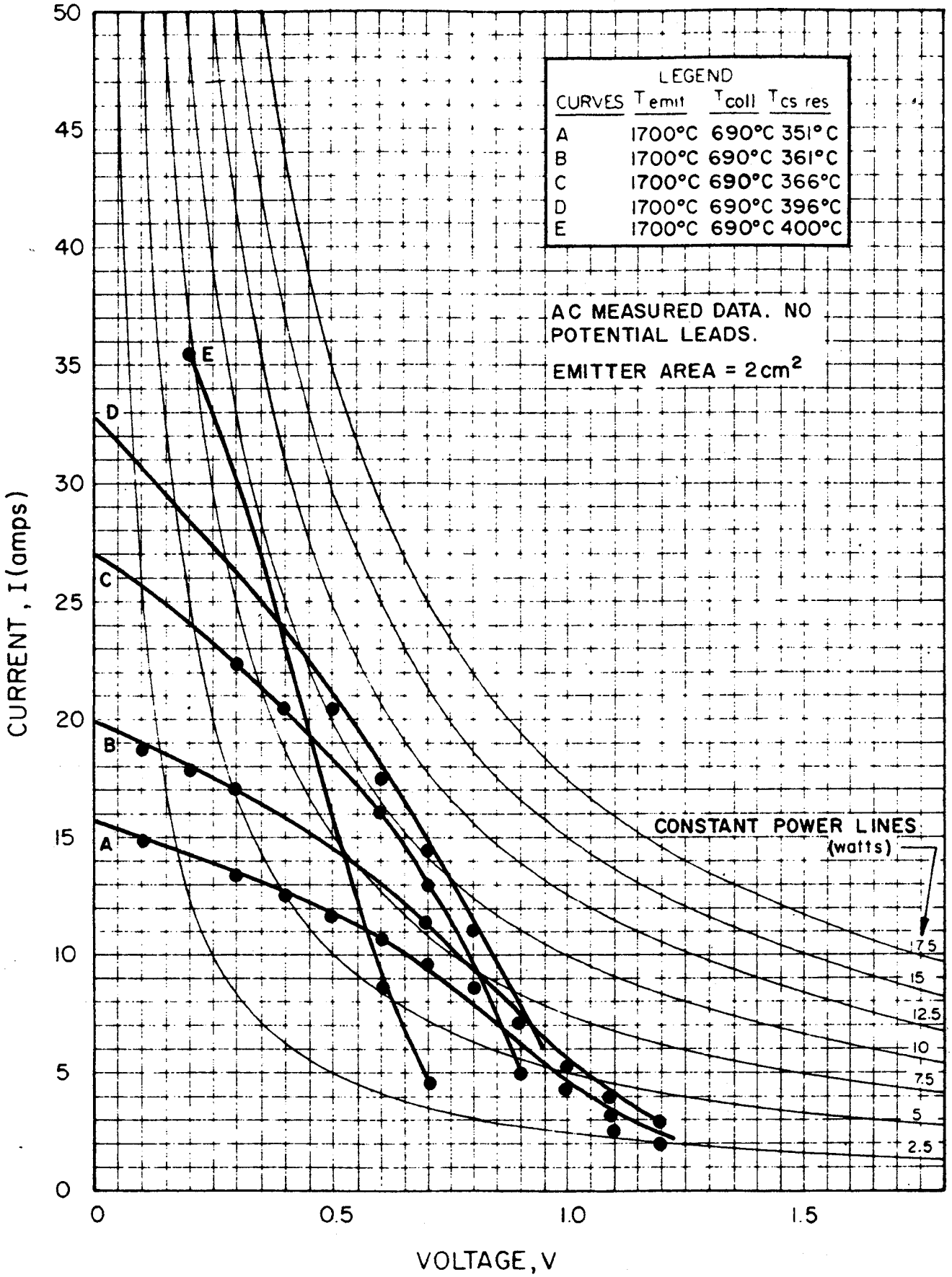

FIG. 3-6 DIODE NO. 2 CURRENT-VOLTAGE CHARACTERISTICS
(T emit 1700°C)

7368671

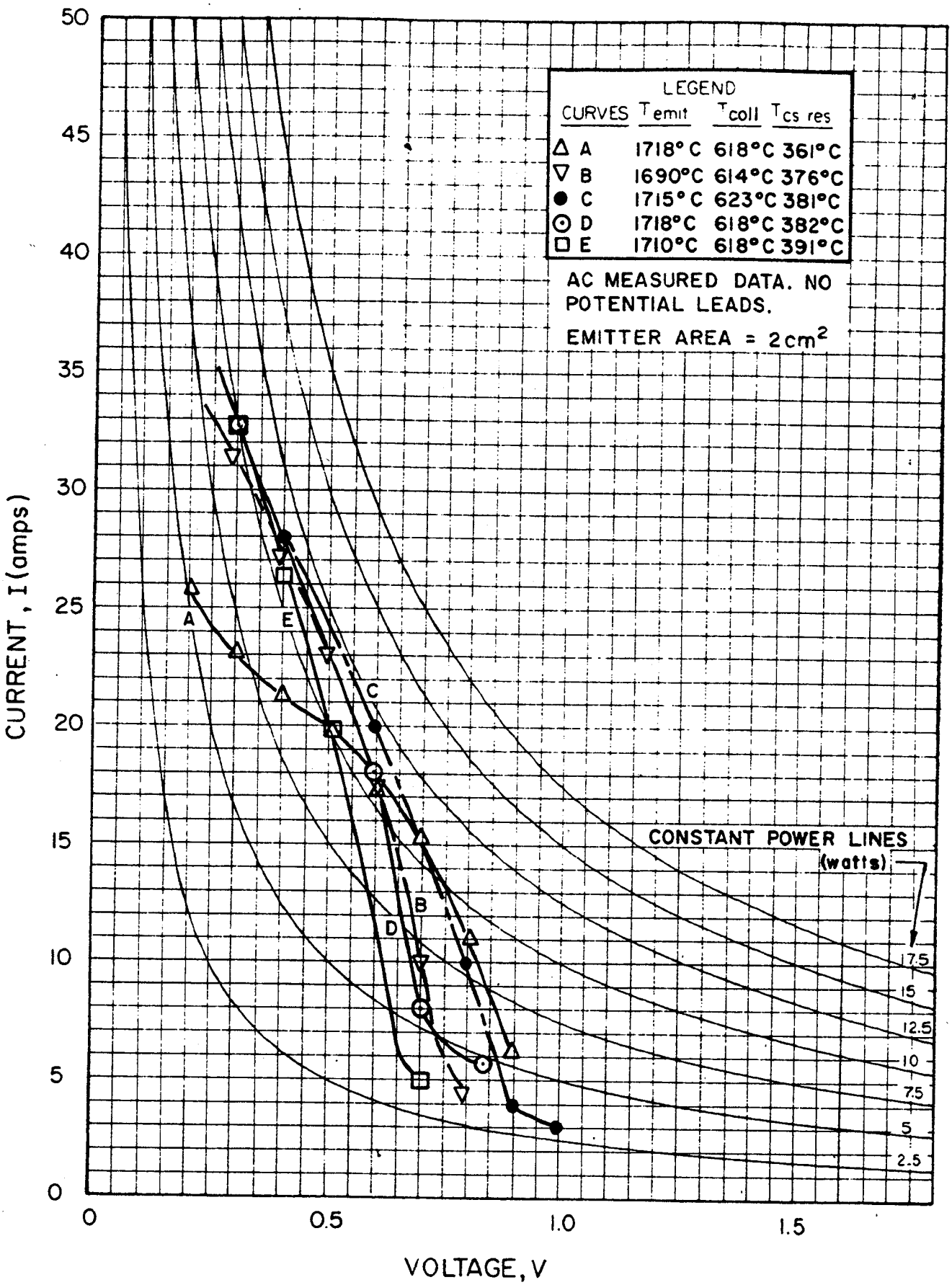

FIG. 3-7. DIODE NO. 2 CURRENT-VOLTAGE CHARACTERISTICS
(T emit 1718°C)

a higher power point. This illustrates the effect of a 70°C change in the collector temperature on converter performance. The change in collector temperature of 70°C has accounted for approximately a 10 percent increase in power output of the converter.

Figures 3-8, 3-9 and 3-10 show the variation in power output from converter No. 2 as a function of cesium reservoir temperature for three different emitter temperatures. Collector temperature is taken as a parameter in these curves. These three curves show in somewhat more detail the affects of cesium reservoir temperature on converter output at a fixed collector temperature. Clearly shown in Figure 3-10 is the affect of too high a collector temperature on the output performance of the converter. A 30 percent decrease in performance of the converter results from operating the collector at a temperature approximately 140°C higher than optimum.

3.3.2 Diode No. 3

In Figure 3-11 are shown the volt-ampere characteristics for diode No. 3 for 1700°C emitter temperature and 610°C collector temperature (cesium reservoir temperature as a parameter). Diode No. 3 has a nominal spacing of 2 mils. This corresponds to approximately a 1 mil closer spacing at operating temperature than that of diode No. 2. The overall major difference between diode No. 3 and diode No. 2 is that at the smaller spacing diode No. 3 had an increased power output. In general, the set of volt-ampere characteristics has moved to the right in the power quadrant, with higher currents being achieved at higher output voltages. Figure 3-12 shows the variation of power output with cesium reservoir temperature for fixed collector temperature. It is not certain from observation of Figure 3-12 that we have achieved as low a collector surface temperature as may be desirable on this converter.

3.3.3 Diode No. 4

In Figure 3-13 are shown volt-ampere characteristics for diode No. 4 for emitter temperature of 1700°C and collector

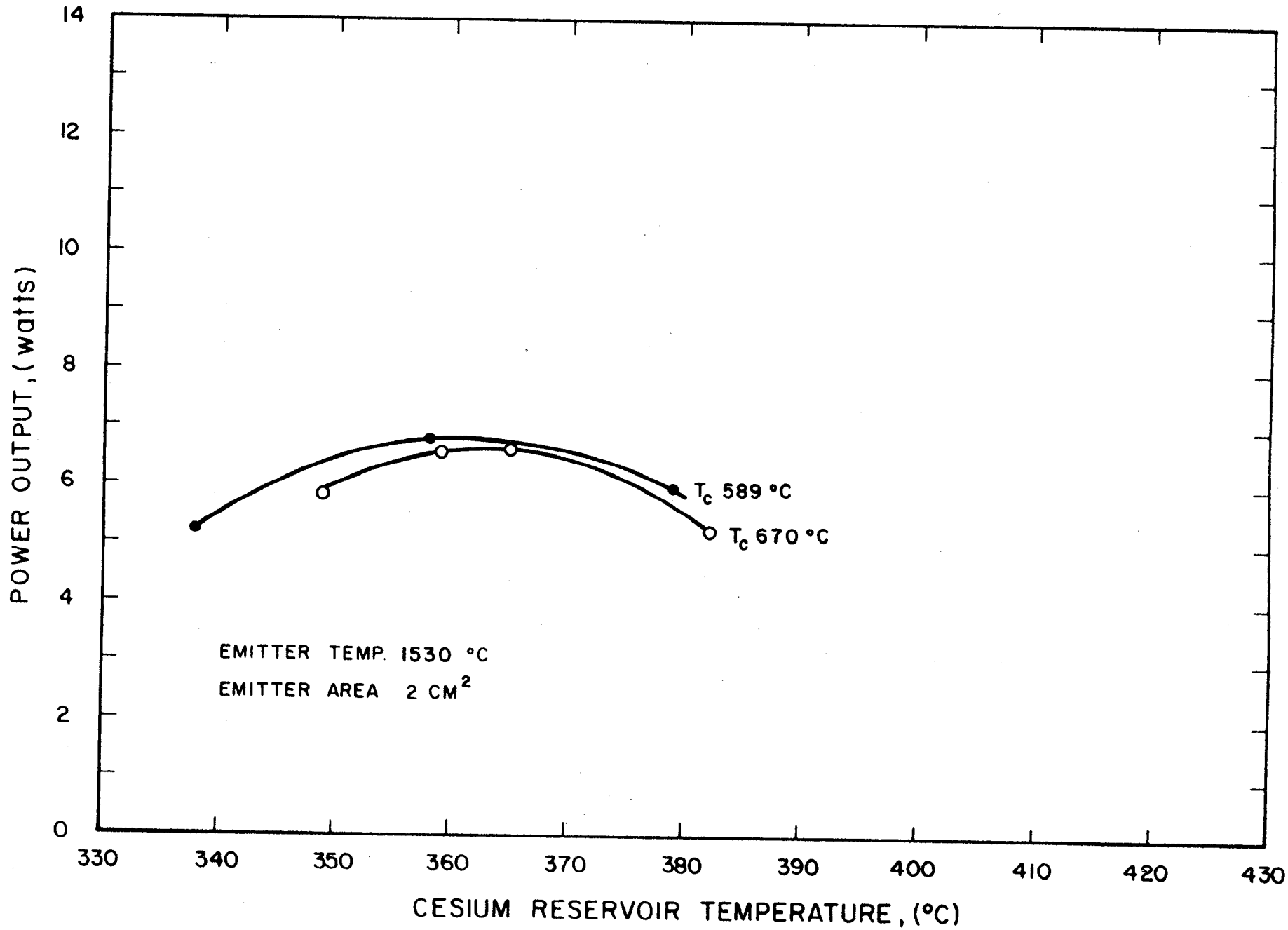

FIG. 3-8. DIODE NO. 2 POWER OUTPUT VS CESIUM RESERVOIR TEMPERATURE FOR COLLECTOR TEMPERATURE AS THE PARAMETER

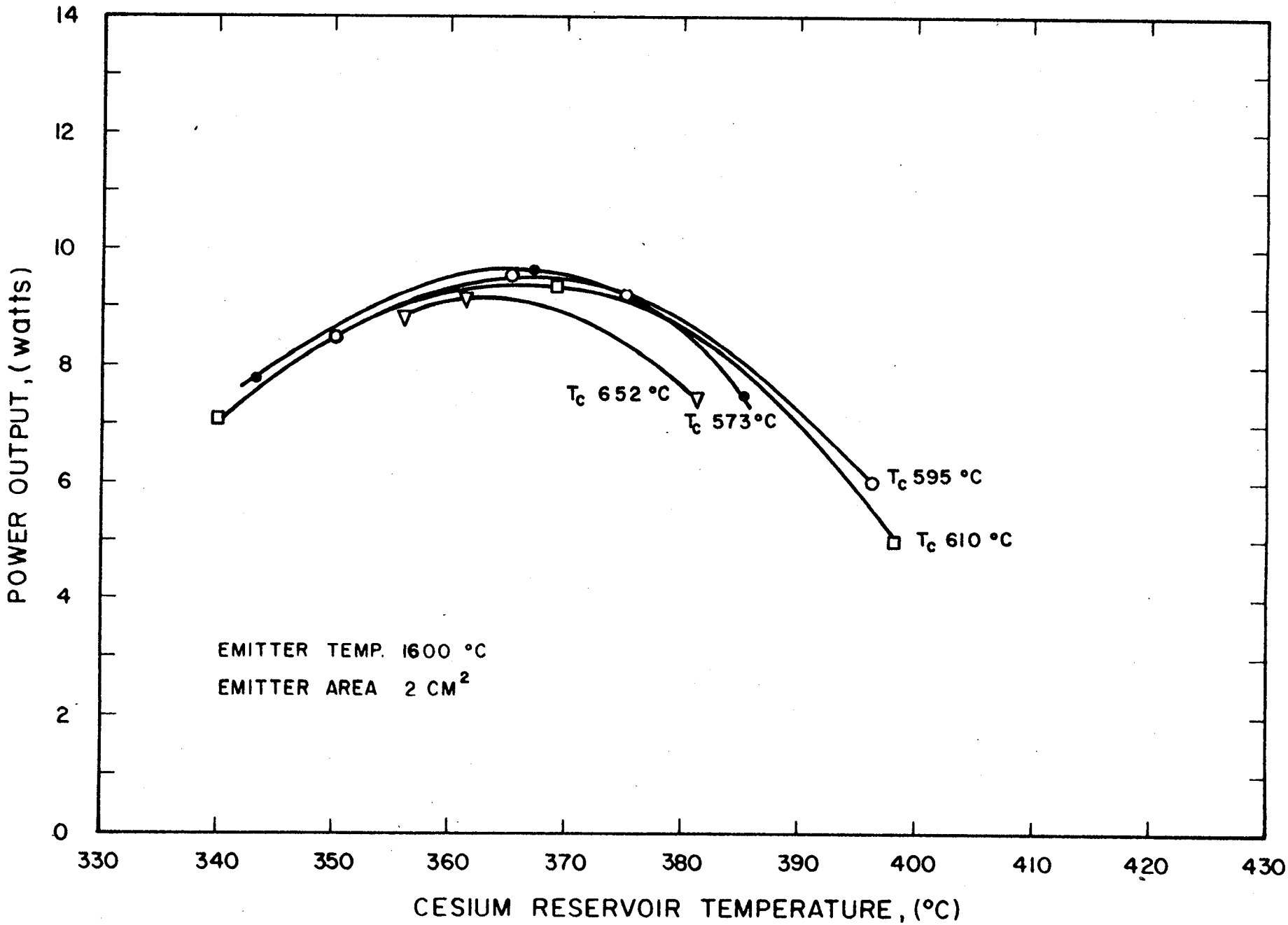

FIG. 3-9. DIODE NO. 2 POWER OUTPUT VS CESIUM RESERVOIR TEMPERATURE FOR COLLECTOR TEMPERATURE AS THE PARAMETER

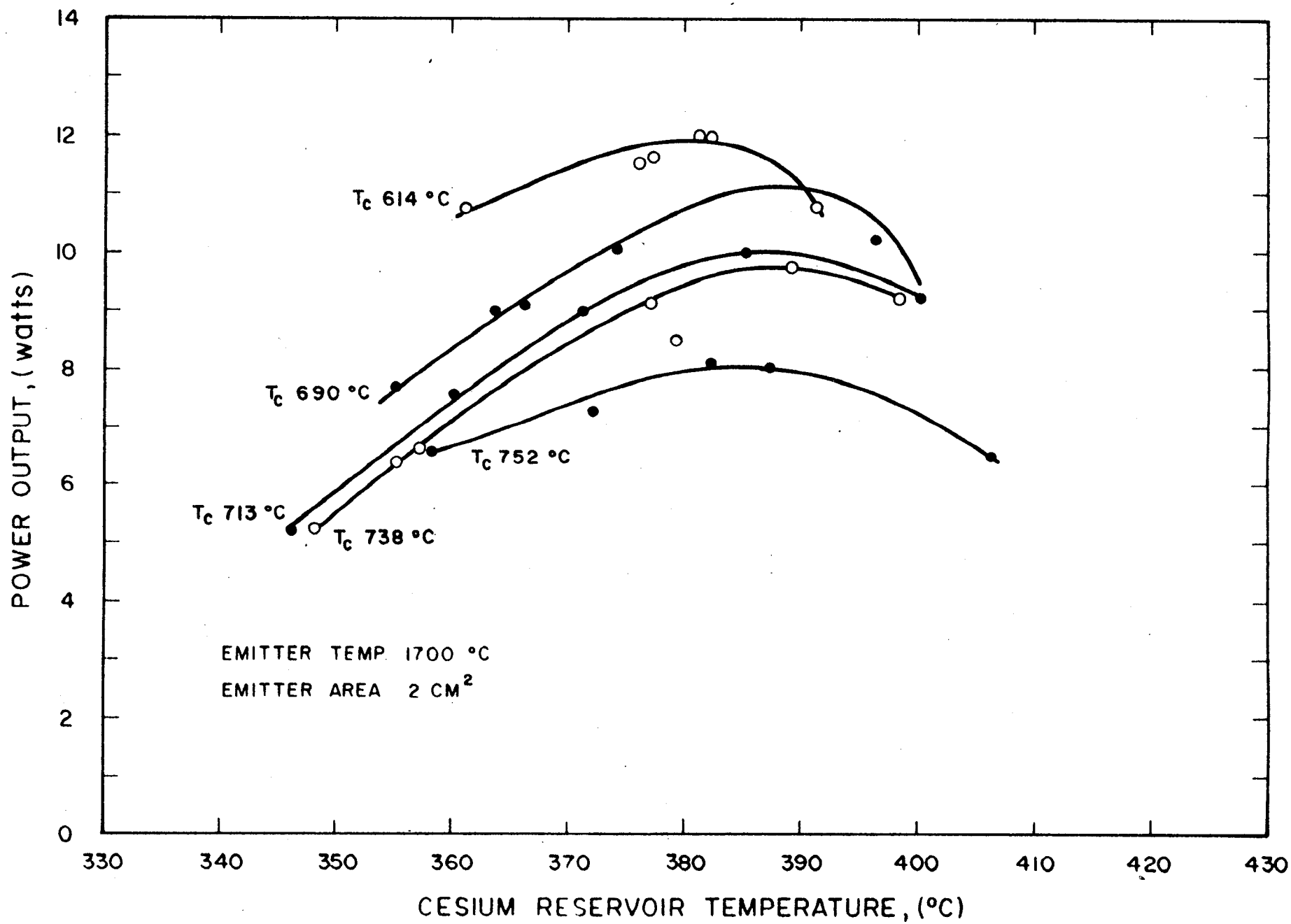

FIG. 3-10. DIODE NO. 2 POWER OUTPUT VS CESIUM RESERVOIR TEMPERATURE FOR COLLECTOR TEMPERATURE AS THE PARAMETER

7368675

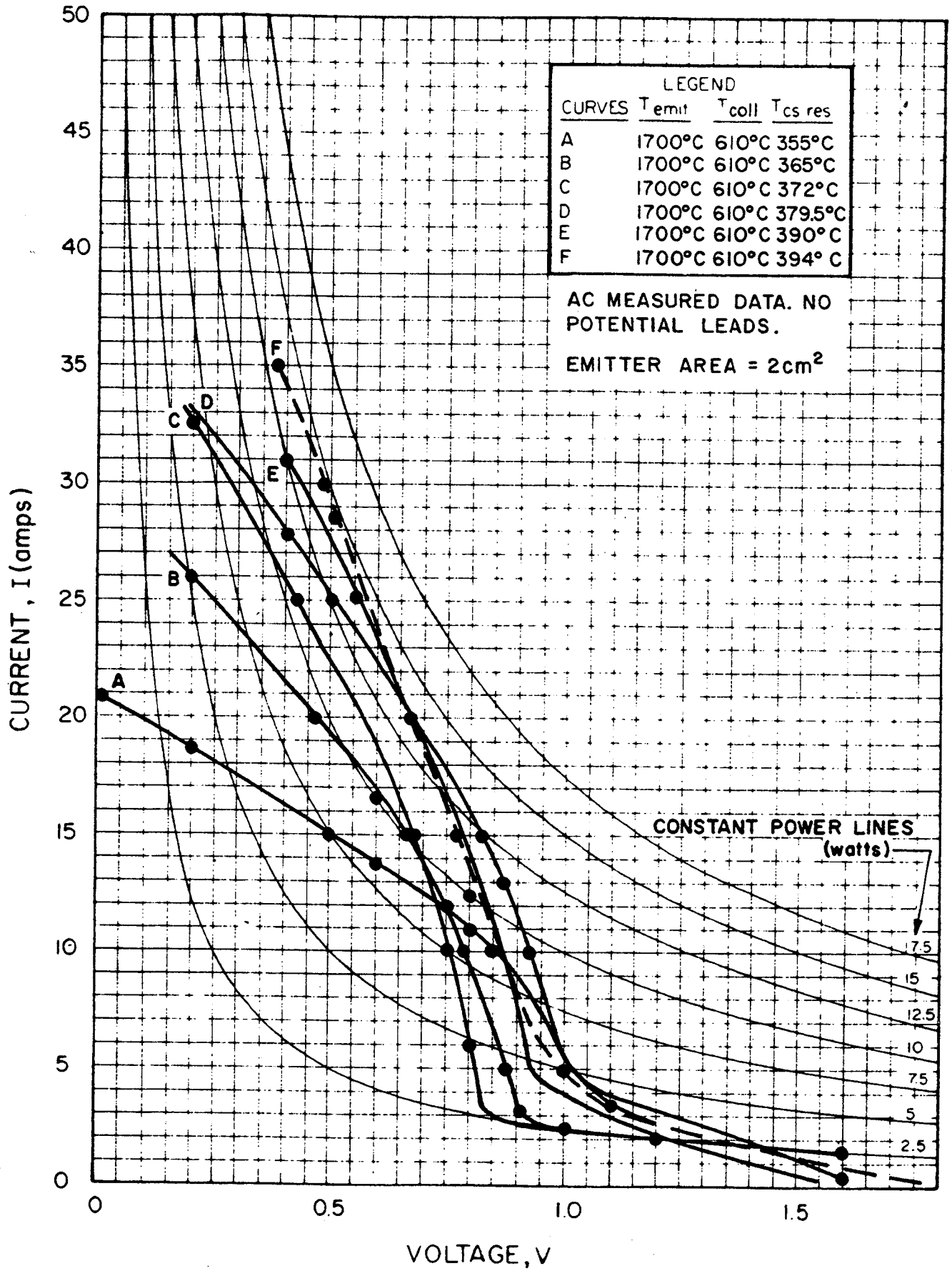

FIG. 3-11. DIODE NO. 3 CURRENT-VOLTAGE CHARACTERISTICS

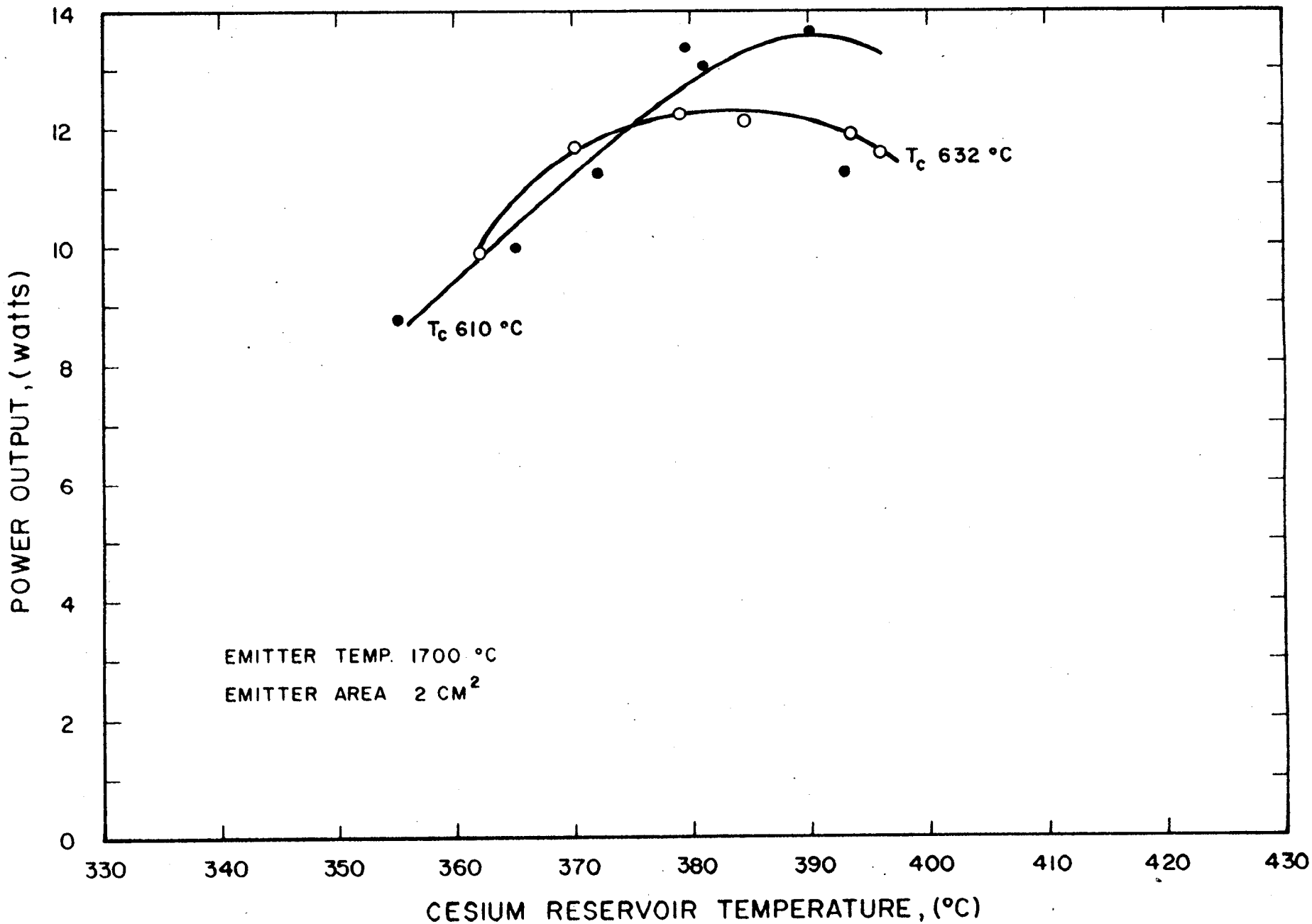

FIG. 3-12. DIODE NO. 3 POWER OUTPUT VS CESIUM RESERVOIR TEMPERATURE FOR COLLECTOR TEMPERATURE AS THE PARAMETER

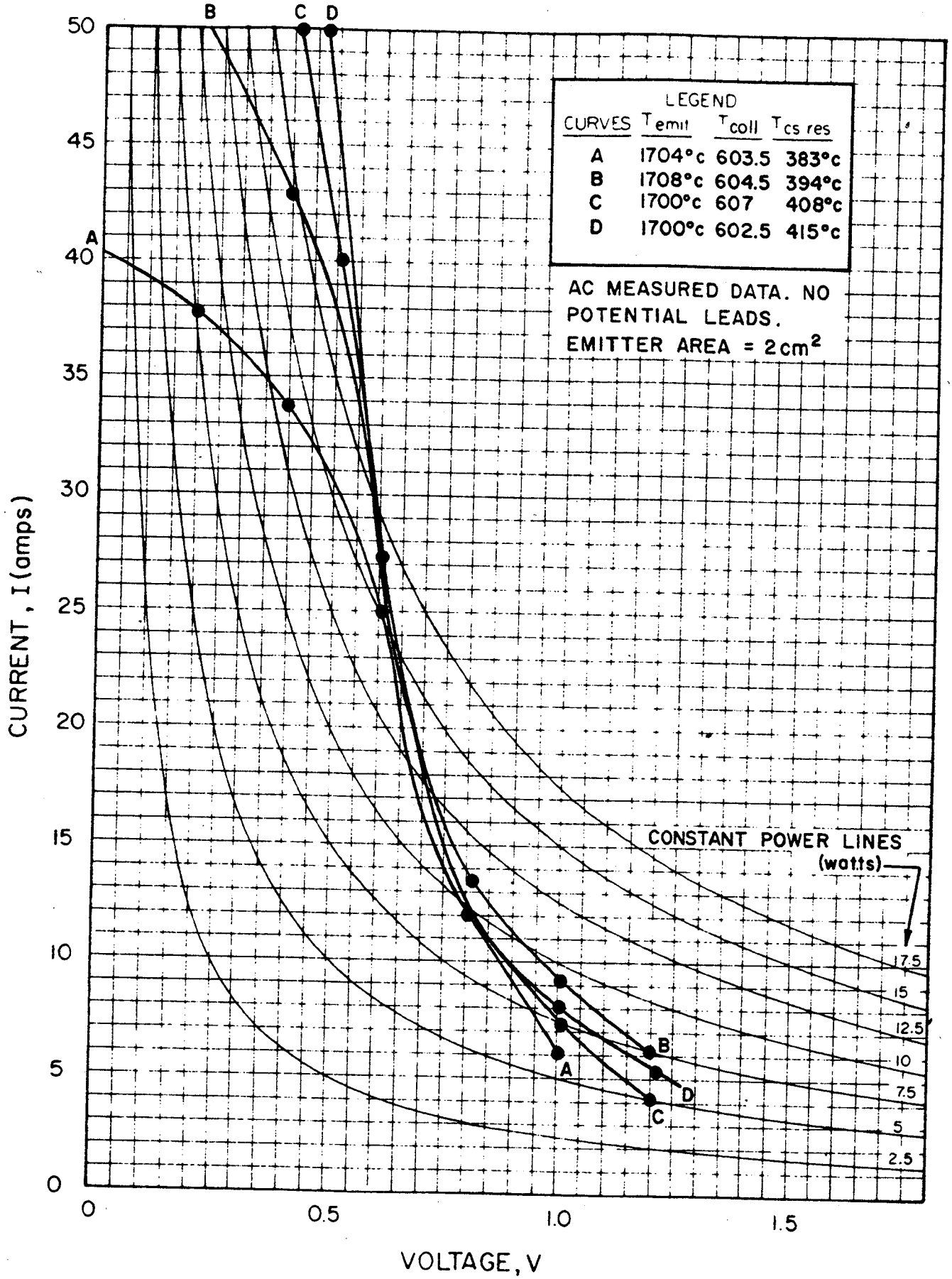

FIG. 3-19. DIODE NO. 4 CURRENT-VOLTAGE CHARACTERISTICS

temperature of approximately 600°C (cesium reservoir temperature as a parameter). This particular diode was constructed to be in shorting contact at the braze temperature of 1000°C. It was found that the converter became unshorted during operation at temperatures on the order of several hundred degrees Centigrade on the emitter structure. The estimated spacing for this particular converter at operating temperatures is between 0.7 mil and 1 mil. The most significant feature of this particular diode as compared to diodes No. 2 and 3 is that for the smaller spacing, the general pattern of volt-ampere characteristics has again shifted consistently further to the right in the power quadrant, yielding higher current outputs at a given output voltage. Saturation current densities between 20 and 30 amps/cm^2 are readily achievable on this particular converter in the power quadrant. Figure 3-14 shows the variation of power output with cesium reservoir temperature (collector temperature as a parameter). Again there is the possibility that we have not been able to achieve low enough collector temperatures under dc operating conditions. Under ac sweep methods of obtaining the volt-ampere characteristics wherein the converter was operated at low average currents (to keep the collector cool) it was found possible to achieve power outputs of approximately 32 watts or 16 watts/cm^2 with the converter emitter operating at 1800°C and the collector at approximately 627°C. The cesium reservoir temperature under these conditions was approximately 423°C. In this particular case it is seen that an increase of 100°C in emitter temperature has accounted for an approximate increase of 50 percent in the power output of the converter. This latter fact illustrates graphically why such great pains have been taken to insure that the emitter temperature measurements are as accurate as possible. At this time it is doubtful whether the power density of approximately 16 watts/cm^2 is achievable over long periods (10,000 hour) of time with the tantalum emitter substrate operating at 1800°C. It is probable that the evaporation rate of the tantalum substrate is too high at these temperatures

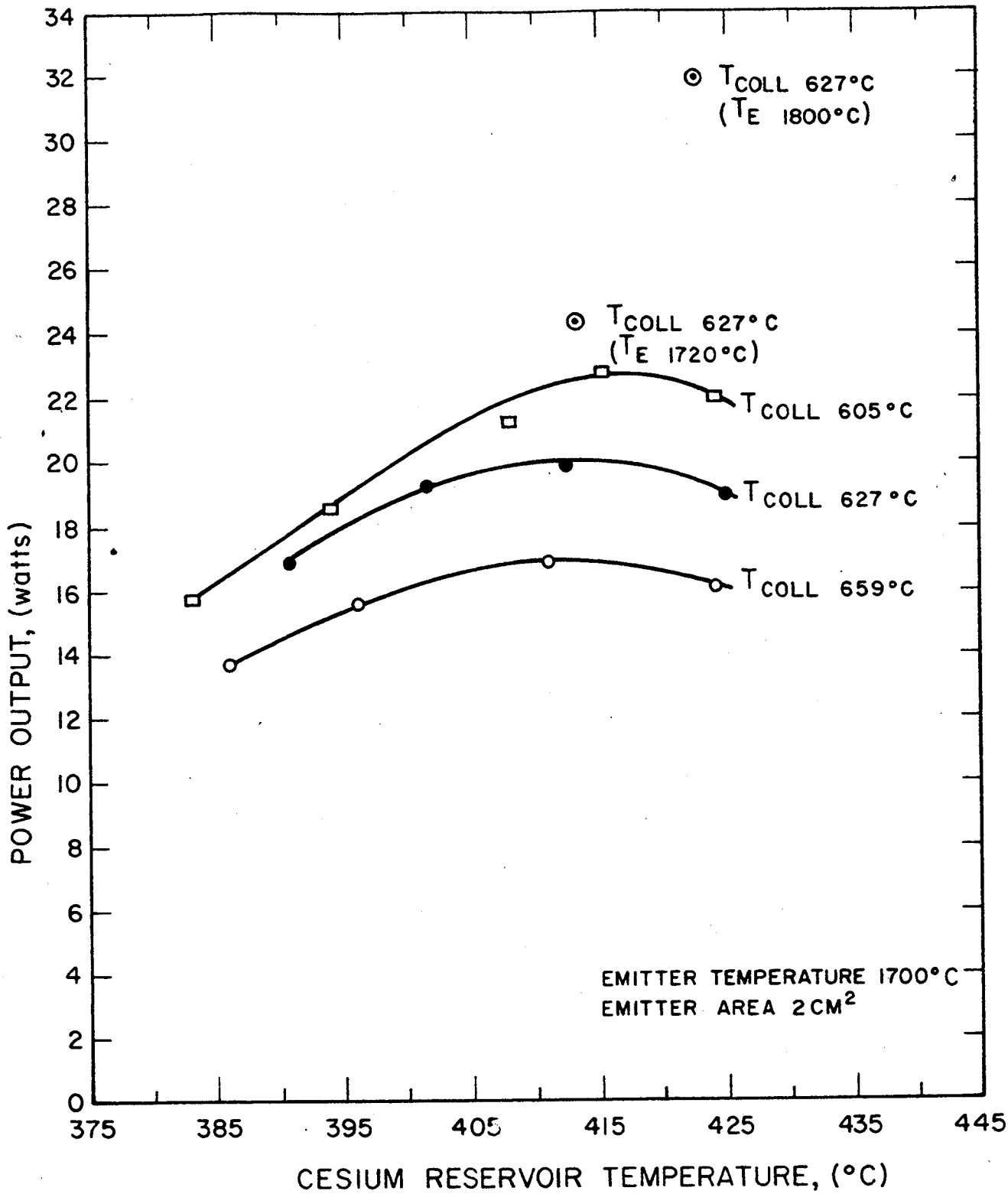

FIG. 3-14. DIODE NO. 4 POWER OUTPUT VS CESIUM RESERVOIR TEMPERATURE FOR COLLECTOR-TEMPERATURE AS THE PARAMETER

7368679

to practially achieve this performance without degradation for periods of time on the order of 1000 hours.

3.3.4 Diode No. 5

In Figure 3-15 and 3-16 are shown the volt-ampere characteristics for the diode No. 5 for 1700°C emitter temperatures and collector temperatures respectively of 630°C and 616°C. The effect of approximately a 15 to 20°C shift in collector temperature is shown by a shift in the sets of characteristics shown in these two figures. The spacing of diode No. 5 is estimated to be on the order of 1-1/2 mils. This particular diode was initially fabricated to give a closer spacing than diode No. 4. Such a result was achieved and it was found that the diode did not unshort until the temperature of approximately 1000°C was reached on the emitter. During the first several test runs on this particular converter, the collector was thermally welded to the emitter with the result that the converter had to be removed from the test set-up and mechanically stretched in order to unshort the emitter and collector. Subsequent to this stretching operation it was found that during operation the collector and emitter unshorted at room temperature, thus, giving a wider spacing than diode No. 4. The results of the wider spacing are apparent when the volt-ampere characteristics are compared. The wider spaced diode having the lower power output under optimum conditions. The possibility of the thermal welding of emitter to collector in a diode which is fabricated with the emitter and collector in contact at the braze temperature has been brought out many times in the past. The occurence of such thermal bonding of emitter to collector under operating conditions in a practical converter generator could be a very serious problem.

Figure 3-17 illustrates the variation in power output versus cesium reservoir temperature for diode No. 5, (collector temperature as a parameter). Of particular interest on this series of curves is the comparison between the curve taken after 3 hours of operation with the collector temperature optimizing at 615°C and that taken after 8

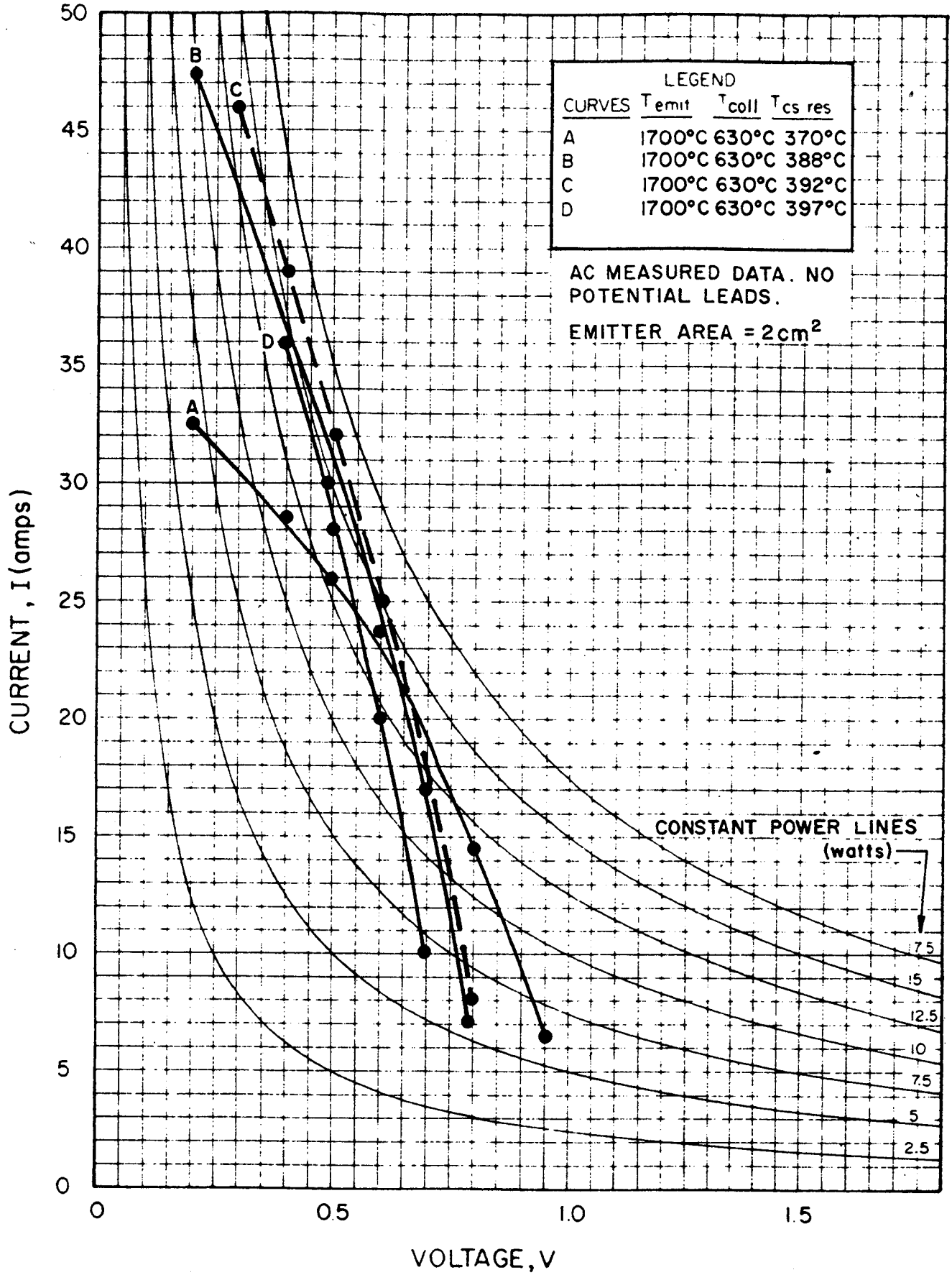

FIG. 3-15. DIODE NO. 5 CURRENT-VOLTAGE CHARACTERISTICS

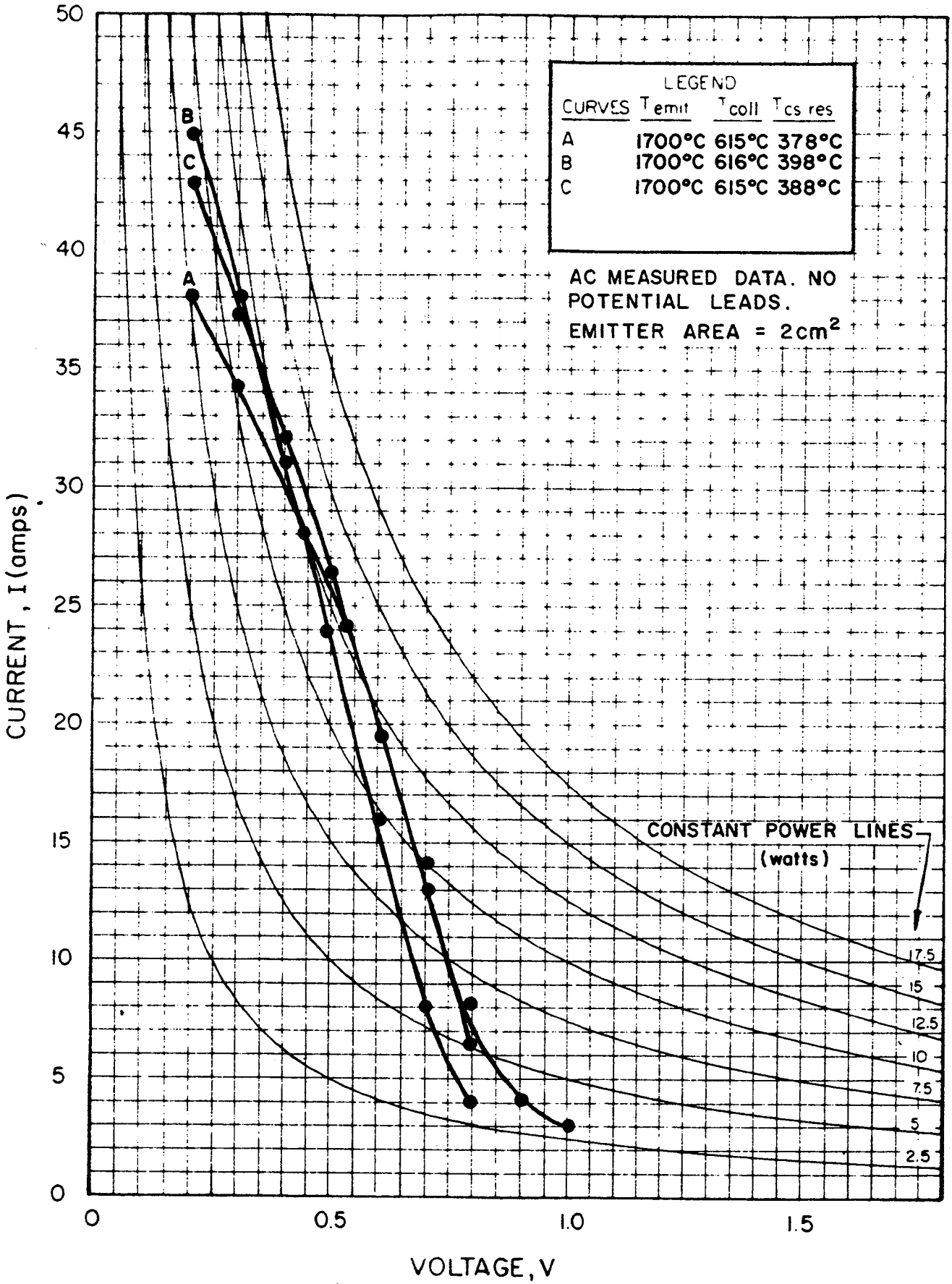

FIG. 3-16. DIODE NO. 5 CURRENT-VOLTAGE CHARACTERISTICS

7368682

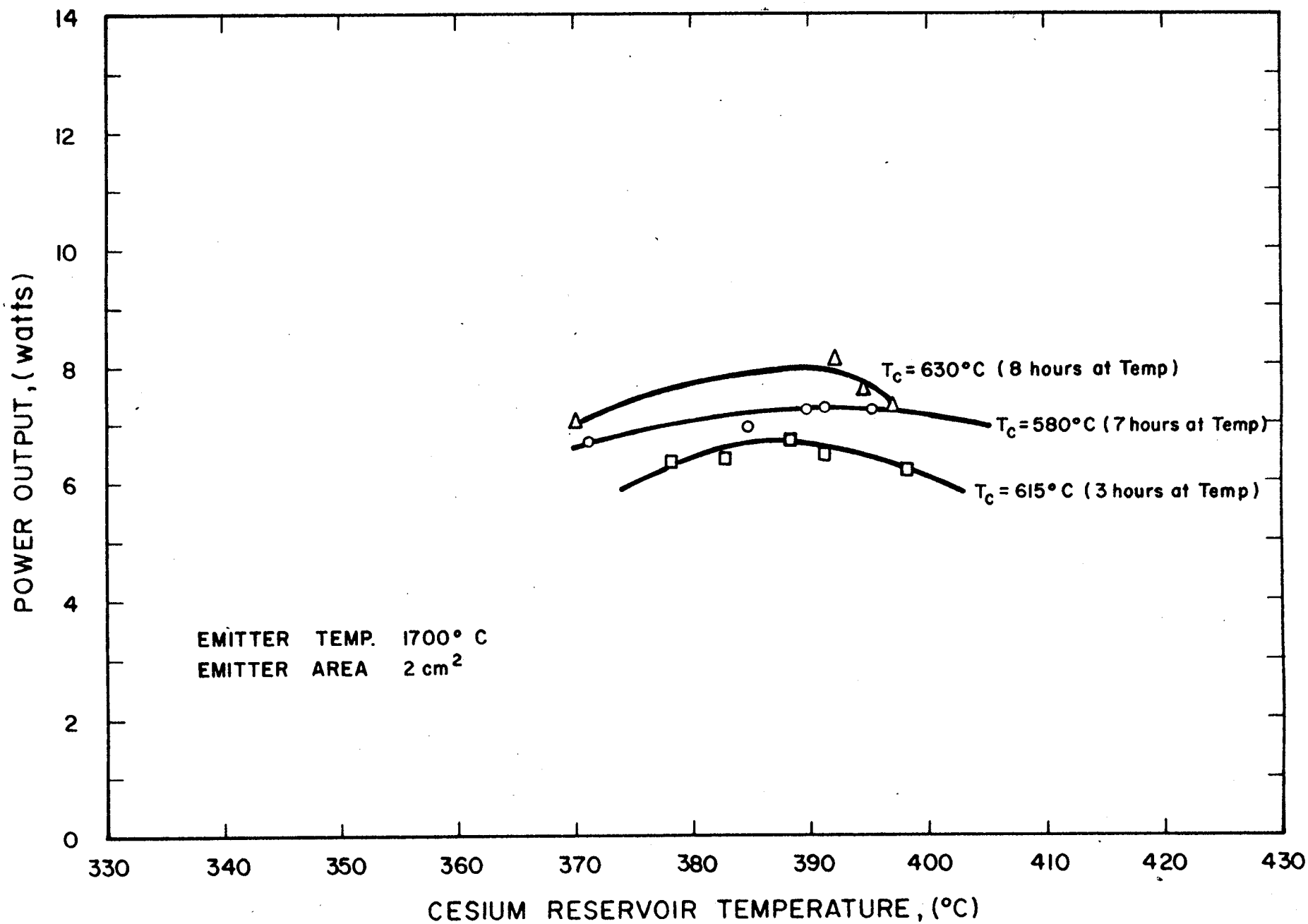

FIG. 3-17. DIODE NO. 5 POWER OUTPUT VS CESIUM TEMPERATURE FOR COLLECTOR TEMPERATURE AS THE PARAMETER

hours of operation where the collector temperature optimized at 630°C and yielded a higher power output. In evidence is the effect of aging the collector for a number of hours at high temperature after the converter has begun operation. It is estimated that the true surface collector temperature in these sets of curves was on the order of 850°C. This particular converter may still be undergoing an "aging-in" process on the collector.

3.3.5 Diode No. 6

Converter No. 6 was fabricated to achieve closer spacing than in converter No. 5. Converter No. 6 did not unshort until an emitter temperature of approximately 950°C is reached. Figure 3-18 compares the volt-ampere characteristics at an emitter temperature of 1700°C. Under conditions of ac sweeping a collector temperature of 605°C was obtained which optimized the output of converter No. 6 at about 19-19.5 watts output. At this optimum output the reservoir temperature was considerably lower than previously noted for other diodes, suggesting that higher cesium pressures would yield higher output, raising the pressure resulted in higher currents from the emitter which raised the collector temperature and deviated from optimum conditions. Figure 3-19 is a display of power output as a function of cesium temperature with collector temperature as the parameter held constant. Random fluctuations in the collector thermocouple offered further evidence that the couple was improperly attached to the collector. Moreover, the inability to optimize the device at the condition of dc operation due to the high collector temperature suggested a new method of radiator attachment.

3.3.6 Diode No. 7

Diode No. 7 was the first EOS converter fabricated without positively spaced electrodes. At room temperature this diode was in a shorted condition, and opened approximately at an estimated emitter temperature of 400-500°C, indicating a slightly wider spacing than diodes No. 4 and No. 6. Diode No. 7 was also the first high

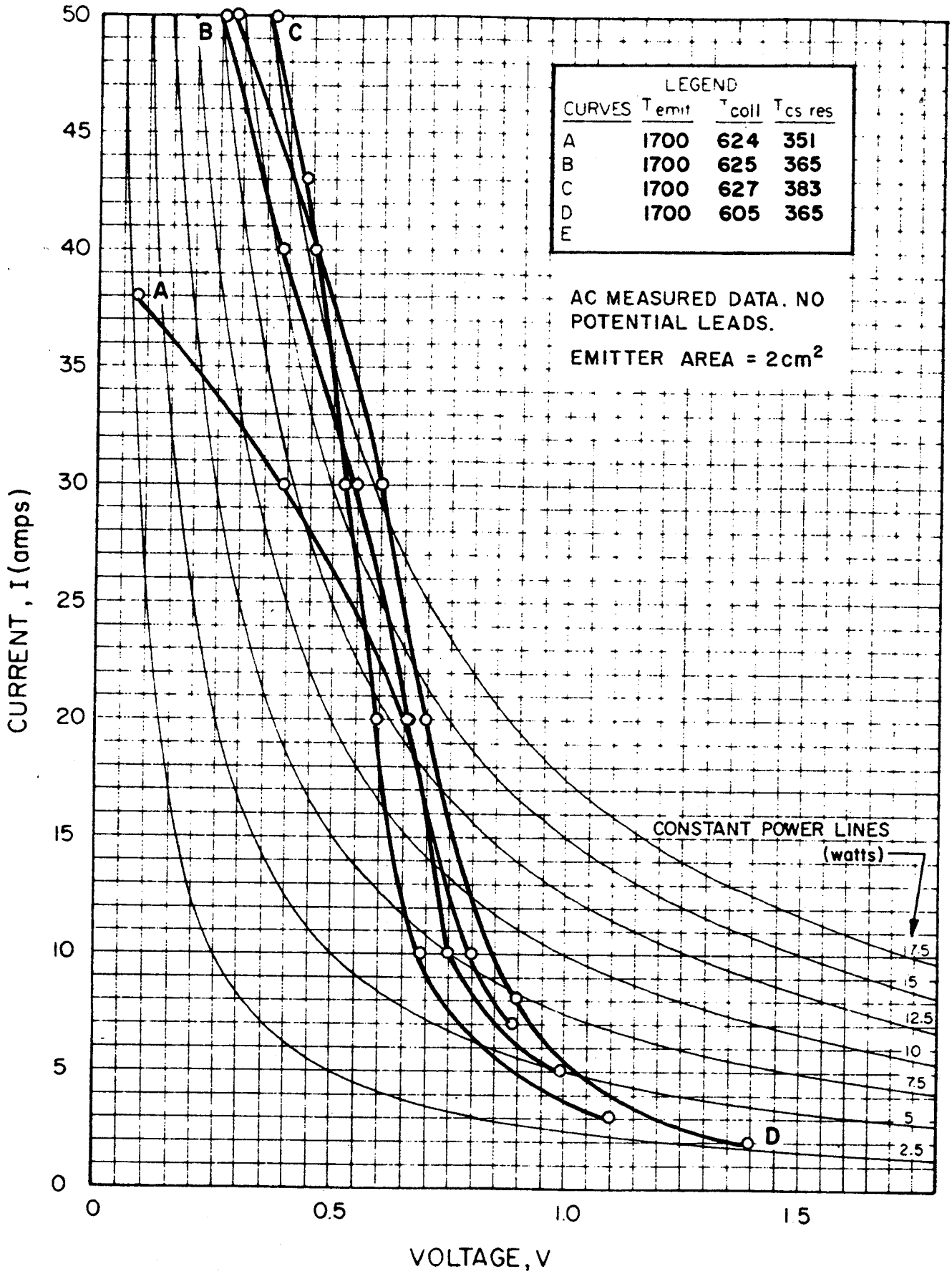

3380-Final FIG. 3-18 I-V CHARACTERISTICS FOR DIODE NO. 6

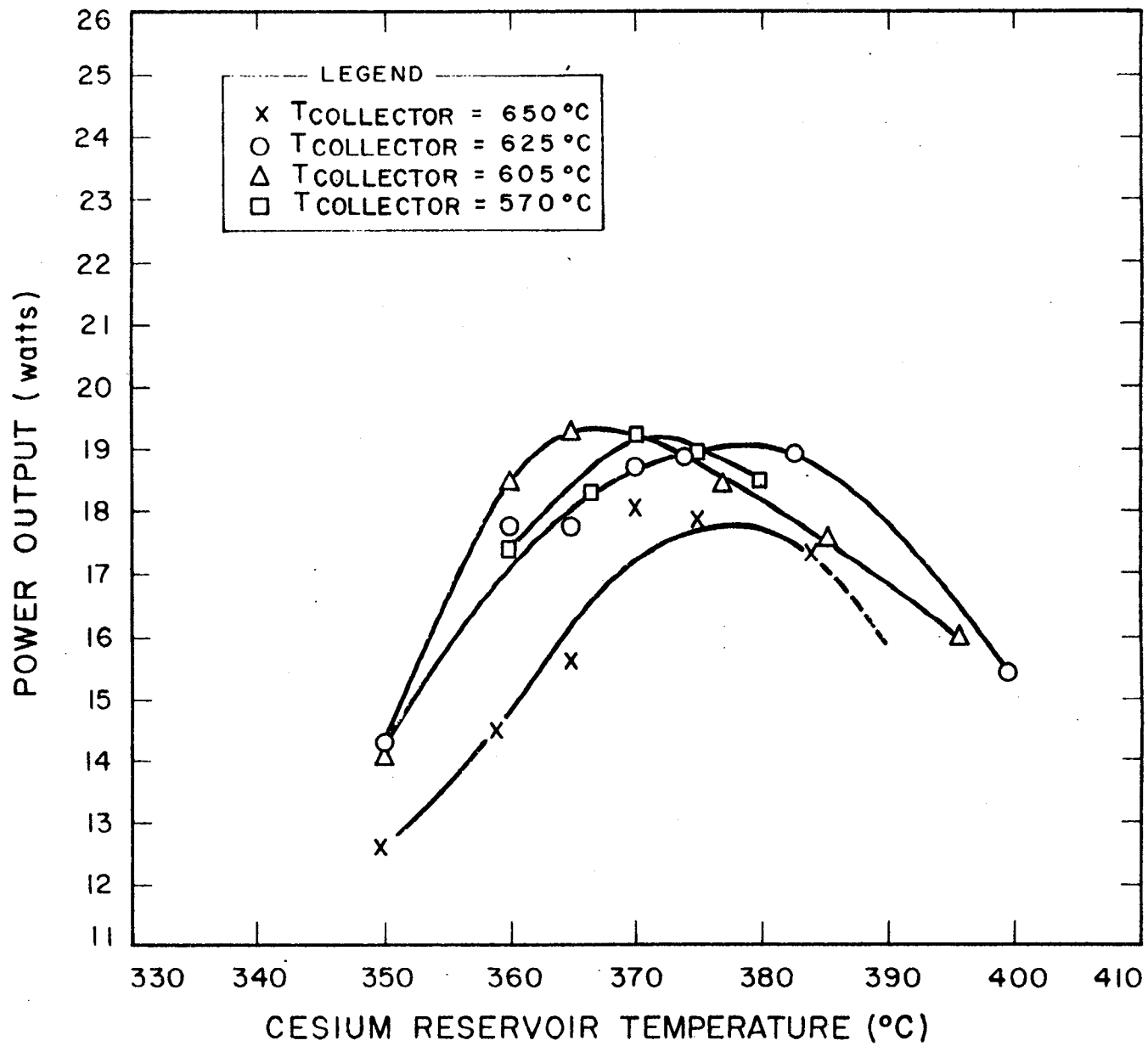

FIG. 3-19 POWER OUTPUT VERSUS CESIUM RESERVOIR TEMPERATURE FOR DIODE NO. 6

performance converter which employed the brazed radiator-collector assembly. Figure 3-20 contains three dynamic I-V curves obtained at an emitter temperature of 1700°C. Figure 3-21 is a plot of the power output as a function of cesium temperature with the collector temperature as the parameter of interest. The curves in Figure 3-21 appear to vary more smoothly than previously noted. This has suggested that the collector thermocouple was bonded to the collector during the braze operation. The braze operation on converter No. 7 appeared reasonably successful since the maximum DC operation point of 25 watts occurred at a collector temperature of 613°C, a temperature previously unobtainable during DC operation.

3.3.7 Diode No. 8

Diode No. 8 was the second EOS converter to be fabricated without positive-spaced electrodes. At room temperature, the electrodes were in a shorted condition which opened after heating the emitter to about 600°C. This spacing was nearly identical to diode No. 7. Diode No. 8 collector was also brazed to the radiator clamp. Figures 3-22 and 3-23 are the I-V characteristics and power output curves for an emitter temperature of 1700°C. In comparison to diode No. 7, the AC obtained power output was slightly less. In addition, the collector temperature operated at 642°C for the maximum DC power output. It is possible that the collector-radiator braze operation on diode No. 8 was not as successful as it was on diode No. 7.

3.3.8 Diode No. 9

Diode No. 9 was fabricated near the conclusion of the program and did receive thorough testing. The I-V characteristics of this diode are shown in Figure 3-24. The emitter was fabricated from tantalum bar stock displaying a saturated emission near 25 amperes. The voltage output of this diode at 25 amperes compared closely with diodes No. 7 and No. 8.

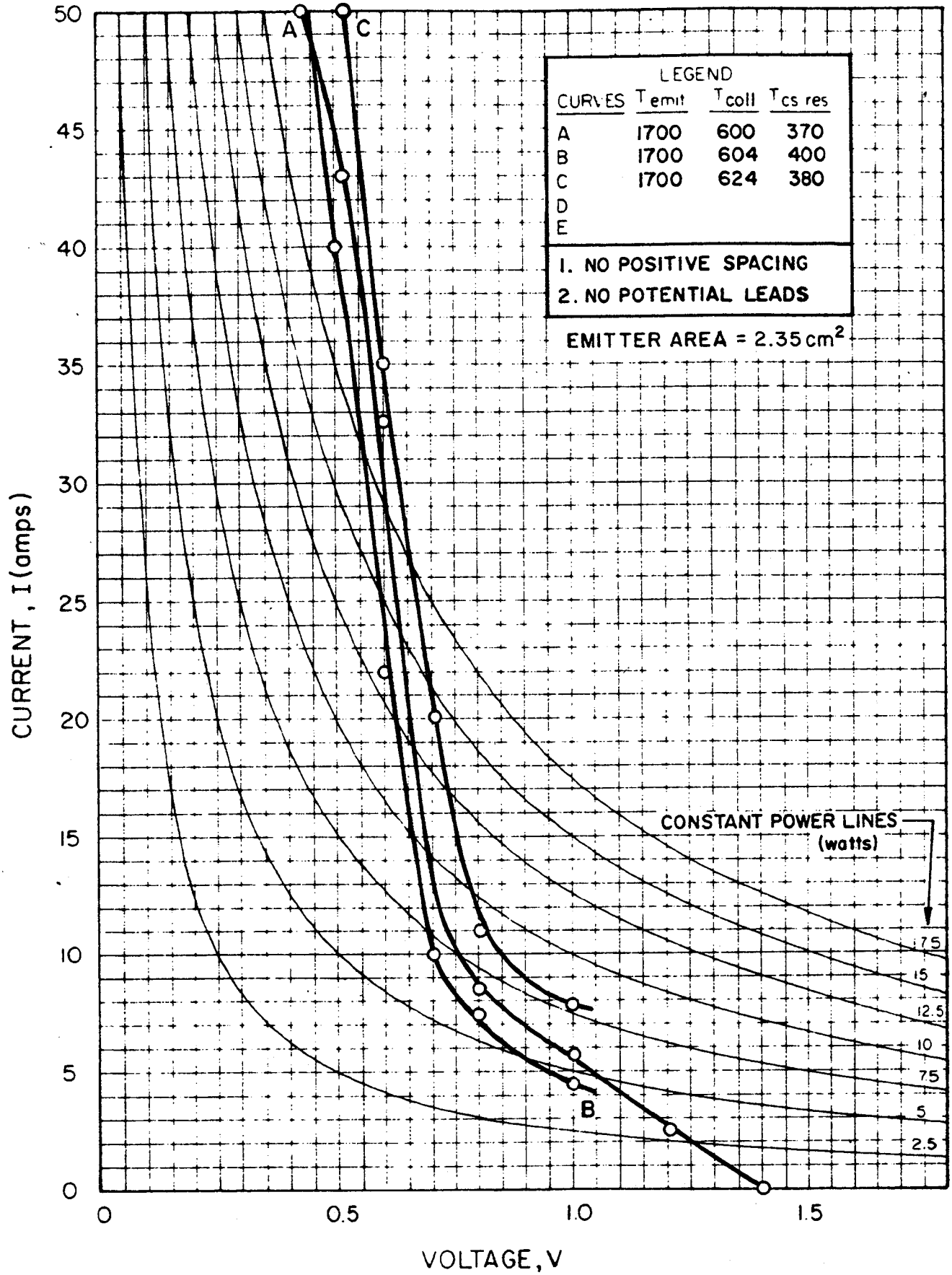

FIG. 3-20 I-V CHARACTERISTICS FOR DIODE NO. 7

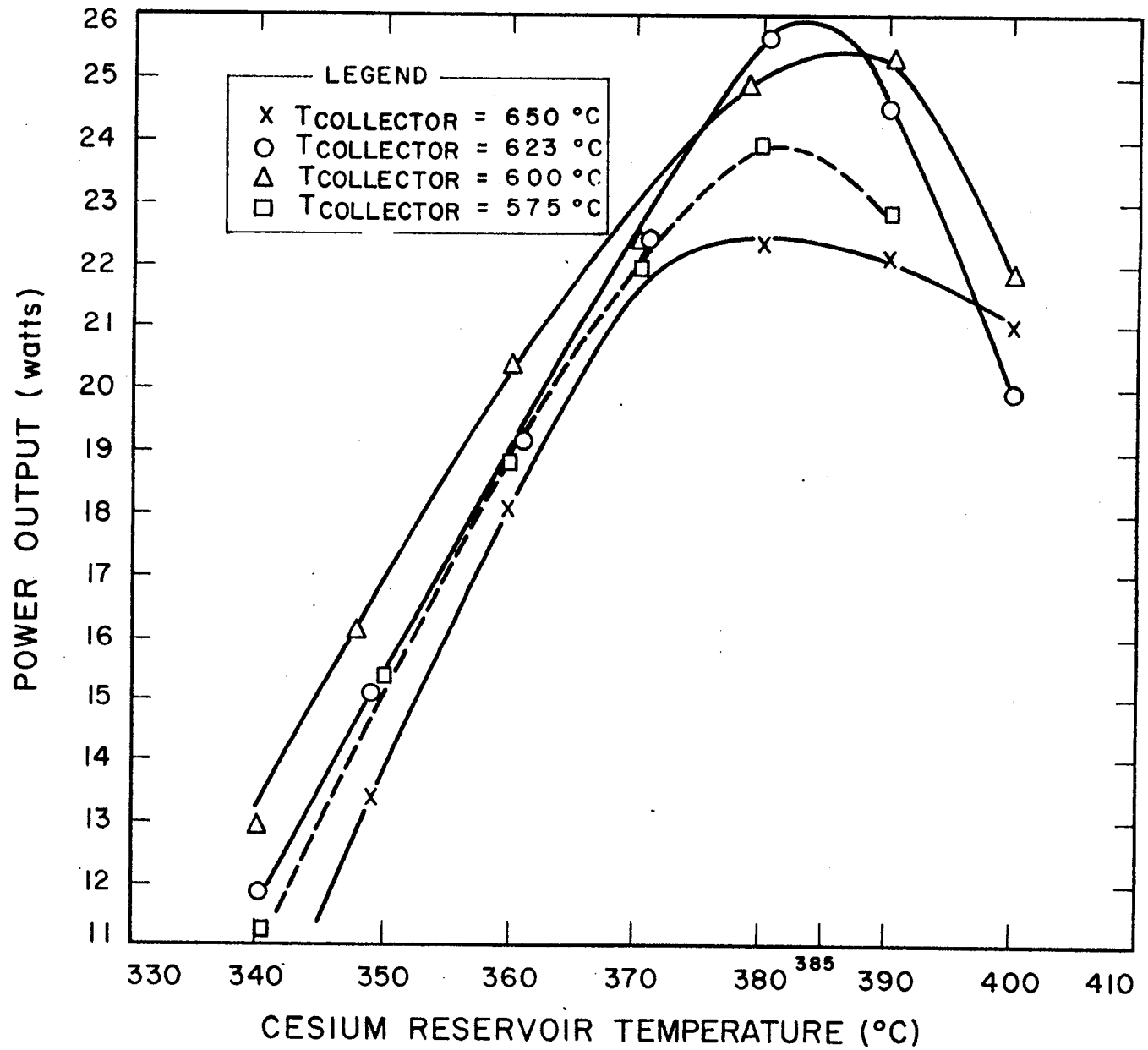

FIG. 3-21 POWER OUTPUT VS. CESIUM RESERVOIR TEMPERATURE FOR DIODE NO. 7

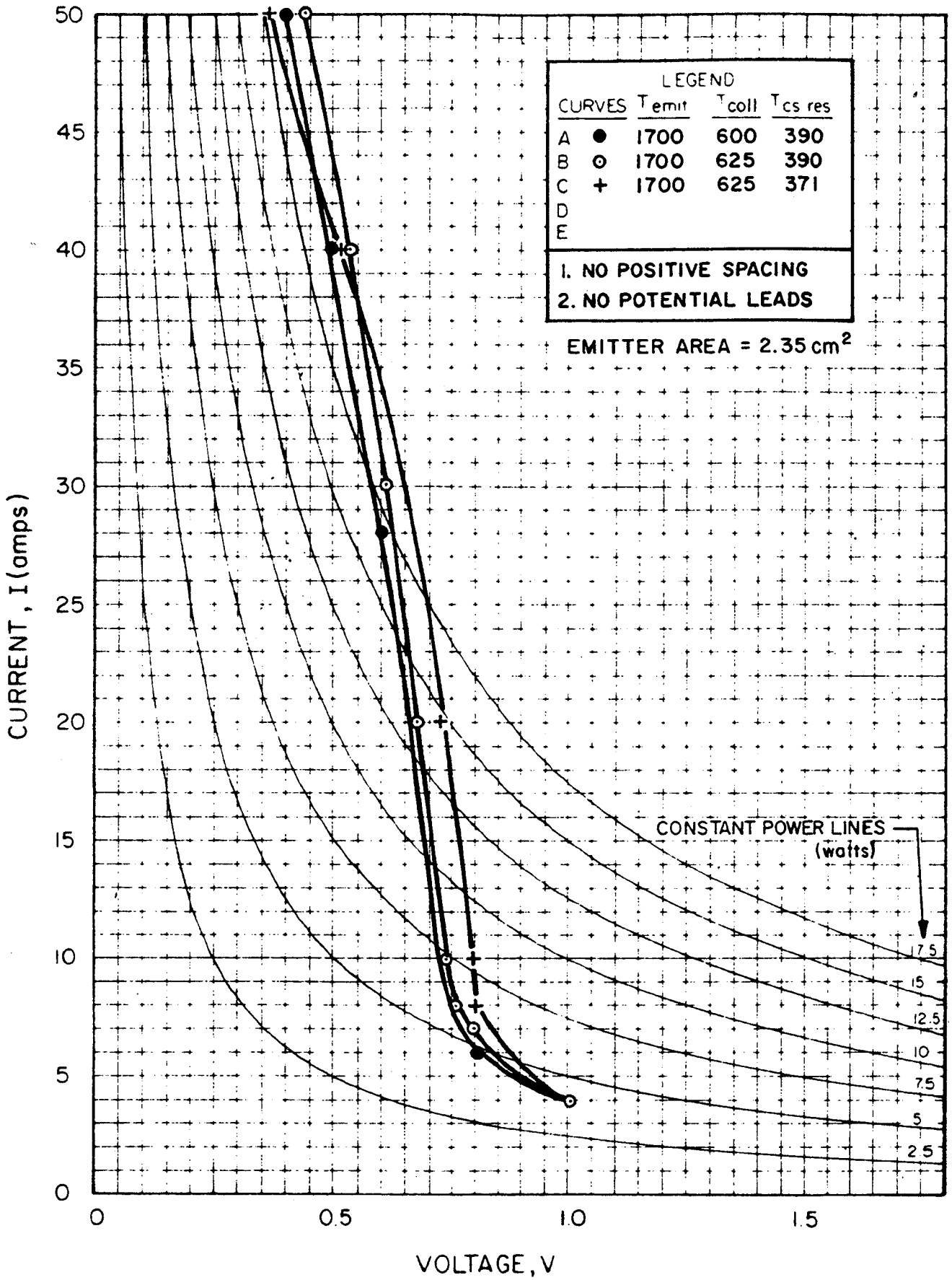

FIG. 3-22 I-V CHARACTERISTICS FOR DIODE NO. 8

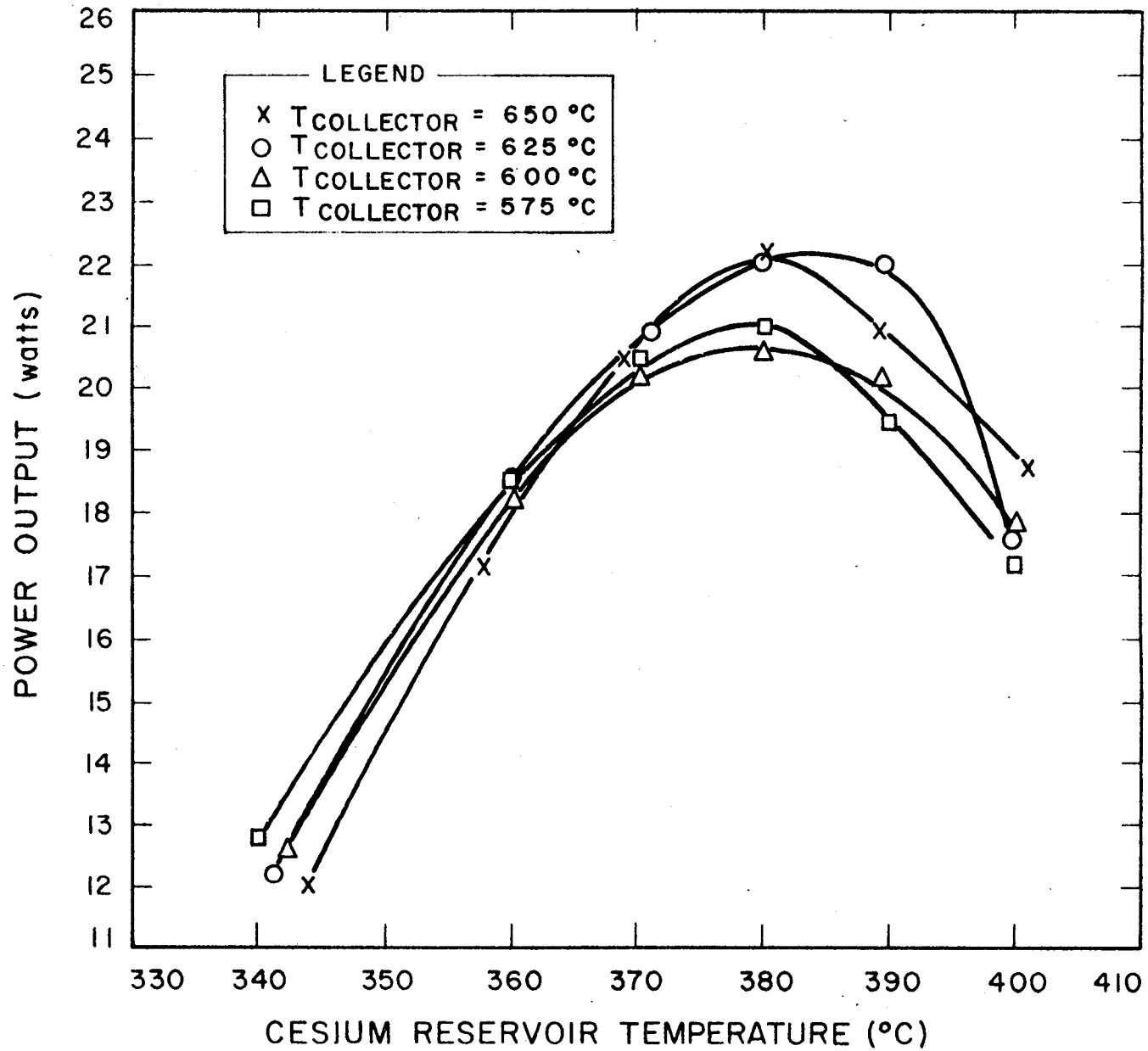

FIG. 3-23 POWER OUTPUT VERSUS RESERVOIR TEMPERATURE FOR DIODE NO. 8

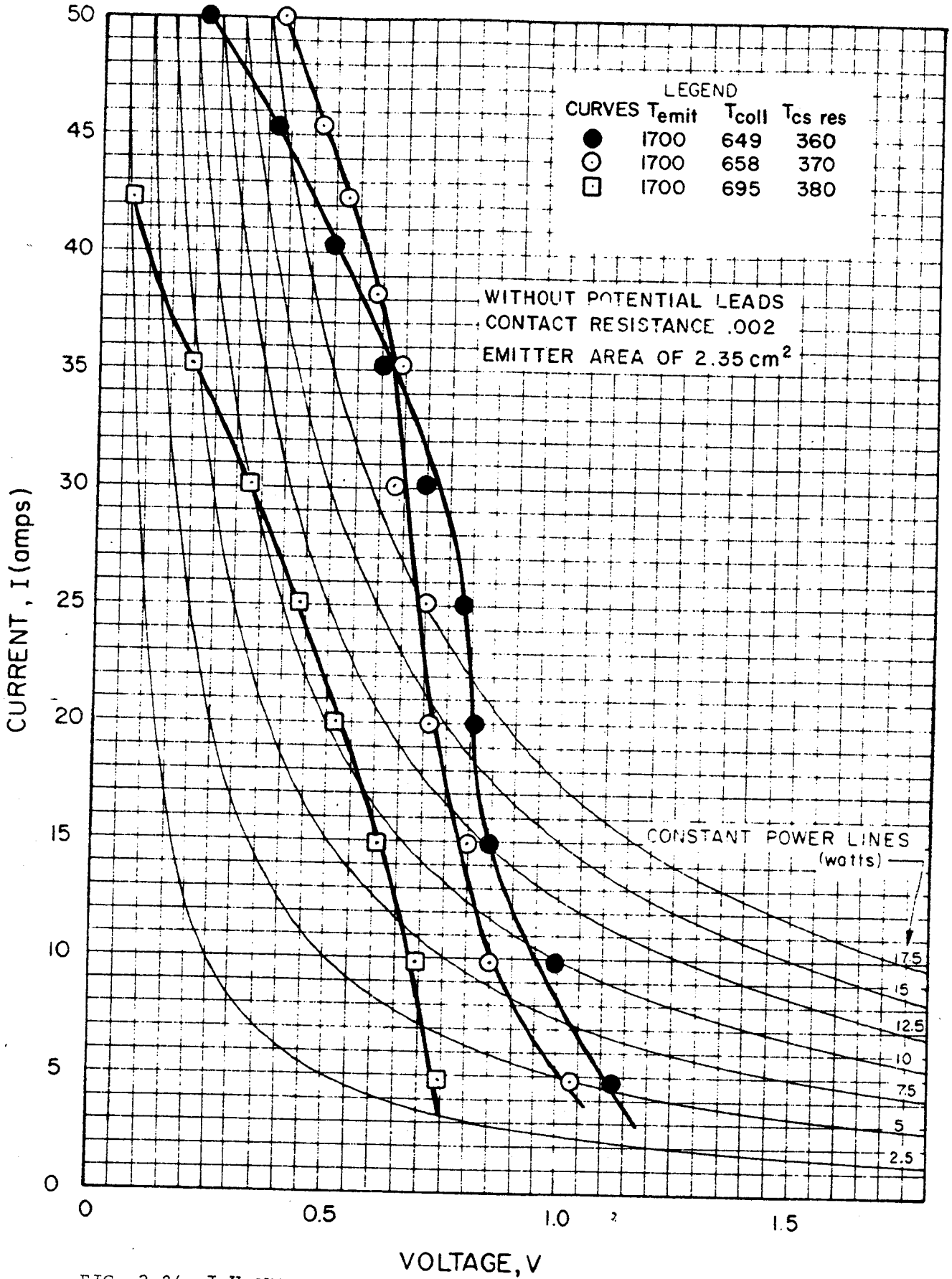

FIG. 3-24 I-V CHARACTERISTICS FOR DIODE NO. 9

3.4 Raw Data From Converter Tests

The raw test data from converters No. 1 through No. 8 are listed in the Appendix on standard diode test sheets that include all pertinent test control points and space for observations and remarks. Unless specifically indicated on the data sheet, voltage measurements were not made with potential leads. AC sweep pictures were not taken at maximum DC operating points, unless specified.

3.5 Metallurgical Examination

The No. 1 converter was operated at 200 hours at an emitter temperature of 1700°C ± 20°C. The cesium vapor pressure approximated 7 to 10 mm Hg. It was felt that 200 hours of continuous operation plus the original parametric testing of 30 hours would sufficiently "age" the component parts for a meaningful metallurgical examination. The areas of interest for examination have been tentatively identified in Fig. 3-25.

3.5.1 Ceramic-Metal Seal

Figure 3-26 is a close-up of the ceramic-metal seal illustrating the arrangement of the ceramic and sealing flanges. Figure 3-27 is a higher magnification of the seal area. Figure 3-28 is a 200 X magnification of the seal that reveals no apparent stress cracks or embrittlement resultant from the sealing operation.

3.5.2 Envelope-Flange Assembly Braze

Figure 3-29, an 11 X magnification of the envelope-flange braze, illustrates the full joining of the tantalum-niobium structure by titanium.

3.5.3 Collector-Reservoir Tubulation Braze

Figure 3-30 is an 11 X magnification of the collector-reservoir tubulation braze. The titanium has appeared to join the niobium properly but has pulled away from the molybdenum collector.

3.5.4 Collector-Clamp Braze

Figure 3-31 illustrates the initial feasibility braze of joining the collector to the radiator clamp. The braze material (B.T.) has not adhered properly over the parts as indicated by large voids in the figure.

3.5.5 Reservoir-Tubulation -- Reservoir Weld

Figure 3-32 displays the copper to niobium weld area at the reservoir-reservoir tubulation junction. The weld appears to possess good integrity at the interface.

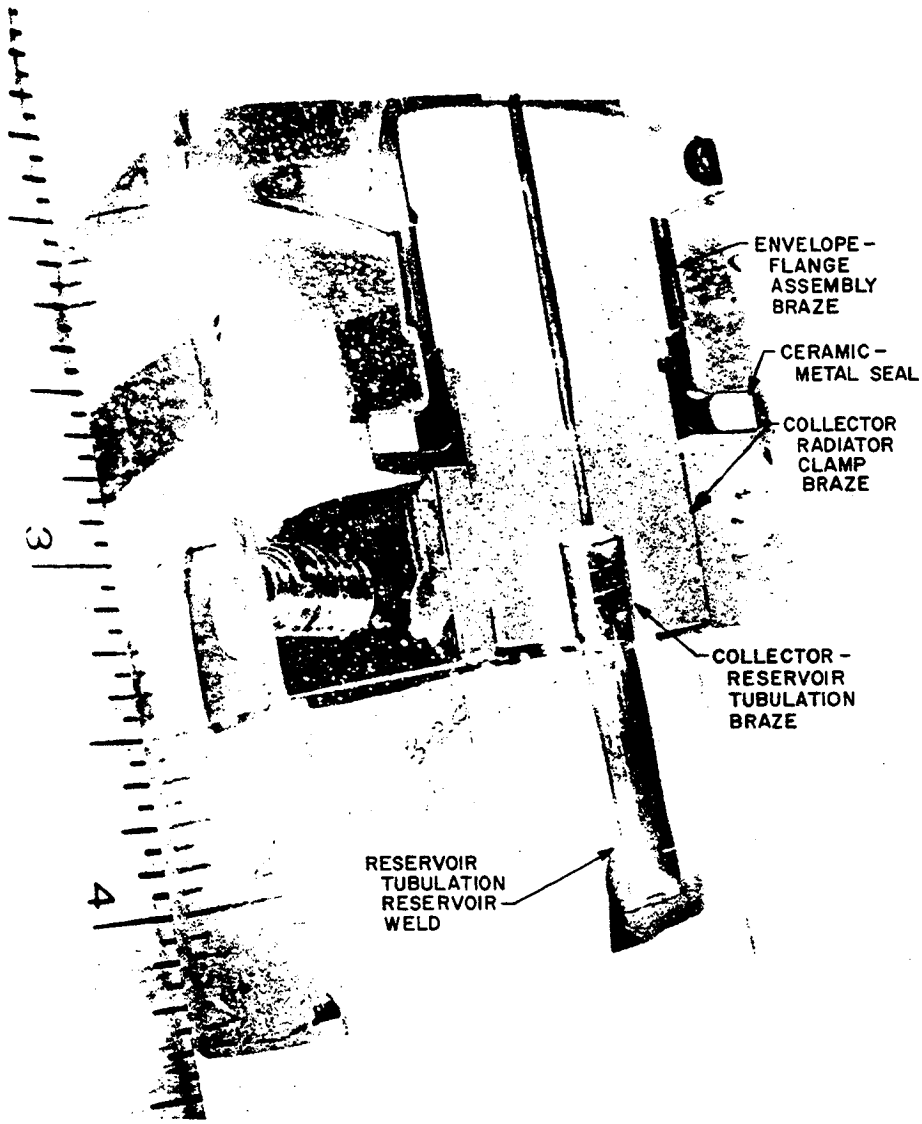

FIG. 3-25 MACRO-SECTION OF DIODE NO. 1 AFTER 200 HOUR TEST

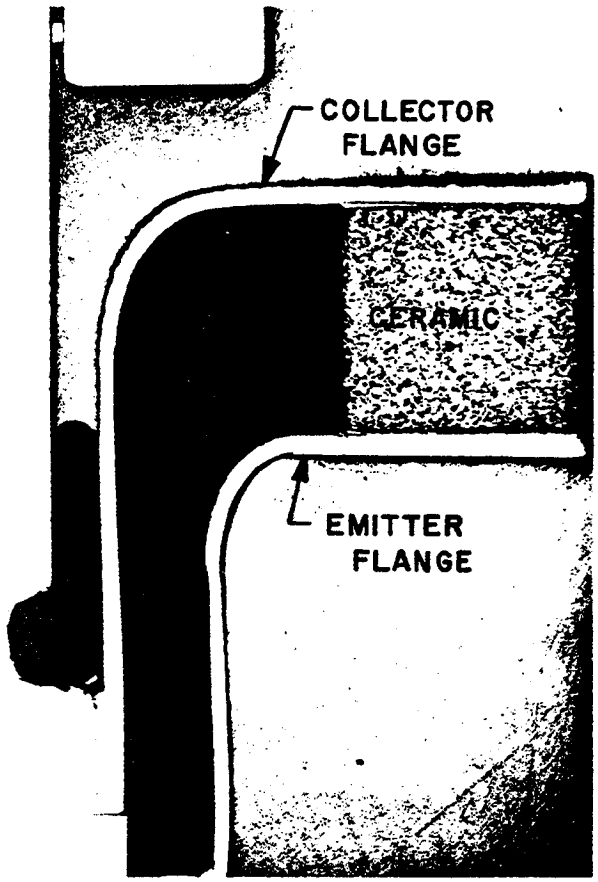

FIG. 3-28 11X MAGNIFICATION OF CERAMIC METAL SEAL

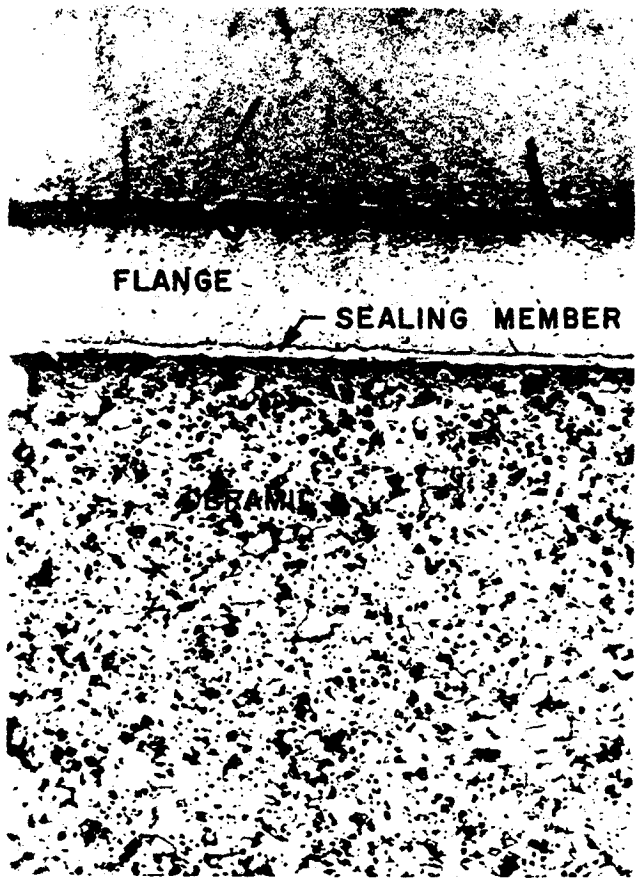

FIG. 3-27 75X MAGNIFICATION OF SEAL AREA

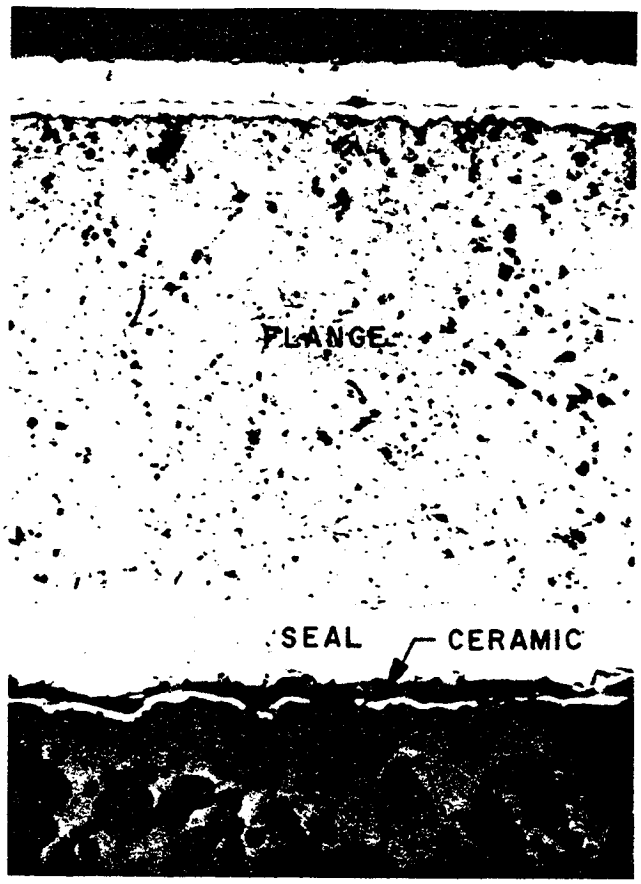

FIG. 3-22 200X MAGNIFICATION OF SEAL

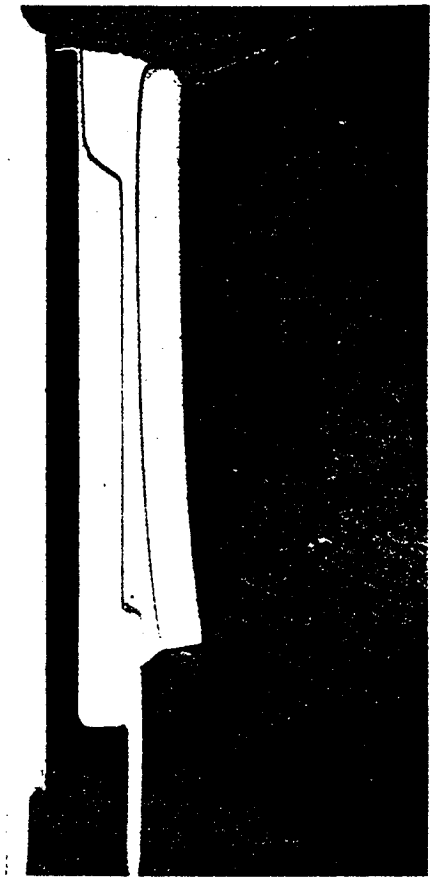

FIG. 3-29 11X MAGNIFICATION OF ENVELOPE-FLANGE ASSY BRAZE

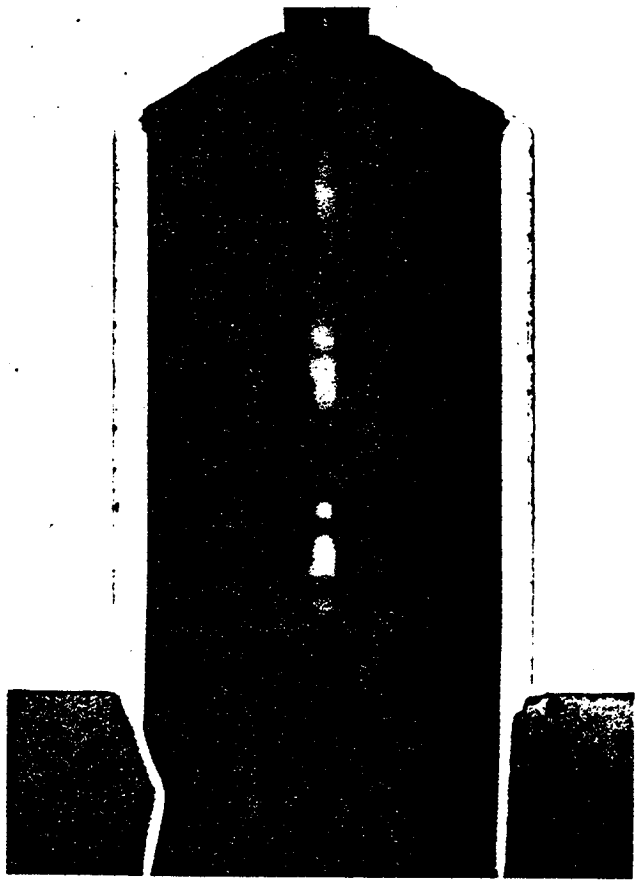

FIG. 3-30 11X MAGNIFICATION OF COLLECTOR RESERVOIR TUBULATION BRAZE

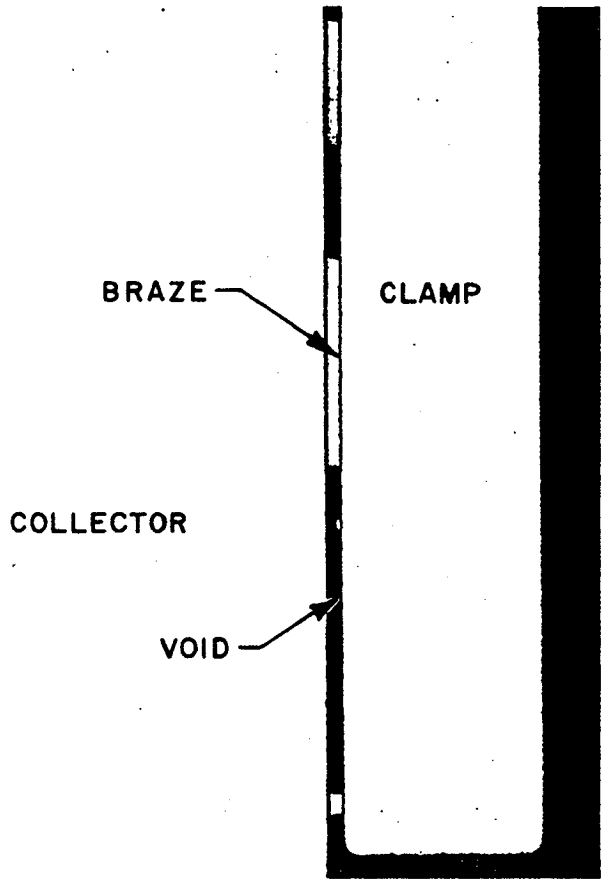

FIG. 3-31 11X MAGNIFICATION OF CLAMP-COLLECTOR BRAZE

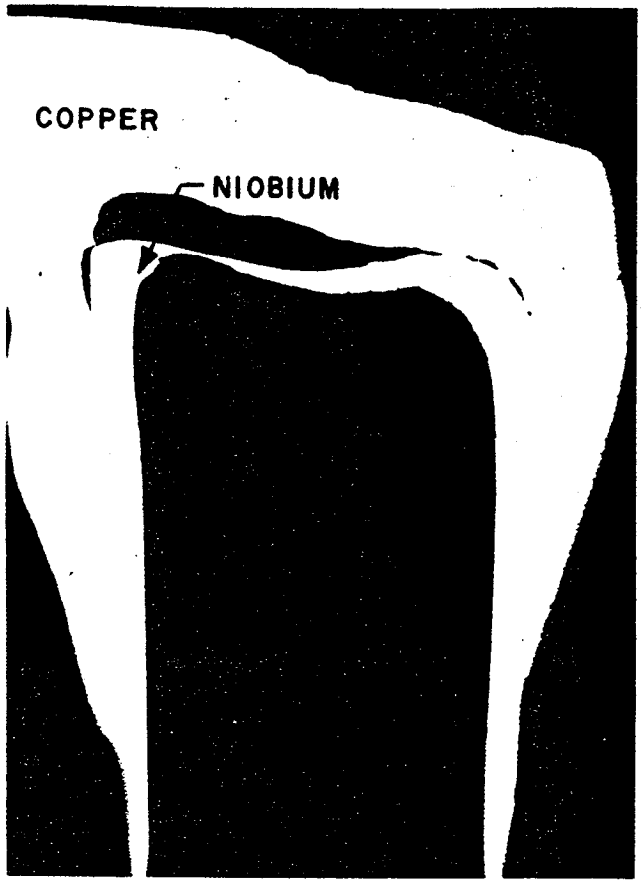

FIG. 3-32 11X MAGNIFICATION OF COPPER-NIOBIUM WELD

4. THREE-CONVERTER GENERATOR

4.1 Generator-Converter Fabrication and Test

4.1.1 Generator-Converter Fabrication

Three generator converters were fabricated for assembly in a three-converter, prototype generator. The converter components for the generator converters remain the same as the components for diode converters 1 through 8, except for the emitter. The emitters for the generator converters were machined from bar stock tantalum to most efficiently and economically accommodate the design as depicted in Drawing No. 12251 in the appendix. However, the unknown crystallographic nature of this surface parallel to the axis of bar stock tantalum is highly oriented in some directions, but not in others. Thus, without x-ray diffraction analysis to indicate the crystallographic direction, the preferred surface may or may not be selected from the bar. This could amount to a penalty for thermionic diodes, since the proper orientation defines the proper work function which, in turn, determines the emission capabilities of the emitter.

The fabrication schedule for diodes 1 through 8 and the generator converters differ in the emitter-envelope joining. Initial attempts at heliarc welding, the most massive emitters to the envelope structure were unsatisfactory. The added thermal capacity of the emitter required greater input of heat to the weld joint, which resulted in the envelope buckling. In place of heliarc welding this assembly, we decided in favor of electron-beam welding. The initial feasibility of the weld and a completed assembly are illustrated in Fig. 4-1.

The cleaning and processing schedules for the generator-converters were in accordance with converters 1 through 8. The flow chart sequence was also the same. The generator-converter emitters were full face, with no positive spacing technique employed. The radiator clamp

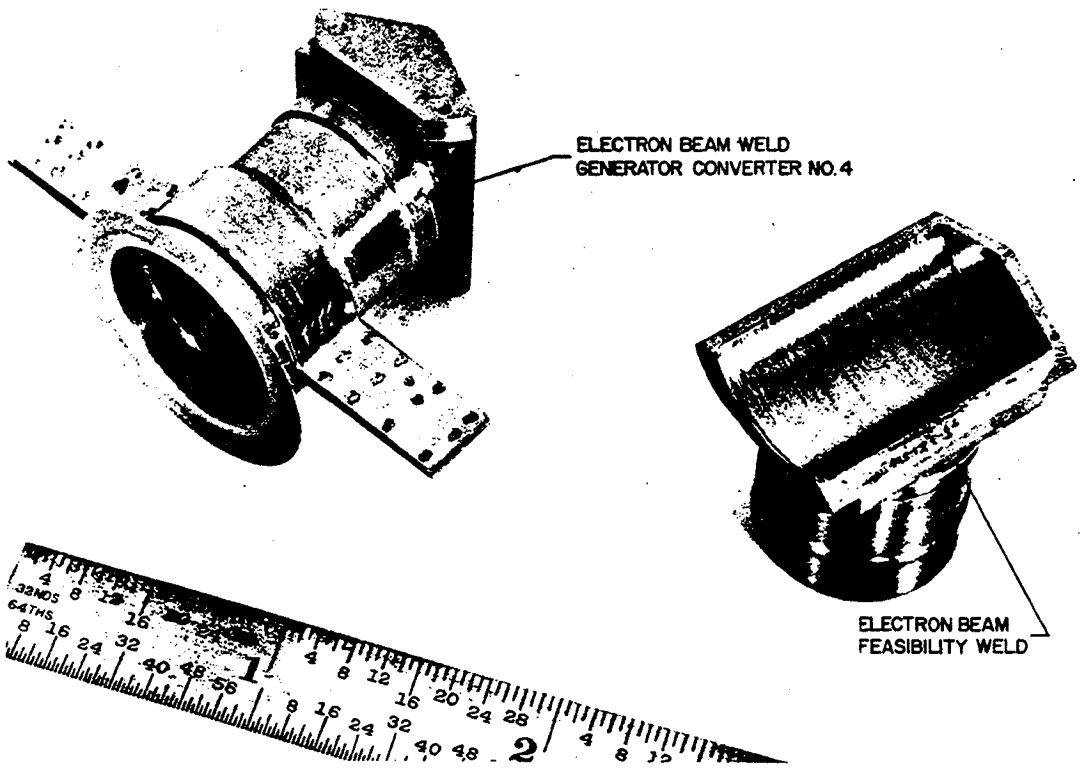

FIG. 4-1 GENERATOR CONVERTER EMITTER STRUCTURE

assemblies were brazed with 0.001 inch B.T. shim, placed between collector and clamp. Moreover, no heaters were added to the radiator fins, since we have identified the collector problem as one of heat rejection, not heat addition.

4.1.2 Generator-Converter Test

The individual generator-converters Nos. 2, 3, and 4 were individually tested for performance prior to assemblying the generator. The purpose of pretesting was two-fold: to ascertain if the diode output was acceptable (on the order of 20 watts or higher), and to obtain individual I.V. characteristics at different emitter temperatures with fixed reservoir and collector temperature. In this manner the converter-emitter temperature could be reasonably estimated during generator operation when the emitter temperature is unknown. The following text is an analysis of the individual I.V. characteristics of generator converters No. 2, 3, and 4.

Converter No. 2. The I.V. characteristics for generator converter No. 2 are displayed in Fig. 4-2 for emitter temperatures of 1500°C, 1600°C, and 1700°C. The maximum dc power output of this diode at an emitter temperature of 1700°C was 19.5 watts (28.2 amperes x 0.685 volts), as measured with potential leads. The cesium reservoir temperature at this maximum was 378°C. The electrodes were opened at room temperature.

Converter No. 3. The I.V. characteristics for generator-converter No. 3 are displayed in Fig. 4-3 for emitter temperatures of 1500°C, 1600°C, and 1700°C. The maximum DC power output of this diode at an emitter temperature of 1700°C was 17 watts (27.2 amperes x 0.618 volts). The cesium reservoir temperature at the maximum was 368°C. The electrodes were opened at room temperature.

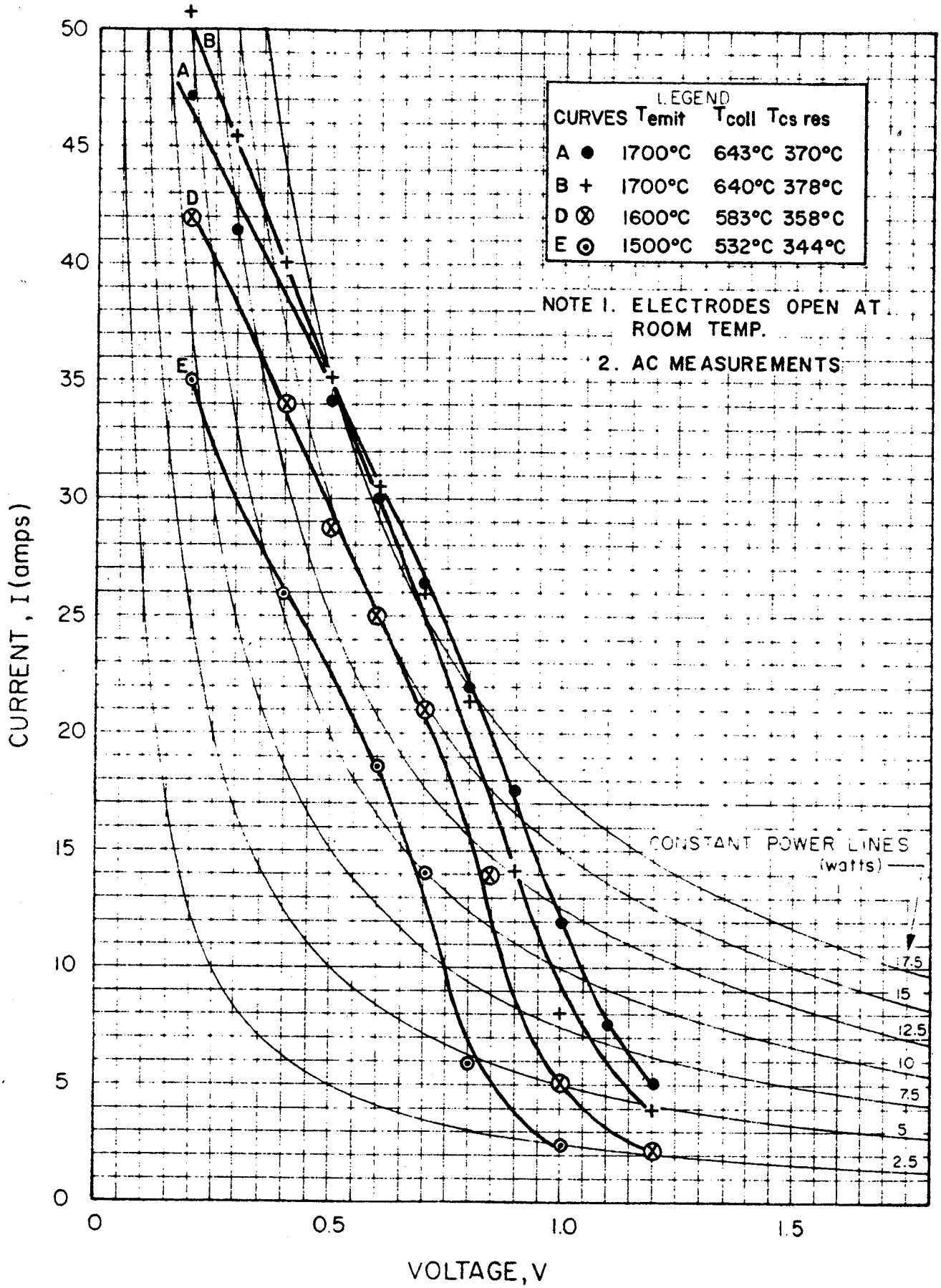

FIG. 4-2 I-V CHARACTERISTICS FOR GENERATOR-CONVERTER NO. 2

7369487

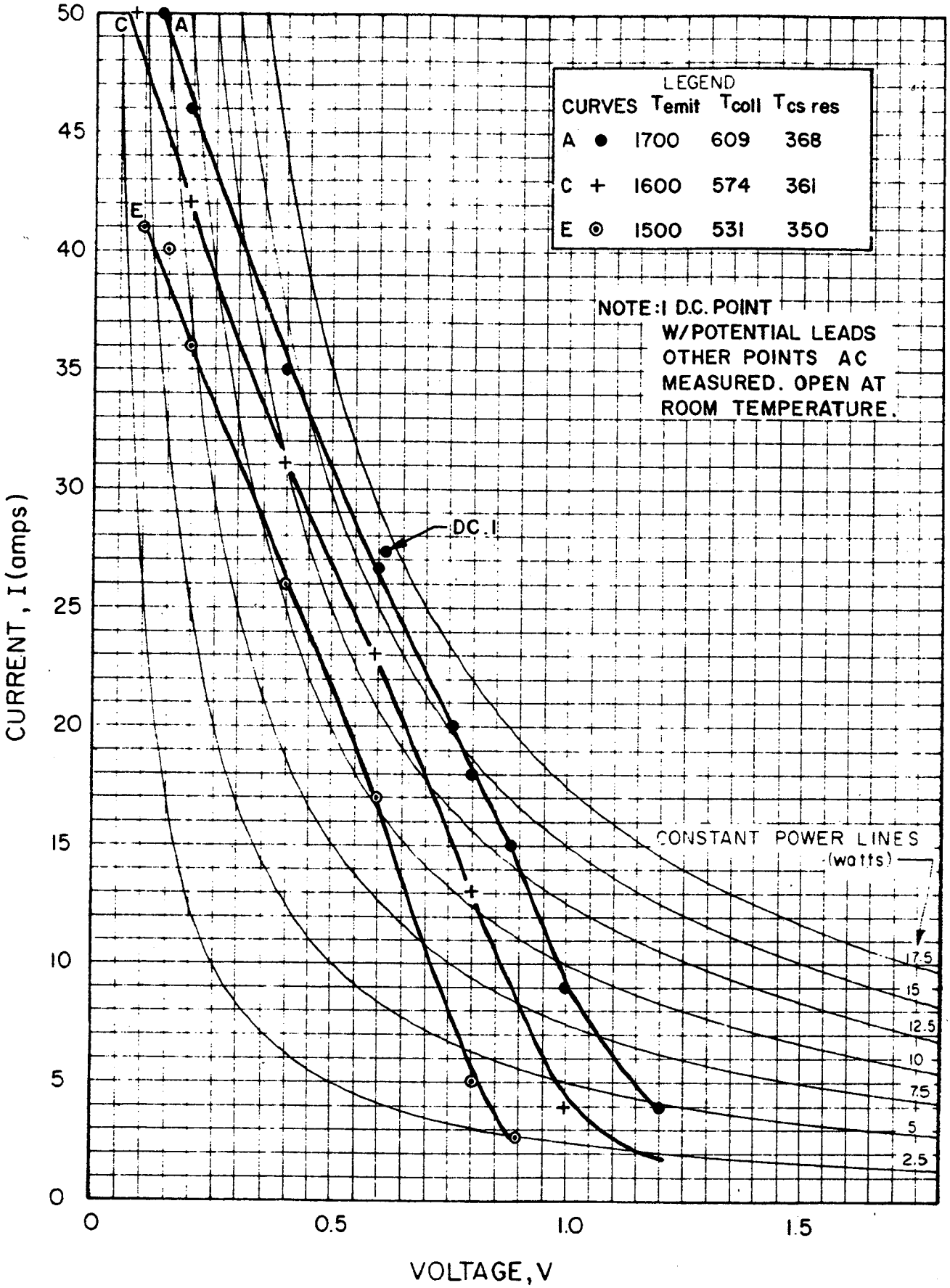

FIG. 4-3 I-V CHARACTERISTICS FOR GENERATOR-CONVERTER NO. 3

Converter No. 4. Generator-converter No. 4 operated at a DC power level of 21.2 watts (without potential leads) at an emitter temperature of 1700°C. Again, the electrodes were shorted at room temperature and parted at 400 to 500 degrees C. The spacing at 1700°C was approximately 1 mil. The saturated emission from each converter was compared at a cesium reservoir temperature of 379°C. Converters No. 2 and No. 3 for these set of conditions each saturated at about 25 amperes, while converter No. 4 saturated at 32 amperes. On this basis we are attributing the enhanced saturated emission from converter No. 4 to the crystal orientation of the emitter. The spacing or collector temperature cannot influence the saturated emission from an emitting surface.

Converter No. 5. Generator-converter No. 5 operated at a DC power level of 21.6 watts (without potential leads) at an emitter temperature of 1700°C. The saturated emission from No. 5 is approximately 25 amperes as indicated in Figure 4-5, which compares closely to generator converter No. 4.

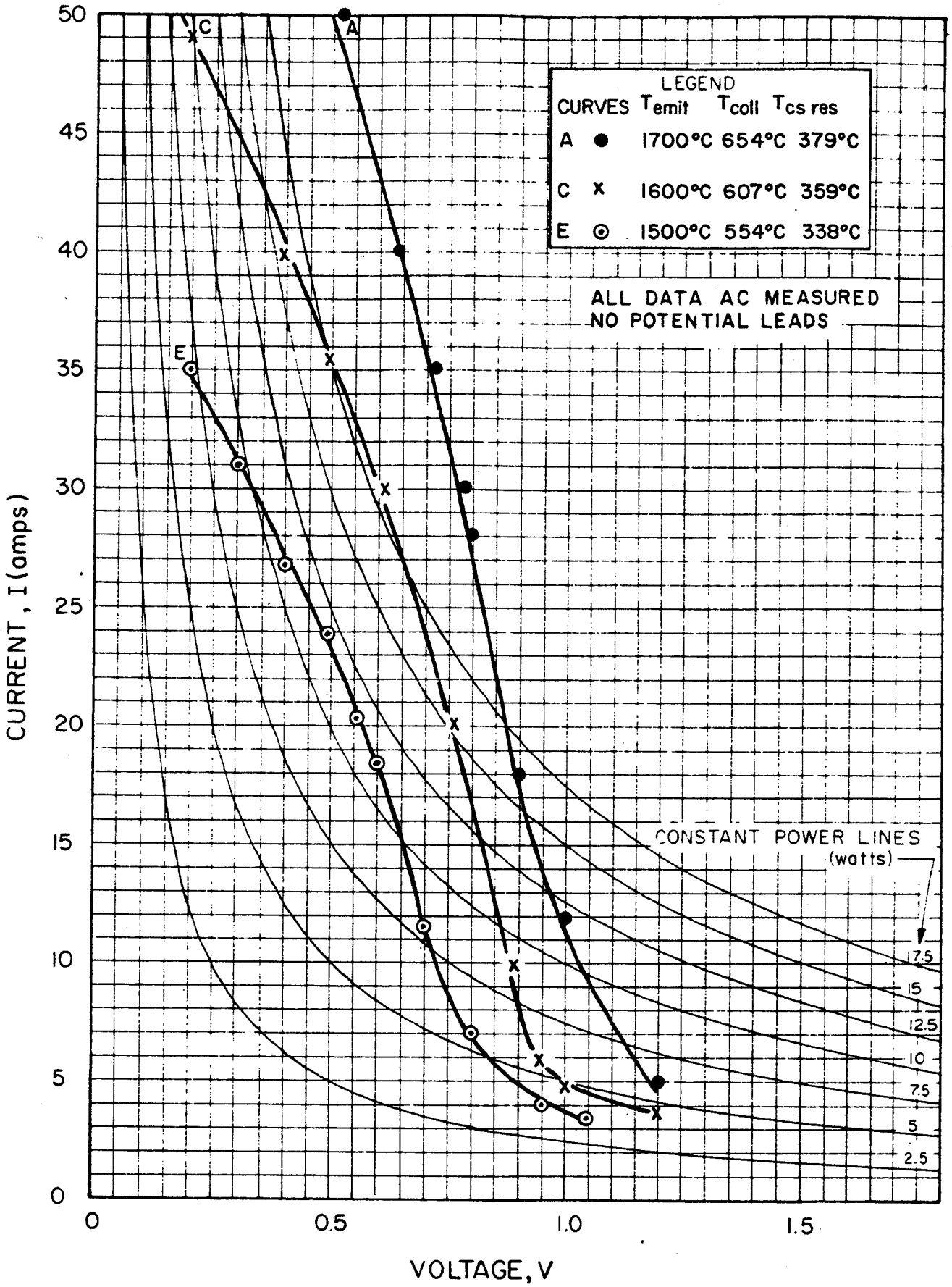

FIG. 4-4 I-V CHARACTERISTICS FOR GENERATOR-CONVERTER NO. 4

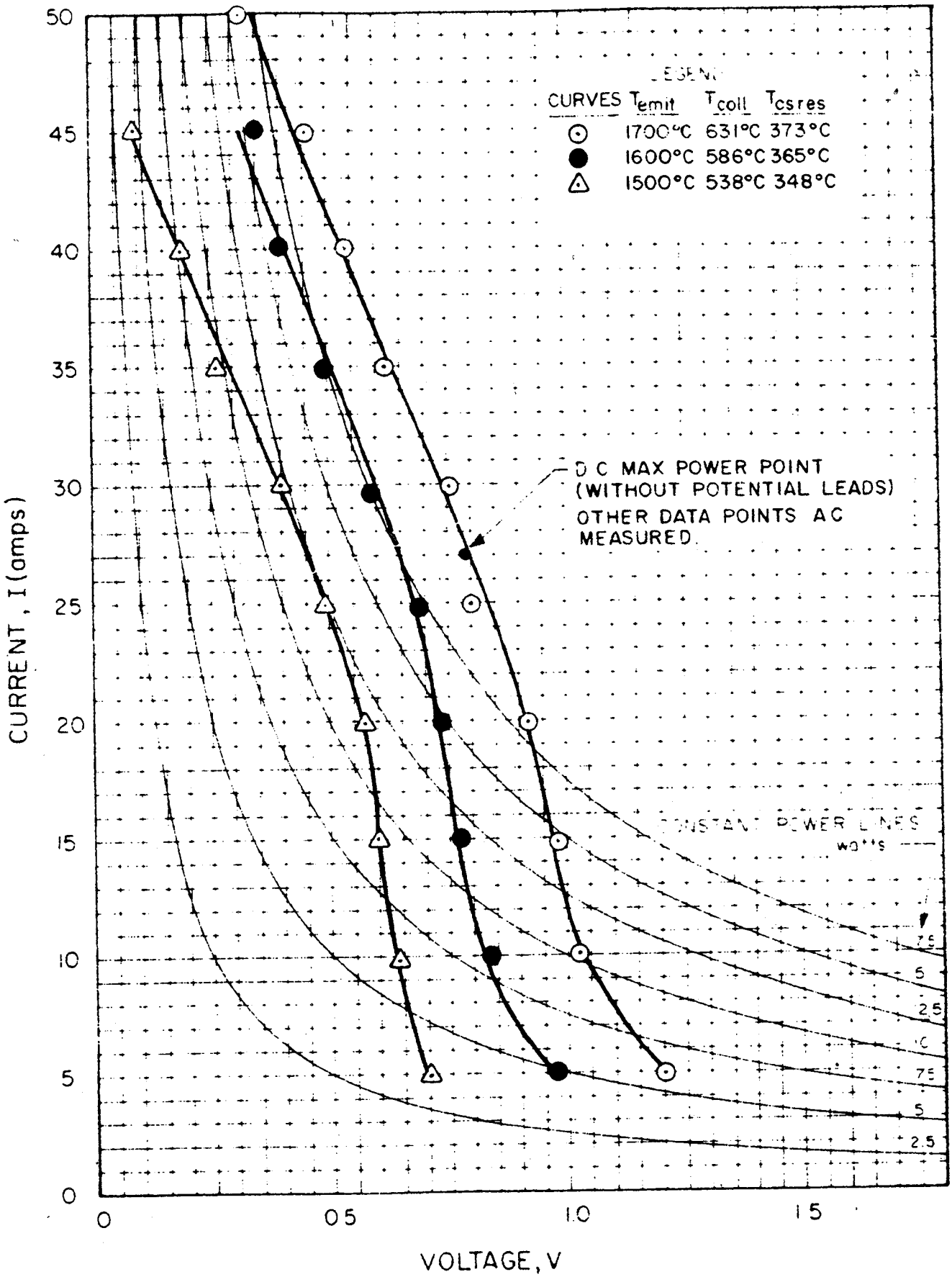

FIG. 4-5 I-V CHARACTERISTICS FOR GENERATOR-CONVERTER NO. 5

4.2 Generator Design

State of the art generators are assembled by mounting the converters in a cavity block. This design concept is penalized since the block conducts heat away from the diode. In addition, the outer surface of the block rejects heat by radiation. The converter prototype generator, photographed in Figs. 4-6 and 4-7, was designed to suffer a minimum of thermal loss by conduction and radiation. To this end, the cavity of the generator was formed by the enclosure of the converter emitter, thus, conduction losses are avoided. Moreover any reduction in radiation losses from the cavity walls is a direct generator saving. Drawing No. 12250 (in the appendix) is the generator assembly in full scale referencing the assembly components. Radiation loss from the cavity is reduced by the inner and outer heat shields, Drawings No. 12246 and 12247 (see appendix). Placed between these shields were eight (8) 0.002 inches tantalum and molybdenum dimpled shields that further impeded radiation heat loss. The individual converters were electrically insulated from 0.002 inch shields by ceramic collars placed around each converter envelope. Tantalum foil was inserted between the collars and the envelopes to prevent interaction with the converter proper.

As noted in the assembly drawing, the structure is maintained rigidly by a series of cross braces. The radiators are braced and held in place by external support straps (Drawing No. 12248 in the appendix). Internally, the generator is supported by the tantalum lead straps, which form a closed ring around the converter envelopes. Both the internal and external straps are electrically insulated with ceramic busings and washers, which prevent short circuiting the electrical leads. The generator cone, Drawing No. 12241 (see appendix) is mounted in place by tripod legs of tantalum strap. The legs (Drawing No. 12249 in the appendix) are in turn secured to the internal lead straps resulting in a rugged, self-contained, light weight, thermionic generator.

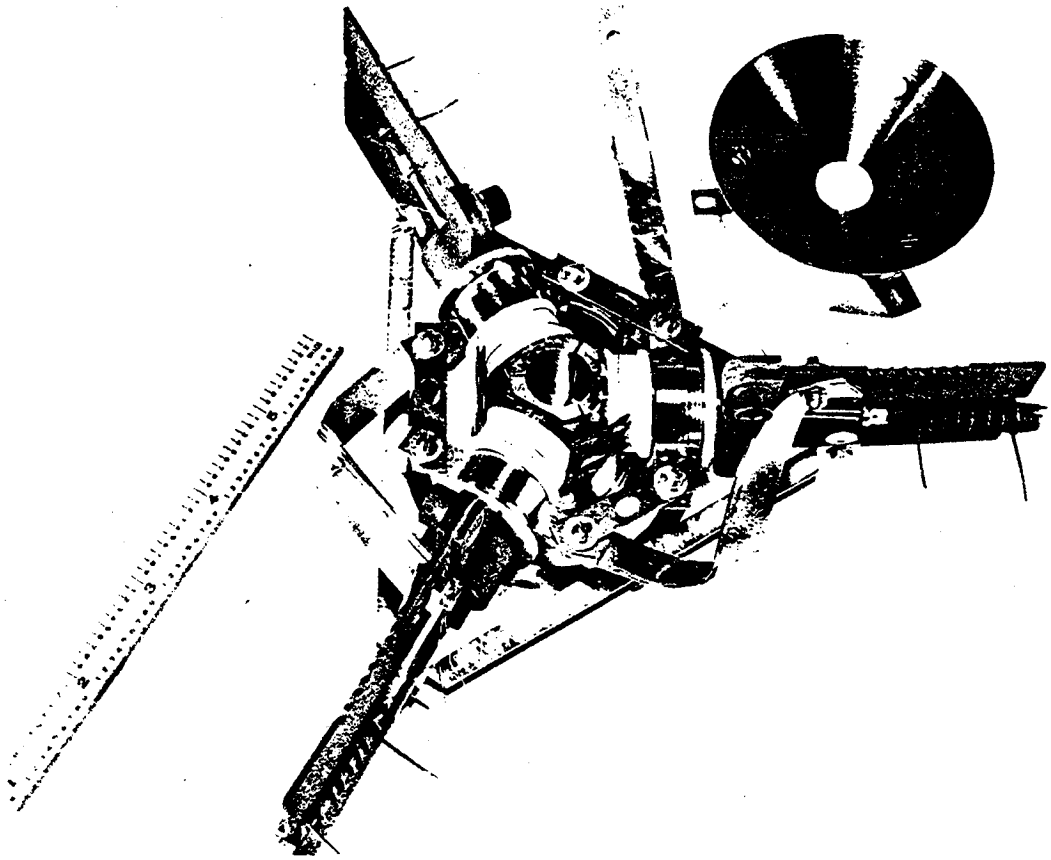

FIG. 4-6 PROTOTYPE 3 CONVERTER GENERATOR

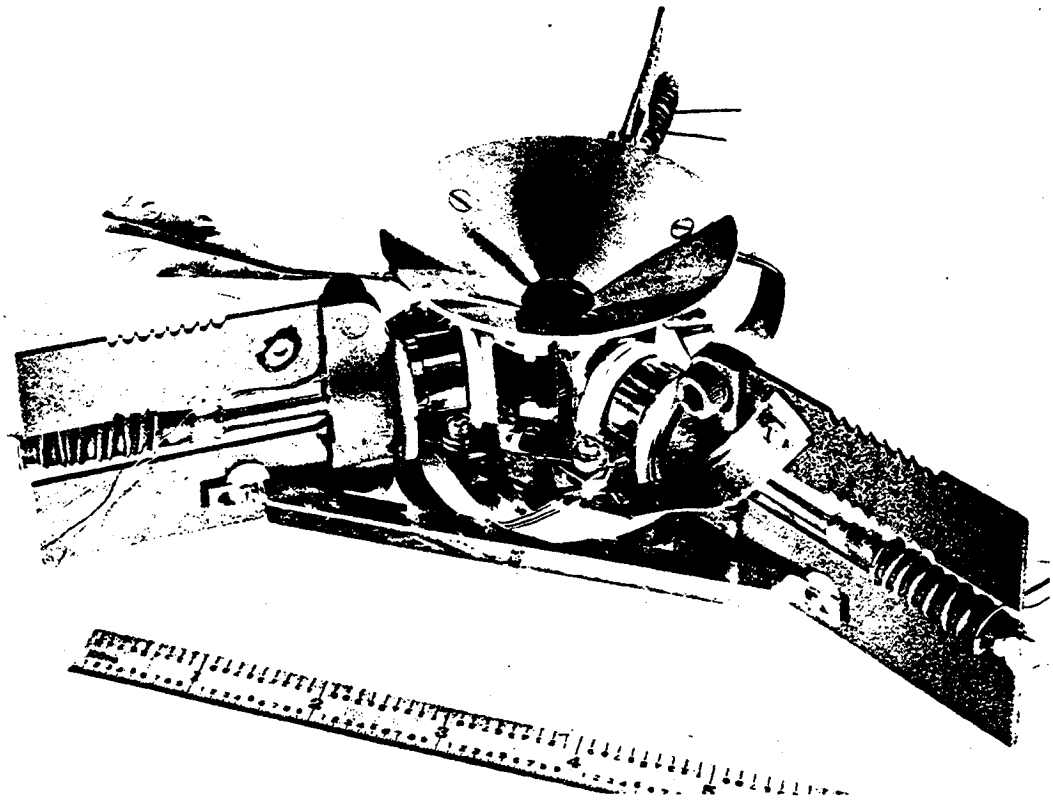

FIG. 4-7 CONE MOUNTED IN PLACE FOR COMPLETED ASSEMBLY OF GENERATOR

4.3 Generator Performance

After assembly the generator was mounted in a high-speed vacuum pump station and instrumented for test. It was originally hoped that the cavity could be brought to temperature by radiation heating alone. However, the maximum cavity input achievable was 770 watts, which was limited by the power supply. Electron bombardment was then employed to obtain higher energy input to the cavity.

An initial shorting problem occurred after first heating caused by a converter whose mounting bolts required retightning. We have previously experienced bolted connections becoming loose after copper and tantalum parts anneal at temperature. The initial testing then proceeded without incident. The significant data is recorded in Table 4-1, however further testing has been conducted with these results:

1. Potential lead measurements of individual diodes undergoing generator test indicate 0.65 w average output for total generator voltages of about 2.0 volts.
2. The outer generator heat shield and cone radiate 150 watts waste heat at cavity power inputs of 1.2 kw. This is significantly higher than originally calculated indicating the requirement of more heat shields to bolster the cavity efficiency.
3. For conditions of cesium pressures, current and voltage output identical in the individual converter test and the converter in generator test, the cavity emitter temperature is estimated at 1700°C ±30°C for 1200 watts input.
4. The one parameter not identical in the individual converter test and the converter in generator test was the collector temperatures, which were some 30 to 80°C higher in the generator test. It is possible the shielding and ceramic collars around the individual converter envelopes forced heat inward to the collector and raised its temperature.

TABLE 4-1 INITIAL TEST DATA FROM THE 3 CONVERTER PROTOTYPE GENERATOR (NO LOSSES ESTIMATED OR INCLUDED)

Filament power input (watts)	Bombardment power input (watts)	Total power input (watts)	Generator current (amperes)	Generator voltage (no potential leads)	Generator power out (watts)	Efficiency (percent)
240	590	830	27.8	1.19	33.1	4.0
247	692	939	28.0	1.4	39.2	4.2
247	749	996	26.1	1.66	43.2	4.3
245	880	1125	26.5	1.82	48.2	4.3
246	950	1196	26.0	1.89	49.4	4.1
245	965	1210	26.7	2.01	53.7	4.5
178	1385	1560	28.4	2.1	56.7	4.1*

*Not optimized

APPENDIX

APPENDIX

CHEMICAL CLEANING SPECIFICATION

MATERIAL: TANTALUM OR MOLYBDENUM

MATERIALS USED

Ethyl alcohol (CH_3CH_2OH)
Hydrochloric Acid (HCl)
Chromic Acid (Saturated solution of Potassium Dichromate in hot concentrated Sulphuric Acid)
Distilled water

PROCEDURE

Step No. 1

Place part in beaker of ethyl alcohol. Place beaker in ultrasonic cleaner. Clean for approximately 60 seconds.

Step No. 2

Remove parts from ethyl alcohol - allow to dry.

Step No. 3

Place parts in beaker of hot hydrochloric acid for approximately 30 seconds.

Step No. 4

Remove from hydrochloric acid and rinse in beaker of boiling distilled water for approximately 2 minutes.

Step No. 5

Remove from distilled water - allow to dry.

Step No. 6

Dip in ethyl alcohol - remove and allow to dry.

Step No. 7

Place parts in beaker of hot chromic acid (110°C)

Step No. 8

Remove from chromic acid and rinse vigorously in large beaker of cold distilled water.

Step No. 9

Rinse parts in hot distilled water for approximately 2 minutes.

Step No. 10

Rinse parts in cold distilled water for approximately 10 seconds.

Step No. 11

Remove parts from distilled water - allow to dry.

Step No. 12

Rinse parts in clean ethyl alcohol - remove and allow to dry.

Step No. 13

Wrap parts in lint free paper. Place in desiccator until ready for use.

CAUTION: All chemical cleaning will be done under the fume hood at all times. Caution should be taken in that the vapors are harmful to the skin and clothes. Rubber gloves and tongs should always be used. The tap water in the fume hood should be kept running constantly in case of any accident. Avoid the inhalation of any of the fumes.

APPENDIX

CHEMICAL CLEANING SPECIFICATION

MATERIAL: NIOBIUM

MATERIALS USED

Ethyl alcohol (CH_3CH_2OH)
20 cc of acetic acid
50 cc of sulfuric acid
5 cc of hydrochloric acid
Distilled water

(Niobium Cleaning Bath)

PROCEDURE

Step No. 1

Place part in beaker of ethyl alcohol.

Step No. 2

Place beaker in ultrasonic cleaner and clean for 60 seconds.

Step No. 3

Remove parts from ultrasonic cleaner and allow to dry.

Step No. 4

Place parts in the niobium cleaning bath solution for approximately 2 minutes.

Step No. 5

Remove parts from bath solution and rinse vigorously in large container of cold distilled water.

Step No. 6

Place parts in boiling distilled water for approximately 2 minutes.

Step No. 7

Remove parts from boiling water and rinse for approximately 30 seconds in cold distilled water.

Step No. 8

Allow to dry.

Step No. 9

Rinse in clean ethyl alcohol and allow to dry.

Step No. 10

Wrap in clean lint free paper and store in desiccator until ready for use.

APPENDIX

CHEMICAL CLEANING SPECIFICATIONS

MATERIAL: SAPPHIRE AND CERAMIC (Al_2O_3)

MATERIALS USED

Distilled water
Detergent

PROCEDURE

Step No. 1

Super saturate the distilled water with the detergent.

Step No. 2

Heat solution to boiling point.

Step No. 3

Place parts in boiling solution.

Step No. 4

Place beaker in the ultrasonic cleaner and clean for approximately 3 minutes.

Step No. 4

Remove from ultrasonic cleaner.

Step No. 5

Stir vigorously in cold distilled water - allow to dry.

Step No. 6

Rinse in clean ethyl alcohol and allow to dry.

Step No. 7

Wrap in lint free paper and place in desiccator ready for next process.

APPENDIX

CHEMICAL CLEANING SPECIFICATIONS

MATERIAL: ZIRCONIUM

MATERIALS USED

Ethyl alcohol
Aqua Regia (3 parts HCl, 1 part HNO_3)
Distilled water

PROCEDURE

Step No. 1

Place parts in beaker of ethyl alcohol and ultrasonically clean for 1 minute.

Step No. 2

Remove parts from ultrasonic cleaner and allow to dry.

Step No. 3

Place parts in solution of aqua regia for approximately 1 minute.

Step No. 4

Remove from solution and vigorously stir in cold bath of distilled water.

Step No. 5

Allow to dry.

Step No. 6

Rinse in ethyl alcohol and allow to dry.

Step No. 7

Wrap in lint free paper and store in desiccator until ready for use.

CAUTION: All chemical cleaning will be done under the fume hood at all times. Caution should be taken in that the vapors are harmful to the skin and clothes. Rubber gloves and tongs should always be used. The tap water in the fume hood should be kept running constantly in case of any accident. Avoid the inhalation of any of the fumes.

APPENDIX

CHEMICAL CLEANING SPECIFICATIONS

MATERIAL: NICKEL

MATERIALS USED

Ethyl alcohol
Nickel cleaning bath
Constituents: 40 cc sodium carbonate
13 cc sodium hydroxide
13 cc sodium cyanide
Distilled water

PROCEDURE

Step No. 1

Place parts in ethyl alcohol and ultrasonically clean.

Step No. 2

Remove from ultrasonic cleaner - allow to dry.

Step No. 3

Place in nickel cleaning solution for approximately 2 minutes.

Step No. 4

Remove from nickel solution and stir vigorously in large bath of distilled water.

Step No. 5

Place in boiling distilled water for approximately 2 minutes.

Step No. 6

Remove from distilled water and allow to dry.

Step No. 7

Rinse in ethyl alcohol and allow to dry.

Step No. 8

Wrap in lint free paper and store in desiccator until ready for use.

CAUTION: All chemical cleaning will be done under the fume hood at all times. Caution should be taken in that the vapors are harmful to the skin and clothes. Rubber gloves and tongs should always be used. The tap water in the fume hood should be kept running constantly in case of any accident. Avoid the inhalation of any of the fumes.

APPENDIX

CHEMICAL CLEANING SPECIFICATIONS

MATERIAL: COPPER

MATERIALS USED

Ethyl alcohol
Hydrochloric acid
Distilled water

PROCEDURE

Step No. 1

Place parts in ethyl alcohol and ultrasonically clean for approximately 1 minute.

Step No. 2

Remove and allow to dry.

Step No. 3

Place in hydrochloric acid until the part is visibly bright.

Step No. 4

Remove and stir vigorously in cold distilled water.

Step No. 5

Place in boiling distilled water for 2 minutes.

Step No. 6

Remove and allow to dry.

Step No. 7

Rinse in clean ethyl alcohol and allow to dry.

Step No. 8

Wrap in lint free paper and store in desiccator.

CAUTION: All chemical cleaning will be done under the fume hood at all times. Caution should be taken in that the vapors are harmful to the skin and clothes. Rubber gloves and tongs should always be used. The tap water in the fume hood should be kept running constantly in case of any accident. Avoid the inhalation of any of the fumes.

APPENDIX

AIR FIRING SPECIFICATION

SAPPHIRE AND ALUMINA PARTS

EQUIPMENT USED

Air Oven designed by the Thermionics Group (EOS)

PROCEDURE

Step No. 1

Place the clean parts on the alumina slab located in the oven.

Step No. 2

Heat platinum can slowly so as not to thermal shock the alumina crucibles.

Step No. 3

Raise heat until 1200°C is reached for a period of 1 hour.

Step No. 4

Lower bombarder power slowly at the rate of approximately 50° per minute.

Step No. 5

When the ceramic or sapphire parts have reached room temperature remove and wrap in lint free paper. Place these in a vacuum desiccator until ready for use.

APPENDIX

VACUUM FIRING SPECIFICATIONS
(Outgassing of Refractory Metals)

Rules to observe in outgassing.

1. No alumina will be used to support any part that is being outgassed.
2. Parts being outgassed will be separated. (Not to touch each other)
3. No dissimilar materials will be outgassed together.
4. The pressure will always be 5×10^{-6} in. Hg or lower.
5. All metals must be chemically cleaned prior to outgassing.
6. Allow at least 90 minutes after the susceptor can has lost its color before permitting the system to go to air.
7. Outgas only the amount of parts that will be used for a short period. (Two weeks)
8. The jar should be clean of any vapor deposition at least after every sixth firing.

NTIS does not permit return of items for credit or refund. A replacement will be provided if an error is made in filling your order, if the item was received in damaged condition, or if the item is defective.

Reproduced by NTIS
National Technical Information Service
U.S. Department of Commerce
Springfield, VA 22161

This report was printed specifically for your order from our collection of more than 2 million technical reports.

For economy and efficiency, NTIS does not maintain stock of its vast collection of technical reports. Rather, most documents are printed for each order. Your copy is the best possible reproduction available from our master archive. If you have any questions concerning this document or any order you placed with NTIS, please call our Customer Services Department at (703)487-4660.

Always think of NTIS when you want:
• Access to the technical, scientific, and engineering results generated by the ongoing multibillion dollar R&D program of the U.S. Government.
• R&D results from Japan, West Germany, Great Britain, and some 20 other countries, most of it reported in English.

NTIS also operates two centers that can provide you with valuable information:
• The Federal Computer Products Center - offers software and datafiles produced by Federal agencies.
• The Center for the Utilization of Federal Technology - gives you access to the best of Federal technologies and laboratory resources.

For more information about NTIS, send for our FREE *NTIS Products and Services Catalog* which describes how you can access this U.S. and foreign Government technology. Call (703)487-4650 or send this sheet to NTIS, U.S. Department of Commerce, Springfield, VA 22161. Ask for catalog, PR-827.

Name _____
Address _____
_____
_____
Telephone _____

- Your Source to U.S. and Foreign Government Research and Technology.